Atmospheric Pressure Non-Thermal Plasma: A Tool for Inactivating Airborne Pathogens

A Thesis

Submitted to the Faculty of the

University of Minnesota

By

Charles Schiappacasse

In Partial Fulfillment of the Requirements

For the Degree of

Master of Science

Advisor

Roger Ruan

December 2019

Acknowledgements

I would like to thank my advisor, Dr. Roger Ruan, for giving me the opportunity to spearhead the efforts of an important project in our lab. Thank you also for your advice and guidance through the duration of this challenging project.

I would also like to thank Dr. Peng Peng and Nan Zhou. I still fondly reflect upon the memories of us working together on the non-thermal plasma milk powder project when I first joined the lab. Despite the frustration and futile feelings associated with that project, I deeply enjoyed that being able to work closely with both of you. Without your mentorship, guidance, and frequent advice I would never have been able to complete this project. Thank you for taking me under your wing and helping navigate the world of research, project management, and graduate school.

For their regular support and frequent advice, I would also like to thank all of the members and visiting scholars of Dr. Ruan's lab in room 42. Thank you Dr. Chen for your regular advice, support, and helpful input, especially during lab meetings. Thank you Dr. Min for your technical advice, hard work in managing equipment orders, and professorial role in several of my classes. Thank you Kirk Cobb for your advice and, perhaps more importantly, being a source of great conversation and debate! Thank you to my undergraduate assistant Nandini Singh. It was a lot of fun having someone in the lab to help with the design and construction of the NTP reactors, and I really appreciate all of your hard work.

To Dr. Liang and all of the members of her lab, thank you very much for all of your hard work and support of this project. Thank you for tolerating the high-pitched

whine of the plasma system, me regularly turning of lights to check plasma discharge, and my frequent calls to ask someone to let me into the lab.

Finally, thank you to my family and girlfriend Theresa. Without your unflinching support outside of the lab I would have permanently morphed into the longhaired, unshaven, madman, endlessly pacing around the room and muttering seemingly nonsensical scientific jargon to myself.

Thank you everyone!

Abstract

Pathogens spread by airborne transmission represent a persistent threat to economic stability and human/animal health. These pathogens are particularly prevalent in the agricultural sector, especially in animal rearing facilities. However, the agricultural industry currently lacks an efficient and cost effective means of controlling airborne pathogens.

The present study explored the possibility of developing a new type of antimicrobial air treatment system based on non-thermal plasma technology. The study consisted of an initial laboratory testing stage followed by a pilot scale study performed in a local poultry rearing facility.

During the laboratory testing stage two prototype non-thermal plasma reactors were developed and challenged in a closed air circulation system with artificially aerosolized Newcastle Disease Virus and avian influenza virus. The results indicated that both viruses could be rapidly inactivated below the limit of detection after sub second exposure to non-thermal plasma. Specifically, Newcastle Disease Virus was completely inactivated after 7.7×10^{-3} seconds of direct plasma treatment with a specific energy input of 171 J/L of air. Although the high virus inactivation effects are believed to predominately be attributable to direct non-thermal plasma exposure, preliminary experiments revealed that liquid-based virus collection strategies (e.g. use of an SKC BioSampler) were susceptible to liquid-based inactivation of collected viruses via indirect non-thermal plasma exposure. Attempts were made to circumvent the issue of liquid-based inactivation by employing a gelatin-filter based virus collection strategy. However, due to the high ozone emissions (80ppm) of the non-thermal plasma reactors, surface-

based inactivation effects of viruses collected on the filters could not be ruled out as a contributing mechanism to the high virus inactivation rates. Due to biosafety concerns, flow rates >28LPM were not tested and the upper limit of non-thermal plasma's virus inactivation efficiency was not determined. Additionally, virus samples taken from the 6-jet collision nebulizer, used to aerosolize viruses in this study, revealed that nebulization stress did not contribute to virus inactivation. Finally, the effects of relative humidity on virus losses within the closed air circulation system were explored. Findings showed a strong correlation (R^2>0.99) between increasing relative humidity and decreasing airborne virus concentrations. This relationship is thought to predominately be due to humid aerosols experiencing greater condensation losses within the closed air circulation system when compared with less humid aerosols. However, the small volume of condensed solution visualized within the system was not sufficient to account for all of the viruses lost between the nebulizer and sampling port (gelatin filters). Correcting for adhesion losses and possible low gelatin filter sampling efficiencies did not completely account for non-plasma treated viral losses. Therefore, it is possible that the viruses used in the present study experience a decrease in infectivity with increasing humidity levels.

The second stage of this study involved the design and fabrication of a pilot scale non-thermal plasma air treatment system and challenging it with ambient aerobic bacteria at a local turkey barn. Technical complications with a commercial high voltage power supply resulted in the pilot scale system operating at approximately 10% of its specified input power resulting in a specific energy input of only ~19.4 J/L. As a result, the pilot system was not able to reduce airborne bacteria concentrations relative to air samples that did not receive plasma treatment.

Overall, the findings from the present study indicate that non-thermal plasma based air treatment technologies can be an effective tool for controlling airborne pathogens. However, the successful industrial implementation of this technology will require appropriate power supplies and methods to mitigate ozone emissions.

Table of Contents

List of Tables

List of Figures

List of Equations

List of Abbreviations

AC	Alternating Current
APNTP	Atmospheric Pressure Non Thermal Plasma
CDC	Centers for Disease Control and Prevention
CFU	Colony Forming Units
COP	Cold Oxygen Plasma
DBD	Dielectric Barrier Discharge
DC	Direct Current
DDB	Double sided Dielectric Barrier Discharge Reactor
dsDNA	Double Stranded Deoxyribonucleic Acid
dsRNA	Double Stranded Ribonucleic Acid
ESP	Electrostatic Precipitator
FBS	Fetal Bovine Serum
GFP	Green Fluorescent Protein
GFU	Green Fluorescent Unit
HEPA	High Efficiency Particulate Air
hPIV	Human Parainfluenza Virus
LPM	Liters Per Minute
MDCK	Madin-Darby Canine Kidney Cells
MEM	Minimum Essential Media
NDV	Newcastle Disease Virus
NTP	Non Thermal Plasma

PBS	Phosphate Buffered Saline
PCR	Polymerase Chain Reaction
PFU	Plaque Forming Units
PR8	Low Pathogenic Strain of Avian Influenza Used in Present Study
RH	Relative Humidity
RNS	Reactive Nitrogen Species
ROS	Reactive Oxygen Species
RSV	Respiratory Syncytial Virus
SDB	Single Sided Dielectric Barrier Discharge reactor
SDB	Single Dielectric Barrier Discharge Reactor
SEI	Specific Energy Input
ssDNA	Short Stranded Deoxyribonucleic Acid
ssRNA	Short Stranded Ribonucleic Acid
UV	Ultraviolet
WHO	World Health Organization

Chapter 1: Introduction

1.1 Airborne Pathogens

1.1.1 Definition of Pathogen

A pathogen is a biological agent capable of infecting a host organism resulting in the development of disease, or death, of the host organism. The colloquial use of the word pathogen typically refers to infectious microorganisms such as viruses and bacteria, however the term also applies to certain species of fungi, protozoa, and worms. For the purposes of this report, the term pathogen will be restricted to referring to viruses, bacteria, and fungal spores.

1.1.2 Modes of Pathogen Transmission

The spread of pathogens follows a cyclical pattern referred to as the "chain of infection" (CDC, 2012). In general, the cycle begins when an infected individual (host/reservoir) sheds pathogens into the environment. The pathogens are then transmitted to a new susceptible host by one or more of several modalities. The first mode is direct contact. Transmission by direct contact occurs when two or more organisms physically touch epidermal or mucosal membranes, such as during kissing, sexual intercourse, or general close proximity. The second transmission modality is vector-mediated transmission. During vector transmission an intermediate organism, such as a mosquito, flea, or rat, carries a pathogen from one host to another. The third mode of transmission is vehicle transmission. During vehicle transmission an object harboring pathogens, such as a piece of food or needle, is directly introduced into/onto a susceptible

host. The three modes of transmission described so far represent significant health risks to humans and animals alike. However, in general these modes of transmission can easily be blocked by control measures including safe/hygienic practices, pesticides, and thoroughly cooking food respectively. Unfortunately, two more transmission modalities exist, which are far more insidious, airborne and droplet transmission.

1.1.3 Airborne & Droplet Transmission

Airborne transmission occurs when an infectious agent becomes suspended in the air, often attached to a dust particle, or in a small water droplet, and is carried to a new host on air currents. These types of airborne pathogens are often referred to as bioaerosols. Droplet transmission is closely linked to airborne transmission. Specifically, droplet transmission occurs when a bioaerosol settles on a surface, forming what is referred to as a fomite. The infection process occurs when a susceptible host touches the fomite, then inadvertently introduces the pathogen to a susceptible tissue, such as rubbing ones eyes, touching ones mouth, etc.

1.1.4 Pathogens with Known Airborne Transmissibility

Although the term pathogen extends to a wide range of organisms, the term airborne pathogen is restricted to organisms small enough to become suspended in the air column while remaining infectious and transmissible. However, despite being a narrower subset of organisms, airborne pathogens include a diverse array of microbes.

- Viruses:

  Viruses are very small microorganisms, typically on the order of 10's to 100's of nanometers that rely on host organisms to replicate. Due to their

small size, the potential of a virus to aerosolize is quite high while outside of a host organism. However, not all viruses are known to utilize air travel as a means of transmission. Some viruses with known airborne transmissibility include influenza, paramyxoviruses such as respiratory syncytial virus (RSV), measles and mumps (Terrier et al., 2009). Perhaps the most common disease associated with airborne viruses is influenza ("the flu").

- Bacteria:

  Bacteria are single-celled microorganism, usually on the order of a few micrometers in diameter. Unlike viruses, bacteria can replicate without a host organism. There are countless species of bacteria and a multitude of pathogenic species with known airborne transmissibility including *E. coli*, *Mycobacterium tuberculosis*, and *S. pneumonia* (Lonc and Plewa, 2009). Some common diseases attributed to airborne bacteria include tuberculosis and pneumonia.

- Fungal Cells/Spores:

  Fungal Cells/Spores are small biological particles on the order of several micrometers in diameter. Fungal cells and spores are often linked to respiratory irritation events and asthma, however there are a variety of opportunistic pathogen species that are known to have airborne transmissibility including A. flavus and A. niger. (Lonc and Plewa, 2009).

1.2 Economic and Health Consequences of Airborne Pathogens

In 1918 the world was devastated by the most severe pandemic in human history, which resulted in the infection of approximately 1/3 of the global population and death of at least 50 million people (CDC, 2019). The cause of this outbreak was a highly pathogenic influenza A virus, which originated from avian sources. Since that time, a variety of pathogens, including influenza, have been shown to demonstrate airborne transmissibility (Herfst et al., 2017). Diseases caused by airborne pathogens have been, and continue to be, a major threat to economic stability and human health worldwide.

1.2.1 Airborne Pathogens & Economic Stability

Threats of airborne pathogen transmission are not limited to human beings. In fact, there have been a variety of disease outbreaks in the agricultural sector, which have raised concern for airborne pathogen transmission among livestock. One of the most prominent disease outbreaks in the United States was the 2014-2015 outbreak of avian influenza. Specifically, an outbreak of highly pathogenic avian influenza H5 viruses, which emerged in the Northwestern states and quickly spread to flocks in 21 US states including Minnesota (CDC, 2015). This particular outbreak resulted in major economic damages in afflicted states. For instance, in Minnesota the outbreak is estimated to have caused over $647.2 million in economic damages, as well as thousands of lost jobs (Center for Animal Health and Food Safety, 2015). A 2009 outbreak of swine influenza also created significant economic issues for farmers (Gatherer, 2009), demonstrating that concerns could not be limited to the poultry sector.

Current projections indicate that the demand for poultry and poultry products (eggs) will grow by 121% and 65% respectively by 2050 and demand for pork will increase by 43% in that time frame (Alexandratos & Bruinsma, 2012). When considering the importance of animal derived protein in the context of increasing global population, it is clear that mass outbreaks of disease in the livestock sector could devastate global economies.

Airborne transmission is of particular concern in the agricultural sector; because of its potential for rapid transmission. Since 1922, an integrated model of animal production has led to the livestock production becoming more localized and in confined settings (i.e. barns) (Silbergeld et al., 2008). The high concentration of animals in confined spaces has increased the total biological load within these facilities, which has resulted in very high local concentrations of airborne pathogens. For example, (Chen et al., 2009) recorded airborne influenza virus concentrations of 6.9×10^4 virus particles per m^3 in a chicken house. Similarly, in barn bacteria and fungi concentrations of 6.43 log CFU/m^3 and 4.0 log CFU/m^3 respectively have been reported (Seedorf et al., 1998). When considering that the risk of infection by airborne transmission increases with an increase in the number/concentration of airborne pathogens, as predicted by the Wells-Riley and dose-response model (To & Chao, 2010), it is easy to understand why airborne transmission within barns can occur rapidly and extend to an entire flock or herd of animals.

Unfortunately, the spread of airborne pathogens in the agricultural sector may not be limited to in-barn transmission. Recent findings have also raised concern for airborne transmission between neighboring barns. This concern is based on multiple studies that have detected airborne pathogens at great distances from the barn where they originated.

For example, (Jonges et al., 2015) detected airborne influenza viruses 60m away from barns housing infected poultry. Similarly, (Kollner and Heller, 2006 & Millner, 2009) reported airborne bacteria concentrations higher than background concentrations 420m downwind from animal farms. The frequent close proximity of neighboring barns, in conjunction with their high, and untreated, ventilation rates has raised significant concern for disease outbreaks caused by airborne pathogens.

1.2.2 Airborne Pathogens & Human Health

Disease outbreaks in the agricultural sector are concerning for more than just economic reasons. The close proximity of humans and livestock presents the risk of zoonotic transmission. Zoonotic transmission, or zoonosis, is the process where a pathogen from an animal host transfers to and infects a human. As previously described, zoonotic diseases, such as influenza (Spanish Flu), have an extensive and deadly history. However, the issue of zoonotic diseases, including those with airborne transmissibility, continues to this day. In fact, zoonotic diseases currently account for 60% of known infectious diseases and 75% of emerging infectious diseases (CDC, 2017).

Influenza is perhaps the most well known zoonotic disease with airborne transmissibility. The 1918 Spanish Influenza virus is believed to have originated in birds (CDC, 2019). However, although there has not been a massive avian influenza outbreak in a human population since the early to mid 1900's, avian influenza viruses have regularly emerged in small groups of people. In 1997, a highly pathogenic avian influenza H5N1 virus emerged in the local population of Hong Kong, China. Since 2003, the virus has caused several hundred human infections across Asia, Europe, and Africa, frequently resulting in human death. In 2013, a new strain of avian influenza virus H7N9

was reported in China, and lead to over 1500 human infections, with high mortality rates (WHO, 2018). The 2015 outbreak of avian influenza, which devastated the Midwestern United States poultry sector, also spread to Asian countries where it caused multiple human infections, many of which were terminal (WHO, 2019 A). Although recent strains of avian influenza have not demonstrated sustained human-to-human transmission, the World Health Organization (WHO) has voiced concern that the diversity of zoonotic influenza viruses necessitates increased surveillance in human and animal populations (WHO, 2018). Though particularly devastating, avian influenza is not the only zoonotic pathogen with airborne transmissibility. The WHO currently recognizes a variety of other pathogen including swine and equine influenza (WHO, 2018), zoonotic tuberculosis (M. bovis), Brucellosis, Severe Acute Respiratory Syndrome (SARS), and others (WHO, 2019 B).

Modern intensive animal rearing practices also produce a variety of non-zoonotic airborne pathogens. Exposure to theses pathogens can result in a variety of chronic respiratory ailments including asthma, chronic bronchitis, chronic obstructive pulmonary disease, and others (Lonc & Plewa, 2009). In their 2009 literary review article (Lonc & Plewa, 2009) compiled a list of pathogenic bacteria and fungal species with known airborne transmissibility, and indicated which species had been detected in animal rearing facilities. The results showed 10 species of pathogenic bacteria including *Psuedamonas, Citrobacter,* and *Bacillus anthracis*, as well as 10 species of pathogenic fungi including *A. niger, Trichophyton,* and *Cladosporium*.

1.3 Importance of Infectious Particle Size

The specific species of airborne pathogen dictates the type of disease that can occur. However, the physical size, or aerodynamic diameter, of a bioaerosol particle determines many of the aerosols' most important characteristics. These characteristics include settling velocity, pathogen infectivity, and the physical mechanics of motion of the suspended bioaerosol.

1.3.1 Factors Influencing Particle Size

There are a variety of factors that influence the size of aerosol particles. In fact, the actual size of an infectious aerosol particle may be much larger than the microorganism itself. Some important factors influencing aerosol particle size include the mode aerosolization, ambient humidity, and the concentration of other airborne particulate matter.

The mode of aerosolization has important implications on aerosol particle size. When an infected individual coughs, sneezes, or otherwise exhales forcefully, pathogens propagating in the lungs can be expelled into the environment (Morawska, 2006). Because the expulsion originates in the respiratory tract, the expelled material often includes other organic matter such as mucous, saliva, and other bodily excretions. Pathogenic microorganisms often adhere to this material, resulting in infectious aerosol particles much larger than the pathogen itself. Other methods of aerosolization include suspension or resuspension of a pathogen into the air by means of an air disturbance, such as a gust of wind (Morawska, 2006). However, this mode of aerosolization likely has minimal impact on final particle size, because the particle has already been generated and reached an equilibrium state with the surrounding environment.

A second important factor influencing aerosol particle size is relative humidity. When a pathogen/particle becomes aerosolized it rapidly gains or loses aggregated water molecules based on the temperature and humidity (absolute humidity) of the local environment. This process is referred to as hydroscopic growth/shrinking. In a very humid environment, water molecules will aggregate on airborne material forming a large aerosol droplet. In contrast, when ambient humidity levels are low, aggregated water molecules quickly evaporate from the droplet nuclei (solid material at center of aerosol droplet) (Tellier, 2006). The hygroscopic grow/shrinking process is incredibly rapid, occurring in just a few milliseconds (Colbeck & Lazaridis, 2014). The process is illustrated in figure 1.3.1.

1.4 Modern Control Technologies & Why they are Insufficient

Airborne transmission of pathogenic microorganisms poses a persistent threat to human health and economic stability. Unfortunately, this threat presents a multifaceted challenge that complicates control efforts. Many of the challenging facets include topics already discussed including the immense biodiversity of airborne microbes, the micrometer and submicrometer size range of microbial aerosols, and the influence of other airborne material such as dust and water vapor.

However, the unrelenting socioeconomic pressure caused by airborne microbes has been met with a variety of research efforts and technological innovations aimed at developing engineering-based control methods for airborne pathogens. These methods are typically based on one of several air treatment technologies including ultraviolet light (UV), air filters, and electrostatic precipitators. Unfortunately, although often demonstrating

success in certain applications, each of these technologies has failed to adequately address the overall problem of airborne pathogen transmission.

1.4.1 Ultraviolet Light

Ultraviolet light, or UV light, describes high-energy photons with wavelengths between approximately 100 and 400 nanometers. However, when applied as an antimicrobial agent, it is common to use light in the UV-C region (~250nm). This particular region is preferred because photons with wavelengths in the UV-C region have been shown to penetrate viruses and bacteria and create single-strand breaks in DNA chains resulting in microbial inactivation (Gurzadyan et al., 1981).

The application of UV light as an antimicrobial technology has a well-documented and extensive history, and the exploration of UV-based air treatment systems is no exception. The first demonstration of UV-light's airborne pathogen inactivation potential was demonstrated in 1935 by Wells and Fair, on airborne bacteria (Wells & Fair, 1935). Shortly thereafter, UV-light was successfully used to inactivate aerosolized influenza (Wells & Brown, 1936).

Since its early inception, experiments and understanding of UV-based inactivation have become much more precise. For example, in 2005 (Tseng & Li, 2005) determined the specific UV dose required for 90% inactivation of four different aerosolized phage viruses including a ssRNA virus, a ssDNA virus, a dsRNA virus, and a dsDNA virus. The study found that the specific UV dosages needed for 90% inactivation were 339-423uW sec/cm^2, 444-494 uW sec/cm^2, 662-863 uW sec/cm^2, and 910-1196 uW sec/cm^2 for each virus respectively. Interestingly, the UV dose required for 99% inactivation was 2 times higher than for 90% inactivation. This study also explored the effects of relative

humidity on UV inactivation efficiency. The researchers found that increasing relative humidity from 55% to 85% required a significant increase in UV dose, in order to maintain inactivation rates. This change was attributed to increased water sorption on viruses (hygroscopic growth) resulting in a shielding effect from UV exposure. The relationship between increasing humidity and decreasing inactivation was also demonstrated by (McDevitt et al.,2012) who challenged a UV air treatment system with aerosolized influenza virus.

Although UV-light is an effective antimicrobial technology, it has some important shortcomings that often make it unsuitable as an air treatment technology. As previously mentioned, increases in relative humidity can lead to rapid hygroscopic growth of aerosolized particles, including pathogens, which leads to a UV-shielding effect for pathogens within the droplet nuclei. A similar problem arises when the air harboring pathogens is laden with dust. Dust, or particulate matter, can also produce a shielding effect for airborne pathogens leading to decreased inactivation (Griffin et al., 2003 & Martin et al., 2008). Finally, UV treatment is not equally effective for all microorganisms. In general, UV treatment is more effective against sensitive microorganisms (smaller and thinner outer membrane) such as vegetative bacteria such as *S. aureus* and *E. coli*, and much less effective against hardy microorganisms (thicker outer membrane) such as sporulating bacteria (*B. anthracis* and *B. subtilis*) and fungal spores (*Aspergillus versicolor* and *Penicillium chrysogernum*) (Martin et al., 2008). Unfortunately, the combination of relative humidity/dust sensitivity and pathogen specificity make UV treatment unsuitable for environments that have dynamic humidity

levels, high dust concentrations, and contain a complex mixture of airborne pathogens, such as animal rearing facilities (Aarnink et al., 2009 and Lonc & Plewa 2010).

1.4.2 Air Filters

Air filtration is the process of removing particles from an air stream by directing the flow of air across a porous material. There are two primary types of filtration: surface filtration and depth filtration. Surface filtration generally utilizes a thin porous medium with a predetermined permeability. As larger particles accumulate on the surface of the filter, they begin to form a cake layer, which decreases the apparent porosity of the filter and leads to an increase in particle capture efficiency and pressure drop across the filter. The second type of filtration is depth filtration. Depth filters are typically much thicker/deeper than surface filters. Therefore, air passing through a depth filter experiences an increased residence time within the filter material when compared to surface filters. Depth filters rely on particles being captured within the bulk of the filtration material.

Although the definition of filtration is broad, and can include complex mechanisms such as thermophoresis, diffusiophoresis, vapor condensation, and bubbling through liquid, in practice basic air filters primarily rely four methods of particle capture: diffusion, interception, inertial impaction, and gravitational settling (Colbeck & Lazaridis, 2014).

- Diffusion: Filtration by diffusion is an important mechanism for small particle capture, including the submicrometer particles subject to Brownian motion. During diffusion filtration, a small particle deviates from the bulk air stream and

impacts the filtration medium (usually a small fiber). If the particle adheres to the filtration medium it is effectively removed from the air stream. (Colbeck & Lazaridis, 2014)

- Interception: Interception is an important filtration mechanism for small particles at high velocities or intermediate sized particles. Filtration occurs when a particle, following the bulk air stream, passes sufficiently close to the filter medium, such that it adheres to the filter and is removed from the air stream. (Colbeck & Lazaridis, 2014)

- Inertial Impaction: Inertial impaction is a primary filtration mechanism for intermediate and large particles. This filtration process occurs when a particle has sufficient inertia such that it deviates from the bulk air stream and directly impacts the surface of a filter. (Colbeck & Lazaridis, 2014).

- Gravitational Settling: Filtration by gravitational settling is limited to very large particles with a settling velocity greater than the convective velocity of the bulk airflow. (Colbeck & Lazaridis, 2014)

Air filters are an important tool for controlling airborne pathogens. Filters can be designed to have very high collection efficiencies for even submicrometer particles such as viruses. Unfortunately, using air filters to control microbial aerosols has some important drawbacks. First, filtration of airborne microbes requires filters with very small

pores, which can be very expensive. Additionally, the small pore size leads to a very large pressure drop across the filter, which requires a powerful and energy intensive air pump. Second, basic air filters do not provide an active means of pathogen inactivation. Therefore, pathogens that accumulate on the filter are still potential dangerous. For example, if the filter was to become punctured, or an instance of backpressure occurred across the filter, captured microbes could become reaerosolized in high concentrations. In fact, bacteria and fungal spores have been known to not only survive, but also propagate on filter mediums (Pyankov et al., 2012). Finally, like UV light, air filters are sensitive to dust and moisture. High efficiency filters operating in a dusty environment, such as a barn, will quickly become clogged by particulate matter and require frequent replacement, which can become very expensive. Also, high moisture content in the air can lead to filter blinding, which can further increase pressure drop across the filter.

1.4.3 Electrostatic Precipitators

Electrostatic precipitators (ESP) are a common tool for controlling airborne particulate matter. The electrostatic precipitation process operates by flowing particle-laden air through a strong electric field, generated between a high voltage (DC) electrode and a ground electrode. The particles pass through a corona region, created by the high voltage electrode, where they become electrically charged (ionized) by impaction from high-energy electrons in the corona discharge region. The charged particles are then subject to the electrostatic force between the high voltage and ground electrode, perpendicular to the air stream, which propels the particles out of the air stream and onto the ground electrode.

Electrostatic precipitators are predominately used to control particulate matter. However, this technology has recently been explored as a means of controlling airborne pathogens with mixed results. Kettleson et al. (2008) demonstrated capture/inactivation efficiencies of aerosolized T3 and MS2 bacteriophages in excess of 6-log reduction during high voltage (-10kV) and low flow rate (10-12.5 LPM) experiments. In a follow up experiment, Kettleson et al. (2013) tested their ESP system's ability to protect rodents from a variety of aerosolized pathogens, including bacteria and viruses. They found that under high intensity corona conditions (-8kV) with low air flow rates (1.5LPM), the rodents were completely protected from viral and bacterial respiratory infection. However, the high pathogen removal efficiencies observed by Kettleson et al. (2008 and 2013) have not been observed in experiments using increased airflow rates. Li and Wen (2003) challenged an ESP air treatment system with a variety of aerosolized bacteria and fungi at flow rates of 60LPM and 90LPM. Despite being operated at voltages similar to Kettleson et al. (2008 and 2013) (+10kV), microorganism penetration rates of 42% and 70% were observed at the flow rates 60LPM and 90LPM respectively.

When electrostatic precipitators are adapted for microbial aerosol control purposes, they utilize two methods of pathogen mitigation: inactivation and precipitation. The inactivation method involves the pathogen being rendered non-infectious regardless of whether or not it is removed from the air stream. The specific mechanism of microbial inactivation from electrostatic precipitator exposure is an ongoing area of research. However, Kettleson et al. (2008) hypothesize that inflight inactivation of aerosolized T3 and MS2 bacteriophages was the result of exposure to a variety of reactive species produced in the high-voltage corona. Specifically, they stated that the reactive species,

such as ozone and various radicals (O*, N*, OH*, and HO_2*), may react with protein or nucleic acid structure of bacteriophages resulting in inactivation. As a surface-based inactivation phenomenon, one would expect this inactivation mechanism to be less effective on microbes with a thicker outer layer. This concept was supported in part by the findings of Mainelis et al. (2002), who showed that when subjected to ESP exposure aerosolized spores of *Bacillus subtilis* were inactivated at much lower rates than the more sensitive *Psuedomonas fluorescens*.

The precipitation method of airborne microbe control is quite well defined, relative to the inactivation method, if one assumes that aerosolized pathogens behave like spherical particulate matter of equivalent aerodynamic diameter. Under these assumptions the collection efficiency of a simple ESP will increase with increasing particle diameter, electric field strength, and collection area (ground electrode), and decrease with increasing flow rate (Manuzon et al., 2014). All of these relationships were observed in the aforementioned microbial aerosol studies. However, this equivalent particle-assumption model neglects two important details pertaining to microbial aerosols. First, many bacterial species have an inherent electrical charge (Sleytr, 1978), which could affect the precipitation process. Second, variations in shape and cell wall structure lead some bacterial species to accept external charges more readily than others, which could lead to different precipitation efficiencies between species (Li and Wen, 2003). Finally, it is important to mention that size-dependent collection efficiencies of ESPs actually follow a U-shaped curve. That is, collection efficiency decreases with decreasing particle size, and bottoms out in the 0.1-1um size range, before increasing for progressively smaller particles. This behavior is a consequence of electrical mobility

(influenced by charge and mechanical mobility) minimizing in the 0.1-1um range, while progressively smaller particles become more amenable to diffusion charging, which leads to subsequent rise in collection efficiency (Kettleson et al., 2013). Unfortunately, this minimum collection efficiency size range encompasses the size profiles of many airborne pathogens.

Despite the mixed results observed in the scientific literature, the overall potential of ESPs as an airborne pathogen control technology is pretty low. This low potential is a consequence of the culmination of several factors. First, ESP systems require very high operating voltages, which make them much more dangerous than other technologies. Second, ESPs appear to have very low pathogen removal efficiencies at higher flow rates (Li and Wen, 2003), which make them unsuitable for commercial applications. Third, the inactivation rates for ESPs are very low for more hardy microbes (Mainelis et al., 2002), which, if taken into consideration with ESP's potential for re-entrainment, inherent variable collection efficiency, and potential sensitivity to naturally charged microbes (Sleytr, 1978), could render the technology completely useless. Finally, the corona discharge produced in an ESP can produce hazardous air pollutants in large quantities. For example, the ESP used by (Kettleson et al., 2013), produced ozone levels as high as 156ppm when operated at -10kV.

1.4.4 Summary

The unrelenting socioeconomic pressure caused by airborne microbes has been met with a variety of research efforts and technological innovations aimed at developing engineering-based control methods for airborne pathogens. These technologies are typically based on ultraviolet light, filtration, or electrostatic precipitation. Unfortunately,

the complex challenge presented by airborne pathogens ensures that each of these technologies is either an insufficient means of controlling pathogens, or not cost effective. Therefore, it is necessary to develop new technologies that can overcome the shortcomings of preexisting technologies. Non-thermal plasma may represent such a technology.

1.5 Non-Thermal Plasma

1.5.1 General Description

In the context of Physics and Chemistry, the term plasma is used to distinguish the fourth state of matter, ionized gas, from the more commonly recognized states including solids, liquids, and gases. Plasmas can be classified as either thermal or non-thermal. Thermal plasmas are ionized gases in which the constituent species (electrons, ions, and neutrals) are in, or very near, thermal equilibrium. In contrast, non-thermal plasmas (NTP), also called cold plasmas, are partially ionized gases in which the constituent species are not in thermal equilibrium. Specifically, the electrons in non-thermal plasma have much higher kinetic energies than the 'heavy' species, such as ions and neutrals. In fact, the mean electron temperature in non-thermal plasma is typically 2-3 orders of magnitude greater than the rest of the gas (Eliasson & Kogelschatz, 1991). It is from this discrepancy in kinetic energies that non-thermal plasma gets its name. The relatively low kinetic energy of the 'heavy' species in non-thermal plasma produces a much lower thermal energy state than that of the high-energy thermal plasmas. In a colloquial sense, non-thermal plasmas 'feel' much cooler than thermal plasmas.

1.5.2 Methods of Plasma Generation

There are a variety of methods used to generate non-thermal plasmas including radio frequency discharges, corona discharges, ionizing radiation, microwaves, and electrical discharge systems (Kim, 2004). However, the relative simplicity and low operational costs of electrical discharge systems have made them a particularly attractive means of NTP generation. Electrical discharge plasma systems produce plasma by subjecting a neutral gas to an external electric field. The presence of the external electric field causes charge carriers (predominately electrons), to accelerate within the electric field, thereby gaining kinetic energy. The accelerated charge carriers then collide with dormant gas species, such as neutral atoms and molecules, and form new charged particles. The newly charged particles are then subject to electromagnetic forces produced by the external electric field, which causes them to accelerate and collide with other gas species. The result is a cascading effect of charged particle collisions, which continues until there is a net balance between charge carrier loss and charge carrier generation within the gas (i.e. a steady-state plasma) (Conrads & Schmidt, 2000).

1.5.3 Conventional Reactor Geometries

Electrical discharge plasma systems include a broad array of reactor geometries, which can be further subdivided based on the type of power supply, inclusion or absence of a dielectric barrier(s), use of a catalyst, and other factors (Kim, 2004). However, most of these reactors are based on one of several conventional reactor configurations.

- <u>Corona Discharge:</u>

Corona discharge plasma reactors come in a variety of geometric configurations. However, in general the reactors utilize a fine wire as the high voltage electrode, and a metal plate or tube as the ground electrode. When a high voltage is applied to the wire electrode, an electric field will form between the two electrodes, but will be focused at the point (or surface) of the wire electrode. The result is the formation of a powerful electric field around the wire electrode, which can ionize the surrounding gas. The ions produced around the HV electrode will then migrate along the electric field towards the ground electrode. This mechanism is the foundation upon which electrostatic precipitators operate. A simple diagram of a corona discharge reactor is illustrated in Figure 1.

The discharge characteristics of corona reactors are predominately dependent on the polarity and voltage applied to the system. Positive polarity corona systems progress from burst pulse corona, to streamer discharge, to glow discharge, and finally electrical arcing as voltage is increased (Chang et al., 1991). In contrast, negative polarity corona systems progress from trichel pulse coronas, to pulseless coronas, and finally electrical arcing with increasing voltage (Chang et al., 1991). The specific discharge characteristics have important implications on the plasma chemistry. For example, the glowing discharge state of a negative corona produces seven times the amount of ozone as a positive corona with the same electrode geometry. However, when operating at the same voltage with a streamer discharge, the positive polarity produces more ozone (Kim, 2004).

- <u>Dielectric Barrier Discharge:</u>

Dielectric barrier discharge (DBD) reactors typically utilize a simple planar or coaxial electrode configuration in which one or more dielectric surfaces separate the high voltage and ground electrodes. The dielectric material, typically silica glass, ceramics, enamel, and certain polymers, acts as an electrical insulator and prevents arcing between the high-voltage and ground electrodes (Kogelschatz, 2003). An illustration of a simple DBD system is depicted in Figure 2.

When utilizing air, at atmospheric pressure, as a feed gas, the plasma produced in a DBD system predominately exists in the form of microdischarges, often called streamers or streamer discharge. However, the discharge modality can change to glow discharge when using other feed gases, such as noble gases (Kim, 2004).

- Gliding Arc Discharge:

Unlike corona discharge and DBD systems, gliding arc discharge reactors are a relatively new method of plasma generation. The basic principle of the gliding arc design was patented in 1988, but has been progressively developed since then (Moreau, 2008). The basic process of gliding arc discharge is relatively simple. Two diverging electrodes are positioned in front of an air stream, such that air flows between the electrodes. Then a potential difference is applied between the electrodes, which causes an arc to form between the nearest points of the diverging electrodes. The arc then propagates along the two electrodes, becoming progressively longer, as it follows the air current between the

electrodes. Near the end of the electrodes the arc 'breaks' and a new arc is formed at the base of the electrodes and the cycle is repeated. The relatively high current produced during the arcing process enables the gliding arc reactor to generally operate at higher power levels than corona discharge or DBD systems (Moreau, 2008). A simple schematic of a gliding arc reactor is depicted in Figure 3.

- Packed-Bed Reactor:

Similar to DBD reactors, packed-bed reactors typically utilize either a parallel plate or coaxial configuration. However, in contrast with DBD designs, packed-bed reactors fill the void space between the two electrodes with dielectric pellets. The pellets, which can vary in size and shape, are typically composed of dielectric materials such as ceramics, glass, aluminum oxides, and ferroelectric materials (Chen et al., 2008). Figure 1.5.4 shows a simple schematic of a coaxial packed-bed plasma reactor. Of note, not all packed-bed reactors will utilize the dielectric barrier between the high-voltage and ground electrodes. A basic packed-bed reactor is depicted in Figure 4.

The distinguishing feature of the packed-bed system manifests in the contact points between adjacent dielectric pellets. As a potential difference is generated between the high voltage and ground electrode, charge accumulates on the surfaces of the dielectric pellets, resulting in increased electric field strength in the gaps between pellets. In fact, the electric field strength between adjacent pellets has been shown to be higher than the mean electric field strength between the high-voltage and ground electrodes of the packed-bed system (Chen et al., 2008 & Chang et al., 2000)

1.5.4 Active Species

The specific chemistry of non-thermal plasma is complex and depends on a variety factors including the method of generation, reactor geometry, input power, gas flow rate, gas temperature, pressure, feed gas composition, and others (Kim 2004 and Al-Abduly & Christensen 2015). However, the following discussion will focus on the chemistry of dielectric barrier systems, utilizing air as a feed gas, and operating at atmospheric pressure.

The reactive chemical constituents produced in a non-thermal plasma reactor can be broadly classified as 'short-lived active species' and 'long-lived active species'. In general, short-lived species include high-energy electrons, ions, and radicals, which are generated in the plasma discharge region, and rapidly react (<1 second) upon leaving the discharge region (Sasaki et al., 2016). When air is used as a feed gas some common short-lived reactive species include high-energy electrons, O*, OH*, N_2* N_2O+, NO, and UV photons (Li et al., 2016). Long-lived active species are typically the product of reactions between short-lived active species and are therefore much more stable outside of the discharge region (Kim, 2004). When utilizing air as a feed gas some common long-lived species include O_3, OH, NO_x, HO_2, and H_2O_2 (Li et al., 2016 and Kim, 2004). Figure 5 provides an illustration of the short and long-lived active species produced by a DBD reactor operating with air as a feed gas.

1.5.5 Mechanism of Pathogen Inactivation

The dynamic physical and chemical nature of NTP has fostered a growing interest in utilizing NTP as an antimicrobial technology. Part of this interest stems from NTP's multiple inactivation mechanisms, which not only make it an effective means of

controlling a variety of microorganisms, but also ensure that organisms struggle to develop any type of immunity to NTP treatment. The specific inactivation modalities that occur during plasma treatment vary based on the geometry and operating parameters of the plasma system. However, in general plasma-based microorganism inactivation will rely on one or more of the following inactivation modalities.

- Etching/Volatilization:

  Plasma etching is one of the primary methods of plasma-based microorganism inactivation. First utilized on microorganisms by (Thomas, 1964), etching refers to the process of surface oxidation and volatilization of a microorganism's outer membrane when exposed to reactive oxidizing species produced by NTP.

  The specific type of reactive species has important implications on how, where, and to what extent it will react with a microorganism's outer membrane. For example, hydroxyl radicals (OH*) are incredibly reactive species, with an average diffusion distance of several nanometers (Farr & Kogoma, 1991). This high level of reactivity allows hydroxyl radicals to effectively react with most surface proteins and lipids (Català et al., 2000). In contrast, less reactive oxygen species, such as the secondary radicals produced by OH* reactions, are likely much more site specific in their reactivity (Gaunt et al., 2006).

  The specific surface macromolecule that is attacked by the plasma species has important implications on the inactivation mechanisms. For example, the

high reactivity of OH* with proteins may be partly responsible for plasma-based inactivation of viruses, which use surface proteins to infect other cells. If the critical surface proteins on a virus are completely oxidized, the virus will likely lose infectivity (Wu et al., 2015). The lipid reactivity has important implications for inactivation of larger cells, such as bacteria and fungal spores. Prolonged exposure to volatilizing plasma species can result in a variety of paths to inactivation, which are typically a function of exposure time. For example, short-duration plasma exposure may lead to localized membrane damage beyond the cell's regenerative capacity, leading to prolonged, but inevitable, cell death (Gaunt et al., 2006). Similarly, longer exposure times may lead to complete cell membrane rupture, and subsequent leakage of intracellular material leading to cell death (Gaunt et al., 2006). Finally, prolonged plasma exposure would likely lead to the complete volatilization of the organic components of the microorganism.

- Reactive Oxygen Species Diffusion:

  Highly reactive plasma species, such as OH*, have minimal penetration abilities, due to their highly reactive nature (Gaunt et al., 2006). However, some less reactive oxygen species, including the secondary reactive products of OH*-based lipid peroxidation, hydrogen peroxide, O_3, and NO, can actually diffuse through cell walls and react with internal cell structures, such as proteins and DNA (Far & Kogoma, 1991 and Gallagher et al., 2007).

- Charge Bombardment:

  Charge bombardment is another surface-based inactivation mechanism. During direct plasma exposure, high-energy electrons and reactive ions bombard a microorganism's cell membrane. These charged species have the potential to break the chemical bonds in membrane molecules, leading to the subsequent rupture of the plasma membrane. The ruptured membrane then allows other "toxic" plasma species, such as reactive oxygen species, to enter the cell and damage or destroy essential organelles or genetic material. (Gallagher et al., 2007)

- UV Irradiation:

  As previously discussed, ultra-violet irradiation can be an effective means of inactivating microorganisms. The literature on non-thermal plasma generated UV photons describes two methods of UV-based inactivation. The first inactivation mechanism is direct DNA/RNA damage from UV exposure. Lower wavelength photons, such as those in the UVC region (~250nm) are able to penetrate a cell's outer membrane and directly react with the otherwise non-exposed DNA and RNA (Lerouge et al., 2001). In contrast, longer wavelength UV photons, such as vacuum UV photons, have less penetration abilities and are typically absorbed in the microorganism's outer membrane (Lerouge et al., 2001).

  Although lacking the direct DNA damaging capacity of shorter wavelength UV photons, longer wavelength photons can still cause significant

damage to a cell. In a process referred to as intrinsic photo desorption, UV photons striking a cell's outer membrane cause atoms intrinsic to the cell to react with one another and form volatile compounds. In this manner, the outer layers of the microorganism are eroded in a process very similar to etching (Moisan et al., 2001).

- Electrostatic Disruption/Electroporation (Gaunt et al., 2006):

  The antimicrobial properties of pulsed-electric fields have been well documented and a corollary inactivation process has been proposed for NTP systems, which utilize pulsating electric fields (Moreau et al., 2008). A study subjecting bacteria to pulsed electric fields (Oshima et al., 1995) showed a correlation between electric field intensity and pore formation in the cellular membrane. This pore formation was shown to cause DNA leakage from the cell and DNA fragmentation. In other words, exposure to sufficient powerful-pulsed electric field can literally rip cells and their DNA to pieces.

- Synergistic Inactivation:

  A final point of interest regarding NTP inactivation is the potential synergistic effects of the various inactivation mechanisms. Non-thermal plasma has four methods of perforating the protective outer membrane of cells including etching, charge bombardment, intrinsic photodesorption, and electroporation. Degradation of the outer membrane of a cell likely makes them more susceptible to internal damage, such as DNA oxidation, from

chemical species which normally cannot penetrate the cells outer membrane, such as OH*, and other highly reactive radicle species. Degradation of the cell membrane may also allow longer wavelength UV photons, normally absorbed in the cell's outer membrane, to penetrate the membrane and react with the critical internal structures of the cell including DNA and RNA. Finally, the culmination of stress placed on the cell from the various inactivation methods may damage the cell beyond its capacity to regenerate. In this manner, no single inactivation modality was responsible for inactivating the cell, but each modes specific contribution helped lead to the eventual death of the cell. Figure 7 provides an illustration of the many inactivation mechanisms of NTP.

1.5.6 Differences Between Non-Thermal Plasma and ESP Technologies

For the purposes of the present discussion it is important to differentiate between ESP-based and non-thermal plasma based antimicrobial air treatment technologies. In the context of airborne pathogen control, the technologies can be differentiated based on their primary method of pathogen abatement and electrical characteristics. Specifically, although ESP systems often utilize corona discharge, which is a form of non-thermal plasma and can lead to indirect pathogen inactivation via indirect ionization and oxidation, the predominant mode of airborne pathogen/particulate removal in an ESP system is precipitation. Furthermore, ESP systems exclusively utilize DC voltages. In contrast, non-thermal plasma antimicrobial air treatment systems predominately rely upon direct inactivation of airborne microbes, through the generation of reactive species. Additionally, non-thermal plasma systems are not limited to DC voltages, but frequently utilize AC voltages.

2 Chapter 2: Laboratory Scale Experiments

2.1 Literature Review

While electrostatic precipitation and indirect ionization of airborne microbes is a relatively well-documented area of research (Mitchell & King 1993, Nishikawa & Nojima, 2003, and Hagbom et al., 2015), airborne microbe inactivation via direct plasma treatment is a relatively new concept. In fact, there are currently only a few articles pertaining to airborne bacteria decontamination with NTP, and even fewer studies investigating airborne virus inactivation. Specifically, at present there are only two articles that explicitly address the topic of airborne virus decontamination via direct NTP exposure.

2.1.1 Previous NTP Virus Inactivation Studies

In 2015 (Wu et al., 2015) investigated the influence of plasma power level and carrier gas composition on NTP's ability to inactivate airborne MS2 bacteriophage. Using a coaxial, wire-to-plate, dielectric barrier discharge reactor (Wu et al., 2015) tested 20, 24, and 28W power levels with ambient air, Ar-O_2 [2% vol/vol], and He-O_2 [2% vol/vol], using an air flow rate of 12.5 LPM. Based on the air flow rate and reactor dimensions, viral aerosols received 0.12s of direct plasma treatment. The study found that virus inactivation rates exhibited a positive linear relationship with increasing power levels, and that generally; air was a more efficient carrier gas for virus inactivation. The study reported a 95% reduction in viral aerosols using 28W of power and air as a carrier gas.

Based on the power level (28 W) and flow rate (12.5LPM), the specific energy input required to achieve a 95% (1.3 log) reduction of the viral aerosol was 134.4J/L air.

The second study investigating the feasibility of adapting direct NTP treatment to airborne viruses was performed by (Xia et al., 2019). This group utilized a tubular, packed-bed, dielectric barrier NTP reactor to inactivate aerosolized MS2 bacteriophage at different flow rates and applied voltages, using air as a carrier gas. This study demonstrated a 2.3-log reduction (inactivation below limit of detection) of aerosolized viruses at a flow rate of 170LPM and input power of 21W. However, the group reports a discharge power of 2.08W under these conditions. In this manner, (Xia et al., 2019) achieved complete virus inactivation with a specific input power of 7.41 J/L of air and a specific plasma discharge power of 0.734 J/L air. Based on the flow rate (170LPM) and reactor geometry, this study had a plasma treatment time of 0.25s. The untreated ozone concentration from the reactor exhaust, at 30kV applied power, was 2.08 ppm.

Though vague in their details regarding reactor design and operation, there are two additional studies that discuss airborne inactivation of viruses using NTP. The first study was performed by (Terrier et al., 2009) and the second by (Bergeron et al., 2011).

The study by (Terrier et al., 2009) investigated three types of air treatment methods and their ability to inactivate three types of aerosolized viruses. The three treatment methods included exposure to a classic UV lamp, exposure to cold oxygen plasma (COP) (generated externally from the treatment chamber), and a commercial device that combines UV and COP. The challenge organisms included respiratory syncytial virus (RSV), human parainfluenza virus type 3 (hPIV-3), and influenza A virus (H5N2). Using an air flow velocity of 0.9m/s (exposure chamber dimensions not

specified) and a treatment time of 0.44s, inactivation efficiencies of 99% or greater were demonstrated for all three viruses when using COP alone. Of note, the other two treatment methods were very similar. Unfortunately, the lack of information about the COP reactor, energy use, and flow rate make it almost impossible to compare the findings of (Terrier et al., 2009) to those of (Wu et al., 2015 and Xia et al., 2019). However, it should be noted that (Terrier et al., 2009) generated COP using deep UV light, as opposed to a high-voltage electrode configuration, and the "COP only" treatment was likely akin to indirect plasma treatment.

The second notable study was performed by (Bergeron et al., 2011). This study reportedly used a NTP reactor, which was initially a component of a larger air treatment system, to treat aerosolized H5N2 influenza virus. This group reports a 4-5 log reduction of virus after a single pass through the NTP reactor at a flow velocity of 1m/s. Although neither the exact flow rates, nor the reactor dimensions, were given, the air flow rate was at least 25LPM, as this was the specified sampling flow rate. Unfortunately, power input, plasma power, and voltage were also not discussed in this paper making direct comparison with other studies impossible.

2.1.2 Justification of Current Study (Laboratory Scale)

The small body of knowledge currently available for understanding NTP's efficacy as an antiviral air treatment technology provides many opportunities for further research. For instance, NTP appears to be effective against MS2 bacteriophage, but is it an effective means of controlling enveloped poultry viruses, such as influenza or Newcastle Disease virus (NDV)? How do input power, treatment time, and flow rate influence inactivation efficiency? And, do other factors, such as relative humidity and

reactor temperature influence NTP performance? The present study sought to answer these questions and fill holes in the current body of knowledge, as well as provide perspective on how future studies should focus their efforts in this field. These objectives were achieved by designing and fabricating two types of plasma reactors, a tubular, double-sided dielectric barrier, discharge reactor (DDB), and a coaxial, tubular, single-sided dielectric barrier reactor (SDB), and challenging them in a single-pass closed airflow system, with two types of enveloped viruses, Newcastle Disease virus (NDV), and/or a low pathogenic influenza A virus (PR8).

2.2 Materials & Methods

2.2.1 Cells and viruses

Madin-Darby canine kidney (MDCK) cells were maintained in Eagle's minimal essential medium (MEM) supplemented with 5% fetal bovine serum (FBS) and 50 μg/ml penicillin/streptomycin. African green monkey kidney Vero cells were maintained in MEM with 10% FBS and 50 μg/ml penicillin/streptomycin. A recombinant Newcastle disease virus expressing GFP reporter gene (rNDV-GFP) was obtained from Dr. Garcia-Sastre (Icahn School of Medicine at Mount Sinai) and grown in 10-day-old embryonated eggs. Influenza virus mouse-adapted laboratory strain A/PR8/34 was grown in 10-day-old embryonated chicken eggs.

2.2.2 Double-Sided Dielectric Barrier Discharge Reactor (DDB)

Figure 7 presents a flow diagram of the DDB reactor and Figure 8 presents the dimensions of the DDB reactor. This reactor consists of steel band (high voltage electrode) wrapped around the outside of a jacketed, tubular, quartz reactor, the center of

which was packed with steel wool (ground electrode). This configuration created a basic dielectric barrier plasma reactor geometry, with both the high voltage and ground electrodes having their own dielectric barriers (i.e. double-sided dielectric barrier).

In the DDB design, infectious aerosols could be pumped into the air inlet and enter the annular space between the two dielectric layers. The aerosols would then flow through the annular space and pass through the plasma discharge region (i.e. the region between the high voltage and ground electrodes). If the plasma was turned on, the aerosols would be subjected to plasma treatment, and if the plasma was left off, the aerosols would pass through the discharge region untreated (i.e. control tests). After passing through the plasma region, the aerosols were channeled through the air outlet, and subsequently exited the DDB reactor.

The aerosol treatment time corresponded to the aerosol residence time within with plasma discharge region. Therefore, the treatment time could be calculated using Equation 1.

$$\boldsymbol{T_t} = \frac{\boldsymbol{V_P}}{\boldsymbol{Q}} \qquad \text{Equation 1}$$

Here, T_t is the aerosol treatment time, or residence time within the plasma discharge region (seconds). V_P is the volume of the plasma region (L), determined by the volume of the annular space encompassed by the high voltage electrode, and Q is the volumetric flow rate of the aerosol through the reactor (L/s).

2.2.3 Experimental Setup (DDB Reactor)

Figure 9 presents a diagram of the experimental setup used to test the DDB reactor. For biosafety purposes, all experiments were conducted in a BSL II safety cabinet. A six jet Collision nebulizer (CH Technologies, USA) was used to generate viral aerosols from a liquid suspension of either NDV or PR8, by pumping filtered compressed air through the nebulizer at a volumetric flow rate of 6 LPM. This concentrated aerosol was then mixed with filtered dry air (6 LPM), from the ambient environment (40% RH and 25° C), for humidity control. The temperature and relative humidity of the combined aerosol were monitored by an inline thermohygrometer (TH-100, Vivarium Electronics, North Carolina), before entering the inlet of the DDB plasma reactor. The DDB plasma reactor was powered by a pulsed AC high-voltage generator (not pictured) (PG100-5D, AA Plasma LLC, Pennsylvania) and the electrical characteristics were monitored by an oscilloscope (Tektronix TDS 2012B). The pulsed power supply power consumption was monitored by a commercial wattmeter (P3 P4400 Kill A Watt Meter). During plasma treatment experiments, the pulsed AC power supply provided an input voltage of 18kV to the DDB reactor, at a frequency of 3500Hz, and 100% duty cycle. The average power input was 80W. During non-treatment experiments (control), the plasma reactor remained off. The temperature and relative humidity of aerosols exiting the plasma reactor were monitored by a second thermohygrometer. After passing the second thermohygrometer, aerosols would reach a bifurcation in the closed air stream. Two ball valves were used to control the path of aerosols. One valve directed aerosols across two gelatin membrane filters (25 mm diameter each) (SKC inc. Pennsylvania) positioned in parallel. The other valve directed aerosols around the gelatin filters. A second valve, located downstream of

the gelatin filters, was used to prevent the back-flow of air across the filters. Whether directed across the gelatin filters, or through the gel filter bypass route, both streams converged at a final HEPA filter, which proceeded a vacuum pump (Vac-U-Go Sampling Pump, SKC inc., Pennsylvania), used to help draw the aerosol, and dry air through the system. All system components were connected via ¼" rubber tubing.

2.2.4 Aerosol Treatment with DDB Reactor

The specific operation of this experimental setup is as follows. First, the nebulizer would be filled with a mixture of 1mL of either stock NDV solution (~10^7 GFU/mL) or 1 mL of stock PR8 solution (~10^8 PFU/mL) mixed with 20 mL of minimum essential media (MEM). Second, the ball valve upstream and down stream of the gelatin filters would be closed, and the valve leading to the filter bypass stream would be opened. In this manner air flow would be directed around the gelatin filters. Third, the vacuum pump would be turned on and adjusted to a negative pressure of 17.5 inHg. This would begin drawing dry filtered air through the system. Fourth, during treatment experiments the plasma would be turned on. However, during control experiments the plasma would be turned off. Fifth, compressed air pressure of 7.5psi would be applied to the nebulizer, producing a flow rate of 6LPM across the nebulizer. The combined positive air pressure produced by the air compressor/nebulizer and negative air pressure produced by the vacuum pump, would draw dry filtered air into the system at a rate of 6LPM and provide an overall system flow rate of 12.5 LPM. Based on the dimensions of the reactor, and the 12.5 LPM flow rate, the aerosol residence time within the plasma region (i.e. treatment time) was calculated to be 0.033 seconds, using Equation 1. In this manner, the system was allowed to run until steady state conditions were achieved (~10min), as determined

by a stabilization of the temperatures and relative humidity of the system. At steady-state conditions, the relative humidity was ~65%, the temperature of the aerosol at the inlet was ~27° and the temperature of the exhaust aerosols were 27° C and 35° C for control and treatment experiments respectively. A digital infrared laser thermometer (Masterforce Dual Laser Infrared Thermometer) was used to measure the temperature of the outer quartz glass surface of the plasma reactor.

After steady state conditions were achieved, the ball valves upstream and downstream of the gelatin filters would be opened, and the filter bypass valve would be closed. In this manner, the aerosol would flow across the gelatin filters. The gelatin filters were used to collect aerosolized viruses, and preserve viability prior to sampling. After 10 minutes of sampling, the valves upstream and downstream of the gelatin filters were closed, and the filter bypass valve opened, to prevent pressure issues. Then the system was turned off. The gelatin filters were then dissolved in 10 mL of MEM solution, and stored at -80C pending sample analysis. Each aerosol experiment (treated/untreated) was repeated in triplicate for both NDV and PR8.

Finally, aerosol experiments led to the accumulation of approximately 2mL of condensed solution within the plasma reactor. Samples of this condensate were taken after plasma treatment tests to determine if there were any viable viruses in the condensate.

2.2.5 Liquid-Based Inactivation with DDB Reactor

Preliminary experiments utilized a vortexing liquid impingement strategy (SKC BioSampler, SKC inc. Pennsylvania) for airborne virus sampling, as opposed to gelatin filters. The experimental setup and operation were the same as DDB aerosol testing with

gelatin filters, with the exception that the gelatin filters were replaced with the BioSampler. To rule out the possibility of liquid-based virus inactivation (i.e. viruses within the BioSampler collection media being inactivated by indirect NTP exposure), the BioSampler was filled with 20mL of MEM solution inoculated with NDV to a concentration of 10^4 GFU/mL. Next, the nebulizer was filled with 20mL of sterile MEM. The system was then operated in the same manner as aerosol DDB experiments (i.e. sampling flow rate of 12.5LPM). Replicate experiments were conducted, but with the addition of sodium thiosulfate to the BioSampler collection media. Single experiments were conducted with the following sodium thiosulfate concentrations: 0M, 0.2M, 0.4M, 0.8M, 1.0M, 1.2M, and 1.4M. pH changes of the BioSampler collection media were monitored with a digital pH meter (Hanna Instruments, HI98103).

2.2.6 Plasma Activated Filter Inactivation

The experiment began by filling 9 50mL vials with 10mL of MEM solution. Each of these vials was then inoculated with either NDV (inoculated concentration of 10^5 GFU/mL) or PR8 influenza (inoculated concentration of 10^6 PFU/mL). The first three vials of each virus received two gelatin filters each, that had been indirectly exposed to NTP in the same manner as during normal aerosol experiments, but using sterile MEM in the nebulizer (i.e. no viruses in the system when filters were exposed to NTP). The second three vials each received two gelatin filters that did not receive plasma exposure. Finally, the third group of vials received no additional input. Each group of vials was subsequently vortexed for ten seconds, and stored at -80C pending sample analysis. The pH of each solution was monitored with a digital pH meter (Hanna Instruments, HI98103).

2.2.7 Single-Sided Dielectric Barrier Discharge Reactor (SDB)

The narrow inlet/outlet apertures of the DDB reactor created a significant restriction to airflow, so experiments with flow rates greater than 12.5LPM were not possible without significant backpressure issues. Therefore, a new reactor (SDB) and experimental setup were developed to enable testing with greater flow rates. Figures 10 and 11 present a component diagram and dimensional diagram of the SDB reactor respectively. The SDB reactor utilized a cylindrical, coaxial, geometry consisting of a stainless steel pipe (ground electrode), encompassed by a quartz glass tube (dielectric barrier), around which was wrapped a copper band (high voltage electrode) inside of a stainless steel band. The geometry of the SDB reactor enabled testing with higher flow rates than that of the DDB reactor.

During operation, infectious aerosols would enter the downstream (bottom) aspect of the stainless steel pipe (ground electrode). Aerosols were prevented from flowing directly through the pipe by a rubber stopper positioned in the center of the steel pipe. Upon encountering the rubber stopper, aerosols would be redirected through the downstream (lower) air slit and enter the annular space between the steel pipe and the quartz glass tube. The infectious aerosols would then flow through the plasma discharge region, defined as the region of the annular space enclosed by the high voltage and ground electrode, where the aerosol would be treated (plasma on) or left untreated (plasma off/control). Upon exiting the plasma discharge region, aerosols were directed through an upstream (upper) air slit, where they could reenter the steel tube, effectively bypassing the rubber stopper, and subsequently are exhausted from the reactor.

2.2.8 Experimental Setup (SDB Reactor)

Figure 12 presents a diagram of the experimental setup used to test the SDB reactor. The experimental setup utilized for SDB experiments utilized many of the same components as the DDB setup. Aerosols were generated with a 6-jet Collision nebulizer, however air was fed to the nebulizer by means of a compressed air cylinder, as opposed to an air compressor. In contrast with the DDB system, a compressed air cylinder, as opposed to using ambient air, supplied dry air. The dry air stream and nebulized air stream were again mixed for humidity and flow rate control prior to entering the plasma reactor. The reactor was driven by the same pulsed AC power supply, which supplied a 15kV input voltage at 3500Hz and 100% duty cycle. The same digital oscilloscope also monitored the specific electrical characteristics of the plasma system. The same digital wattmeter was used to record the systems input power. Exhaust air from the plasma reactor was again split into two air streams. However in contrast with the DDB system, the air streams did not recombine. Instead, one air stream was impinged on a 10% bleach solution, while the other was drawn across two gelatin filters, positioned in parallel, similar to the DDB system. The sampling air stream (gel filter stream), was drawn across the gelatin filters using the same vacuum pump as before. The same infrared laser thermometer was used to measure the temperature of the quartz glass of the plasma reactor. In contrast with the DDB system, the SDB system components were connected via ½" rubber tubing, as opposed to the ¼" rubber tubing used for the DDB system. Ozone emissions were recorded using a digital gas analyzer (IMR 1400c Flue Gas Analyzer, Florida).

2.2.9 Aerosol Treatment with SDB Reactor

The specific operation of this experimental setup is as follows. First, the ball valve leading to the gelatin filters would be closed. Second, the nebulizer would be filled with a 20mL of MEM combined with 1mL of stock NDV solution (10^8 GFU/mL). Third, filtered dry air would be pumped into the system at a flow rate of 10, 15, or 20 LPM. Fourth, during treatment experiments the plasma reactor would be turned on and during control experiments the reactor would remain off. Fifth, compressed air would be fed to the nebulizer at a pressure of ~20psi, which produced a flow rate of 8LPM across the nebulizer. The combination of nebulized air and dry air would produce flow rates of 18, 23, and 28 LPM corresponding to the dry air flow rates of 10, 15, and 20LPM respectively. Using equation 2.2.1 the aerosol residence times for the flow rates 18, 23, and 28 LPM were $1.2x10^{-2}$, $9.5x10^{-3}$, and $7.7x10^{-3}$ seconds respectively. In this manner the system would be allowed to run until it reached steady-state conditions, as determined by the stabilization of the exhaust temperature and relative humidity. The specific temperature and RH depended on the specific flow rates utilized for the experiment. After steady-state conditions were achieved, the ball valve leading to the gelatin filters was opened and the vacuum pump turned on, such that a slipstream of 5LPM flowed across the coupled gelatin filters. At this flow rate, the negative pressure provided by the vacuum pump was not quantifiable using the pumps analog pressure gauge. The exhaust air from the plasma reactor was sampled for 5 minutes, at which time the vacuum pumped was turned off and the ball valve closed. The filters were then replaced with fresh gelatin filters, followed by another 5 minutes of sampling. The four gelatin filters provided 10 minutes of total sampling time, or 50 liters of sampled air. The filters were

immediately dissolved in 10mL of MEM (all four filters in the same 10mL), and subsequently stored at -80C pending sample analysis.

Six independent replicate trials were conducted for both the control experiments and plasma treatment experiments. Additionally, six independent samples were extracted from the nebulizer before nebulization, and after 20 minutes of nebulization to determine if viruses were being inactivated during the nebulization process.

2.2.10 Quantification of rNDV-GFP

Vero cells were seeded into 96-well plates and reached 90% confluence the next day. After PBS wash, cells were infected with 40 µl of serial 10-fold dilutions of rNDV-GFP virus in fresh media for 1 h at 37°C. After removing the virus, the Vero cells were incubated with fresh media (MEM with 10% FBS) for 24 h at 37°C. GFP-positive cells in each well were observed and counted under fluorescence microscope. Viral titer of rNDV-GFP was calculated with dilution factors and presented as GFP focus-forming unit per ml (GFU/ml).

2.2.11 Plaque assay of Influenza virus A/PR8

MDCK cells were seeded into six-well plates and reached 90% to 100% confluence the next day. After PBS wash, cells were infected with 0.5 ml of serial 10-fold dilutions of influenza virus A/PR8 in MEM for 1 h at 37°C. After the infection media was removed, the cells were incubated in 1% agar layer prepared with L-15 medium (15 mM HEPES, pH 7.5; nonessential amino acids; 0.75 g of NaHCO3 per liter; and 0.125% bovine serum albumin) in the presence of 2 µg/ml TPCK-treated trypsin, and cultured for 2-3 days at 37°C. After carefully removing the agar layer, plaques were stained with 1%

crystal violet and 20% methanol. Viral titer of A/PR8 was calculated with dilution factors and presented as plaque-forming unit per ml (PFU/ml).

2.2.12 Calculation of Airborne Virus Concentrations

Samples collected from aerosol experiments are analyzed in liquid form. However, the average concentration of airborne viruses can be calculated using Equation 2.

$$\boldsymbol{C_{Air,Downstream}} = \frac{\boldsymbol{C_{Liquid}} \times \boldsymbol{10\ mL}}{\boldsymbol{Q \times t}} \qquad \text{Equation 2}$$

Here, $C_{Air,Downstream}$ is the airborne virus concentration downstream of the NTP reactor, as PFU/L air or GFU/L air for PR8 and NDV respectively. C_{Liquid} is the virus concentration in the liquid sample with units PFU/mL or GFU/mL for PR8 and NDV respectively. 10 mL is the volume of liquid samples (i.e. volume of the MEM used to dissolve gel filters). Q is the volumetric flow rate of the air-sampling stream used in the experiment, and t is the sampling time. The air concentration can be converted to virus per cubic meter by multiplying C_{Air} by 1000.

Estimates of the airborne NDV concentrations upstream of the NTP reactor can be calculated in a similar manner to the downstream air concentrations using Equation 3.

$$\boldsymbol{C_{Air,Upstream}} = \frac{\boldsymbol{C_{Neb}\ x\ \dot{V}_{Neb}}}{(\boldsymbol{Q_{Dry}} + \boldsymbol{Q_{Neb}})} \qquad \text{Equation 3}$$

Here, $C_{Air,\ Upstream}$ is the theoretical air concentration of NDV upstream of the NTP reactor. C_{Neb} is the average NDV concentration in the nebulizer before nebulization is

initiated. V_{neb} is the rate of nebulization (0.4mL/min) and Q_{Dry} and Q_{Neb} are the volumetric air flow rates of dry air and nebulized air respectively.

2.2.13 Calculation of Condensation Losses

The volume of nebulized solution lost due to condensation and adherence to the inner walls of the experimental setup was calculated using (Equation 4).

$$V_{loss} = \frac{(Q_{dry}+Q_{Neb})(t_{run})(C_{Air,Upstream})-C_{Air,Downstream})}{C_{Neb}} \qquad \text{Equation 4}$$

Here V_{loss} is the volume of nebulized solution that did not make it through the experimental system (mL) and t_{run} is the total run time of the experiment (20 min).

2.2.14 Statistical Analysis

The experimental data, including treated/untreated aerosol samples, nebulizer samples, and relative humidity were analyzed using either a two-tailed Mann-Whitney U-test (alpha = 0.01) or a linear regression analysis.

2.3 Results

2.3.1 Aerosol Treatment with DDB Reactor

Figure 13 summarizes the data obtained from aerosol testing with the DDB reactor for PR8 influenza virus. The mean concentration of samples from control experiments (i.e. plasma off) was 4.9×10^3 PFU/mL. This liquid sample concentration correlates to air concentrations of 3.92×10^2 PFU/L air or 3.92×10^5 PFU/m^3 air, when using Equation 2. All plasma treatment experiments (plasma on) yielded samples with virus concentrations below the limit of detection (10 PFU/mL). Of note, a 2mL sample of

condensed PR8 solution in the plasma reactor from a plasma treatment experiment showed no detectable virus (data not shown). The reactor temperature varied over the length of the reactor, with peak temperatures occurring near the discharge region. Plasma region temperatures were typically around 68°C, but recorded as high as 80°C. The reactor temperature ~1" downstream of the discharge region was 58°C. Inlet aerosol temperatures were 25-27°C and exhaust temperatures were as high as 34°C. Based on the specific reactor geometry, and aerosol flow rate through the reactor (12.5LPM), the residence time of the aerosol in the plasma discharge region (i.e. direct plasma treatment time) can be calculated as 3.3×10^{-2}s.

Figure 14 summarizes the data obtained from aerosol testing with the DDB reactor for NDV. The mean concentration of samples from control experiments (i.e. plasma off) was 1.3×10^{2} GFU/mL. This liquid sample concentration correlates to air concentrations of 10 GFU/L air or 10^{3} PFU/m^{3} air, when using Equation 3. All plasma treatment experiments (plasma on) yielded samples with virus concentrations below the limit of detection (25 GFU/mL). Of note, a 2mL sample of condensed NDV solution in the plasma reactor from a plasma treatment experiment showed no detectable virus (data not shown).

2.3.2 Liquid-Based Inactivation with DDB Reactor

Figure 15 shows a plot of the change in NDV concentration in the BioSampler, before and after indirect exposure to NTP, at various concentrations of sodium thiosulfate, which was added to the BioSampler. All experiments demonstrated complete inactivation (below limit of detection, 25 GFU/mL) of aqueous NDV after indirect NTP exposure, regardless of the amount of sodium thiosulfate added.

2.3.3 Plasma Activated Filter Inactivation

The data for the liquid-based virus inactivation, via the addition of plasma exposed/unexposed filters, are summarized in Figures 2.3.4 and 2.3.5 for PR8 and NDV respectively.

Figure 16 shows mean PR8 concentrations of $4.3x10^5$, $3.5x10^5$, and $3.3x10^5$ PFU/mL for solutions mixed with two plasma-activated filters; two untreated filters, and no added filters respectively.

Figure 17 shows mean NDV concentrations of $6.4x10^3$, $5.6x10^3$, and $1.2x10^4$ PFU/mL for solutions mixed with two plasma-activated filters; two untreated filters, and no added filters respectively.

Of note, the pH of the solutions containing two plasma exposed filters, two untreated filters, and without the addition of filters (pure MEM), were 6.8, 6.9, and 7.2 respectively for both PR8 and NDV solutions.

2.3.4 Aerosol Treatment with SDB Reactor

This study utilized three different flow rates, at a fixed power input, to determine NTP's ability to inactivate aerosolized NDV. At each of the flow rates tested (18, 23, and 28 LPM) the viruses were inactivated below the limit of detection (25 GFU/mL) when exposed to NTP. In contrast, when the NTP reactor was turned off, the mean virus concentrations were $1.8x10^3$, $3.6x10^3$, and $4.9x10^3$ GFU/mL for the flow rates 18, 23, and 28 LPM respectively (Figure 18). Based on the sampling flow rate and sampling time, these liquid concentrations correspond to air concentrations of $3.6x10^2$, $7.2x10^2$, and $9.8x10^2$ GFU/L air for the flow rates 18, 23, and 28LPM respectively. The difference in virus concentration between treated and untreated samples was deemed statistically

significant with 99% confidence, when using the Mann-Whitney U-test with a p-value of 0.005 for all flow rates. This data is summarized graphically in figure 2.3.6. Using the power input for the pulsed AC power supply and the specific flow rate, the specific energy inputs for the plasma system were calculated as 267, 209, and 171 J/L for the flow rates 18, 23, and 28 LPM respectively.

Figure 19 presents the airborne NDV concentrations upstream and downstream of the SDB reactor. The upstream and downstream air concentrations were calculated using Equations 2 and 3 respectively. Additionally, Figure 19 includes downstream air concentrations corrected for possible low sampling efficiencies of the gelatin filters (discussed later).

Figure 19 shows a substantial difference between airborne virus concentrations upstream and downstream of the NTP reactor in the absence of NTP treatment. Upstream air concentrations were calculated to be 8.5×10^4 GFU/L air, 6.7×10^4 GFU/L air, and 5.5×10^4 GFU/L air for the flow rates 18, 23, and 28 LPM respectively. Downstream air concentrations, based on collected sample concentrations were 3.6×10^2 GFU/L air, 7.2×10^2 GFU/L air, and 9.8×10^2 GFU/L air for flow rates 18, 23, and 28 LPM respectively. Similarly, downstream air concentrations, corrected for possible low (1.5%) gel filter sampling efficiencies were 2.4×10^4 GFU/L air, 4.8×10^4 GFU/L air, and 6.5×10^4 GFU/L air for flow rates 18, 23, and 28 LPM respectively.

Figure 20 presents the same data as Figure 19, but as a scatter plot. From this perspective one can more clearly distinguish the convergence of the calculated upstream NDV concentration and the downstream air concentration, as flow rate increases. Note, that when the downstream NDV concentration is corrected for low collection efficiencies,

the lines converge around 25LPM. The difference between upstream and downstream NDV concentrations decreases from 2.37-log GFU/L air at 18LPM, to 1.97-log GFU/L air at 23 LPM, and finally to 1.75-log GFU/L air at 28LPM. Similarly, the difference between upstream air concentrations and corrected downstream air concentrations decreases from 0.55-log GFU/L air at 18LPM, to 0.14 log GFU/L air at 23 LPM, and finally to -0.07-log GFU/L air at 28LPM.

Figure 21 presents a scatter plot of the estimated mean air concentrations of NDV at different flow rates. Here, we see that upstream and downstream concentrations converge at lower flow rates (~45%), and diverge as RH increases. The differences between upstream and downstream NDV concentration at each RH value is the same as the difference found at the corresponding flow rate (e.g. difference at 62% RH is equal to difference at 18LPM equals 2.37-log GFU/L air).

The temperature of the aerosol leaving the NTP reactor was relatively stable for each of the flow rates tested. When the NTP reactor was turned on, exhaust temperatures were approximately 27 °C for the flow rates 23 and 28 LPM, and 29°C for 18LPM. When the NTP reactor was left off, exhaust aerosol temperatures were approximately 26 °C for all flow rates tested. The plasma reactor temperature (just downstream of the discharge region), was 74°C for the 18LPM flow rates and approximately 62°C for 23 and 28LPM flow rates when the plasma was turned on. When the plasma was turned off, reactor temperatures were around 21°C for all flow rates tested.

The relative humidity values were 62%, 51% and 44% for the flow rates 18LPM, 23LPM, and 28LPM respectively. The apparent relationship between the relative humidity and virus concentration is illustrated in Figure 22. A linear regression analysis

of the NDV concentration/humidity relationship revealed a very strong relationship (R^2 >0.99). Ozone concentrations were recorded at 80ppm at all flow rates during plasma testing.

The specific reactor geometry and volumetric air flow rates were used to calculate the aerosol residence times in the plasma discharge region and reactor. At 18, 23, and 28 LPM the aerosol residence times in the plasma discharge region were $1.2x10^{-2}$ s, $9.5x10^{-3}$ s, and $7.7x10^{-3}$ s respectively. Similarly the reactor residence times for 18, 23, and 28LPM were $9.6x10^{-2}$ s, $7.6x10^{-2}$ s, and $6.1x10^{-2}$ s respectively.

Based on the changes in airborne virus concentration upstream and downstream of the SDB reactor, the estimated volume of nebulized solution lost to condensation and adherence to the walls of the experimental system was calculated using Equation 4. The data for the estimated volume loss is presented in Table 1. Table 1 presents volume loss based on air concentrations calculated from sample concentrations, as well as air concentrations based on sample concentrations corrected for possible low sampling efficiencies (1.5%).

Samples were taken from the nebulizer before (0 min nebulization time) and after (20 min nebulization time) nebulization. The data are summarized in Figure 23. The mean NDV concentration prior to nebulization was $3.8x10^6$ GFU/mL. The mean NDV concentration after nebulization was $9.2x10^6$ GFU/mL. The difference in NDV concentration between nebulized and non-nebulized samples were determined to be insignificant with 99% confidence when applying the Mann-Whitney U-test. The p-value for the nebulization tests was 0.23.

2.4 Discussion

2.4.1 Airborne Virus Inactivation

The present study demonstrates that infectious aerosols containing enveloped poultry viruses can be completely inactivated (below the limit of detection) by single pass exposure to NTP at high flow rates. Limitations on safety hood ventilation rates prevented experiments with flow rates higher than those tested in these experiments. Therefore, the upper limit of NTP's inactivation potential was not determined. Manipulation of specific plasma energy input via voltage and/or frequency adjustment was not explored to avoid altering plasma chemistry, and duty cycle was maintained at 100%, as time between pulses at lower percentages created periods where aerosols could pass through the plasma region without plasma exposure.

This study's demonstration of a rapid inactivation of viral aerosols via direct NTP exposure is in agreement with findings from previous studies (Wu et al., 2015 & Xia et al., 2019). However, directly comparing these studies is difficult do to differences in reactor design and operating parameters. An incomplete, but important, comparison between the studies can be made on the basis of specific energy input. (Wu et al., 2015) demonstrated a 95% reduction in aerosolized bacteriophage with a specific energy input of approximately 134 J/L of air (based on their stated power input and sampling flow rate). The present study demonstrated complete inactivation of aerosolized virus with a specific energy input of 171 J/L. If inactivation efficiency is independent of virus species, then it is possible that the minimum specific energy input required for complete inactivation of aerosolized viruses, with a DBD reactor, is somewhere between 134 and 171 J/L of air. However, this conclusion is very unlikely due to the changes in plasma

chemistry that occur when power input parameters such as voltage, current, and frequency change. Comparisons between this study and the study conducted by (Xia et al., 2019) are even more difficult due to the fact that they used a packed-bed plasma reactor, as opposed to an unpacked DBD design. However, it should be noted that they report complete bacteriophage inactivation with as little as 7.41 J/L air of input power, indicating that it is likely that other plasma parameters, such as plasma chemistry, play an important role in inactivation efficiency.

Another important distinction between this study, and the previous studies mentioned, is the specific challenged microorganism. Newcastle Disease Virus and PR8-influenza are enveloped single-stranded RNA (ssRNA) viruses, whereas some bacteriophages, such as the MS2 phage used in previous studies, are non-enveloped ssRNA viruses. Previous studies suggest that plasma-based bacteriophage inactivation occurs as a result of plasma-induced RNA damage, surface protein damage, and cell fragmentation (Wu et al., 2015). Similarly, previous studies into the plasma-induced liquid-based inactivation of NDV and influenza demonstrated RNA damage and surface protein degradation, as well as viral envelope (lipid) degradation (Sakudo et al., 2013). The findings from the present study seem to support an airborne inactivation mechanism similar to that of bacteriophages used in previous studies, based on the rapid inactivation rates.

The possibility of airborne virus reductions via electrostatic precipitation was considered and determined to be highly unlikely. This conclusion is based on the fact that the pulsating AC voltage used to drive the plasma reactor would produce both positively

and negatively charged species resulting in rapid neutralization of charge carriers and reentrainment of precipitated charged species.

Of note, a small amount of precipitated moisture was observed in the DDB reactor, and to a much lesser extent in the SDB reactor, following aerosol testing. However, this precipitation was more likely the result of a temperature difference between the aerosol and walls of the plasma reactor than an electrostatic precipitation effect. Furthermore, samples of the condensation from plasma testing showed no detectable virus (PR8 or NDV). Therefore, any condensed virus was likely inactivated.

A final point of consideration, with respect to NTP reactor comparison, is the production of ozone. Ground level ozone is an important pollutant, linked to cardiovascular and respiratory disease in humans (Sheffield et al., 2011 & Goudarzi et al., 2015). Therefore, it is critical to monitor, and minimize, the emission of ozone by an NTP air treatment system. The present study recorded an ozone emission of 80 ppm for all flow rates tested. This finding was much higher than that of (Xia et al., 2019) who reported an ozone emission concentration of 2.08 ppm for a 30kV voltage input. This large discrepancy is likely due to the fact that the current study utilized a much higher specific energy input (171J/L) than (Xia et al., 2019) (7.41 J/L). However, it should be noted that previous findings have indicated that the addition of packing material, such as the borosilicate beads utilized by (Xia et al., 2019), generally increases the ozone production efficiency of an NTP reactor (Chen et al., 2008). Fortunately, ozone production can easily be mitigated by the addition of an O_3 adsorbent media, such as activated carbon, downstream of the NTP reactor. (Xia et al., 2019) was able to return O_3

emissions from their reactor to near background levels with the addition of an O_3 adsorbent with minimal pressure drop.

2.4.2 Liquid-Based Inactivation with DDB Reactor

Though not explored with sufficient depth to warrant statistical analysis, the preliminary findings of liquid-based virus inactivation via indirect NTP exposure warrant discussion. To reiterate, preliminary experiments utilized an SKC BioSampler for airborne virus sampling, as opposed to gelatin filters. However, after only 3-5 minutes of sampling, during plasma treatment experiments, the MEM solution in the BioSampler would change from it's characteristic red color, to a very light pink coloration (Figure 24), indicating some type of chemical change within the media. Further investigation revealed that MEM contains a pH indicator (Phenol Red Indicator), which was likely responsible for the color change. This rapid and dramatic change led to a brief investigation of possible liquid-based virus inactivation, in which the BioSampler was inoculated with NDV and indirectly exposed to NTP. Samples taken from the BioSampler, after 20min of indirect NTP exposure, showed complete virus inactivation (4-log reduction) (Figure 15). These findings indicated that aerosol experiments would not be able to distinguish between liquid-based and air-based virus inactivation effects (i.e. aerosolized viruses may be inactivated in the air, but are certainly inactivated when collected in solution).

A review of literature indicated that the liquid-based inactivation observations were not unique. (Wang et al., 2016) demonstrated complete inactivation of liquid-based NDV and influenza with only 2 min of indirect NTP exposure (plasma jet). (Aboubakr et al., 2015) demonstrated a 5.5-log reduction of feline calicivirus after only 1.5 minutes of

indirect NTP exposure. Finally, (Zimmermann et al., 2011) demonstrated a 6-log reduction of a solution containing adenovirus after 4 min of NTP treatment. The findings of these studies were not only consistent with the liquid-based inactivation results obtained in the present study, but indicated that simply reducing the sampling time to a few minutes would not be sufficient to ensure virus survival.

However, additional attempts were made to improve the collection mediums resistance to the indirect inactivation effects of NTP. First, a pH analysis demonstrated that 20 minutes of indirect NTP exposure decreased the pH of MEM (pH = 7.2) to a pH of 5.9. However, this mild decrease in pH was not determined to be a significant contributor to virus inactivation, because previous studies have indicated that influenza, considered here as a surrogate for NDV, can survive in liquid solutions with pH between 5 and 7 for 18 to >24 hours respectively (Shahid et al., 2009). Furthermore, in their indirect plasma treatment experiments (Wang et al., 2016) reports that a slight decrease in pH (6.5) had minimal impact on virus inactivation. Interestingly, (Uhm et al., 2009) found synergistic effect between low pH (4) and high ozone concentrations (>20mg/L) when inactivation aqueous influenza. However, this pH was far lower than any measured in the present study. Therefore, it was deemed much more likely that inactivation was the result of the accumulation of long-lived reactive oxygen species (ROS), specifically ozone, which was recorded at concentrations of 80ppm (157.06mg/m^3) during plasma experiments.

In an attempt to prevent virus inactivation from the accumulation of ROS/RNS in solution, sodium thiosulfate was added to the collection media. Sodium thiosulfate is a known scavenger of reactive oxidizing species and has been shown to be an effective

means of neutralizing long-lived reactive species, produced by NTP, in solution (Aboubakr et al., 2015).

Unfortunately, the present study observed the same rapid MEM color change and complete virus inactivation in solutions containing up to a 1.4M concentration of sodium thiosulfate. The reason sodium thiosulfate failed to preserve virus viability in solution in the present study, as opposed to that of (Aboubakr et al., 2015) is as follows. First, the present study likely utilized a much higher plasma power level (80W input power) than that used by (Aboubakr et al., 2015) (2.5W plasma discharge power). Second, the present study utilized air as a feed gas, which has a much higher N_2 and O_2 content than the Ar + 1% O_2 feed gas utilized by (Aboubakr et al., 2015). The combination of these parameters likely led to the present study generating far more ROS/RNS than (Abooubakr et al., 2015).

Finally, it should be mentioned that (Xia et al., 2019) was able to successfully collect viable viruses, with a liquid impingement device, from an air stream that had received plasma treatment (i.e. they prevented the liquid-based inactivation observed in this study). The success of (Xia et al., 2019) is likely due to the combination of several factors. First, they utilized a much lower sampling flow rate (1LPM) than that used in this study (12.5LPM). A lower sampling flow rate, in general, would mean fewer active species absorbed in solution. Second, as previously described, their specific energy input was lower than that used here, which may have led to a decrease in the amount of ROS/RNS produced. This hypothesis is partially supported by their low ozone emissions (2.08ppm) compared to that of the present study (80ppm). Finally, (Xia et al., 2019)

added 50mM of anhydrous sodium sulfite to their collection media, which was sufficient to control “ozone” accumulation in their impingers.

The present study did not attempt to circumvent the issue of active species accumulation in the BioSampler by decreasing the sampling flow rate because, as per the manufacturer’s instructions, a minimum pressure drop of ~17inHg must be maintained across the BioSampler to produce the characteristic vortexing motion of the collection media responsible for particle capture. Previous studies have shown that the BioSampler loses the vortexing motion at lower flow rates, which can lead to a sharp decrease in collection efficiency (Hogan et al., 2005). Finally, the sampling time of the BioSampler was not decreased from 20min, as preliminary experiments with lower sampling times were not able to collect adequate quantities of virus in sampling times shorter than the 3-5min, required to create a drastic color change in the BioSampler.

It should be noted that (Xia et al., 2019) did not explore pH changes in their collection media. However, they were able to control liquid-based inactivation effects with an ROS scavenger. This finding lends further evidence to the fact that mild to moderate pH changes do not substantially contribute to liquid-based virus concentration. This also supports the hypothesis that liquid-based inactivation is a result of ROS/RNS accumulation in solution.

2.4.3 Plasma Activated Filter Inactivation

In an attempt to collect viable airborne viruses, while circumventing the issue of liquid-based inactivation, gelatin filters were utilized in place of the SKC BioSampler. According to the manufacturers, gelatin filters contain a high moisture content, which prevents desiccation stress and preserves microbial viability. Furthermore, the filter’s

porous nature would presumably allow ROS species to pass through the filter, therefore preventing the issue of ROS accumulation and indirect virus inactivation during sampling. However, to extract viruses from the filters, the filters must be dissolved in solution. Preliminary plasma exposure experiments using gelatin filters showed that when the plasma exposed filters were dissolved in MEM for sample collection, the MEM turned a similar light yellow color to the MEM used in BioSampler experiments (Figure 25) indicating a pH change. This coloration was much different than the mild color change that occurred when dissolving non-NTP exposed gelatin filters (Figure 26).

It is known that the dissolution of gelatin filters can mildly decrease the pH of the solvent (Jaschhof, 1992). When two non plasma-exposed filters were dissolved in MEM, the pH dropped from 7.2 to 6.9. Similarly, when two plasma-exposed filters were dissolved in MEM, the pH dropped from 7.2 to 6.8. While it is possible that the more dramatic color change observed in MEM containing plasma-exposed filters was the result of the slightly lower pH, this conclusion seemed unlikely. This apprehension was due to the fact that the solution containing two plasma-exposed filters (Figure 25) had almost identical coloration to the MEM that received substantial indirect NTP exposure (Figure 24), while their pHs were markedly different, 6.8 and 5.9 respectively. Therefore, it was hypothesized that the color change observed in MEM was not merely a result of pH change, but also the result of dissolved ROS. It was believed that the high moisture content of the filters allowed ROS to dissolve in the filter, and subsequently be released into solution when the filter was dissolved. This of course raised concerns for the same liquid-based virus inactivation observed in BioSampler experiments.

Interestingly, the liquid-based inactivation experiments yielded very different results depending on the virus used. Specifically, experiments using PR8 showed the highest virus concentrations for solutions treated with dissolved, plasma-exposed, filters, with the lowest virus concentrations occurring in solutions that did not receive any filters, activated or otherwise (Figure 16). However, the opposite occurred with NDV. Solutions with NDV had lower virus concentrations when plasma-exposed filters were dissolved, when compared with the control solution (i.e. not filters added) (Figure 17). However, it is interesting to note that the lowest mean NDV concentrations occurred when untreated filters were dissolved in solution.

The findings from the plasma activated filter inactivation experiments seem to indicate that filters exposed to NTP treatment do not lead to liquid-based virus inactivation when dissolved in virus containing solutions. This would seem to imply that ROS do not accumulate in, or at least are not released from, gelatin filters that are indirectly exposed to NTP. However, the question regarding the difference in MEM color change between solutions receiving plasma-exposed versus non plasma-exposed filters remains unanswered. It is possible that the very minimal pH difference between solutions receiving these filters is responsible for the color change observed. Future studies may wish to test this by adding acid to MEM to achieve pHs of 6.9 and 6.8 and observing the difference in coloration.

Finally, the somewhat dramatic differences between PR8 and NDV's response to filter dissolution must be addressed. As previously mentioned, (Wang et al., 2016) concluded that a pH drop from 8.5 to 6.5 was not a significant contributor to influenza or NDV inactivation. The present study observed a much less dramatic drop (7.2 to 6.8),

which would indicate that the slight virus reduction (~1-log) observed in NDV solutions that received gelatin filters was not, or only mildly, the result of the pH change. Of course, it should be noted that only three replicate experiments were conducted for these experiments. Therefore, differences between treatment groups may simply be the result of statistical error. The important point is that NDV concentration differences between samples receiving activated and non-activated gelatin filters were not different, so the comparison between control and NTP exposed aerosol experiments is not affected by liquid-based inactivation as a result of plasma activated filters.

2.4.4 Surface Inactivation

Surface-based inactivation refers to the inactivation of viruses collected on, or within (depth filtration), the gelatin membrane filters. Possible modes of surface inactivation include, thermal inactivation, desiccation stress (RH-inactivation), and exposure to long-lived plasma species. However, thermal inactivation and desiccation stress will be discussed in subsequent sections. The current section will restrict the conversation to possible surface-based inactivation effects due to indirect NTP exposure.

As previously discussed (section 1.5), NTP produces a variety of long-lived plasma species, which can exist for extended periods of time outside of the plasma region. The present study monitored the air concentrations of two long-lived plasma species, ozone and NO_x. NO_x was not detectable during plasma experiments, however ozone was measured at sufficiently high concentrations (80ppm or 157.06mg/m^3) to warrant concern for surface-based inactivation.

The use of ozone as an antimicrobial agent is well documented in the scientific literature, but information is predominately focused on dissolved ozone and liquid-based

inactivation (Lazarova et al., 1998; Shin & Sobsey, 2003; Uhm et al., 2009). However, a study performed by (Tseng & Li, 2008) did explore the antiviral effects of ozone on surfaces. This study is a particularly relevant source of information, because it plated a variety of viruses (bacteriophages) on a gelatin surface and exposed the viruses to gaseous ozone at moderate humidity levels (55%) and time durations (<1 hour) similar to those used in the present study. (Tseng & Li, 2008) found that all tested viruses required ozone doses of 20-112 min(mg/m^3) to achieve 90% inactivation and 47-223 min(mg/m^3) to achieve 99% inactivation. Based on the ozone concentrations (80ppm or 157.06mg/m^3) and sampling times (5 min for the SDB reactor and 10min for the DDB reactor), the theoretical ozone dosages were 785.3 min(mg/m^3) and 1570.6 min(mg/m^3) for the SDB and DDB respectively. According to the findings of (Tseng & Li, 2008), these dosages were more than sufficient to cause significant inactivation of viruses collected on the gelatin filter surfaces.

However, there are a few important details that may challenge the idea of complete inactivation of collected viruses as a result of ozone exposure. First, the viruses used in the present study were enveloped viruses, as opposed to the non-enveloped bacteriophages used by (Tseng & Li, 2008). Therefore, it is likely that the specific inactivation mechanism, and therefore dosage-inactivation relationship, is different for the viruses used in the present study. Second, the gelatin membrane filters used in the present study rely on depth filtration as a means of virus collection. Therefore, it is possible that many viruses collected had some degree of shelter from gaseous ozone within the filter media. Finally, viruses in the present study were generated and sampled in an ongoing manner. Therefore, viruses collected at the beginning of the experiment

and viruses collected towards the end of the sampling process did not receive equal ozone dosages. However, due to the high ozone concentrations generated by the SDB and DDB reactors, only viruses collected in the final 18 seconds of sampling would receive ozone dosages lower than the minimum dose (47 min(mg/m^3)) required to cause 99% inactivation, reported by (Tseng & Li, 2008). Therefore, despite possible added protection from the viral envelope or gelatin filter media, it seems likely that viruses collected on the gelatin filters were inactivated by high ozone dosages.

2.4.5 Thermal Inactivation Effects

During aerosol testing the temperature of the plasma reactor and the temperature of the air exhausted from the plasma reactor were closely monitored. Both the DDB and SDB reactors displayed non-uniform temperature distributions over the length of the reactor. Specifically, the DDB reactor showed peak temperatures near the plasma discharge region, typically around 68°C, but recorded as high as 80°C and exhaust air temperatures of 34°C. The SDB showed peak temperatures as high as 74°C for 18 LPM flow rates and 62°C for 23 LPM and 28 LPM flow rates. Similarly exhaust aerosol temperatures from the SDB reactor were 29°C for 18LPM flow rates and 27°C for 23 and 28 LPM flow rates. When the NTP was not initiated (control experiments), both reactor and aerosol temperatures remained at, or slightly below, room temperature (25°C) for both reactors.

Viruses, such as NDV and influenza, are well known to be highly susceptible to thermal inactivation. For example, (Thomas et al., 2008) found that NDV and influenza viruses in chicken meat were completely inactivated in the 34s it took for the heating unit to increase from 25C to 73.9C. They also showed D-values (time required to reduce virus

concentration by 1-log) on the order of 200 s for temperatures of 57°C, and 20-30s for temperatures of 61°C for both NDV and influenza. Similarly, in an experiment exploring thermal inactivation of NDV and influenza in various egg products, researchers found D-values less than 20 seconds, at 63°C, for two strains of influenza and three strains of NDV, in a liquid egg white product (Swayne & Beck, 2004). Finally, an investigation into the thermal inactivation rates of avian influenza and NDV in fat free egg product found Z-values (increase in temperature required to cause a 1-log reduction in D-value), of 4.4°C and 0.4°C for two different strains of influenza (H5N2 and H7N2 respectively), and 4.7°C and 1°C for two different strains of NDV (vNDV and INDV respectively) (Chmielewski et al., 2011).

The data and Z-values obtained for virus inactivation in egg products by (Chmielewski et al., 2011) can be extrapolated to get an estimation of D-values at higher or lower temperatures using Equation 5.

$$\boldsymbol{Z} = \frac{T_2 - T_1}{logD_{T1} - logD_{T2}} \qquad \text{Equation 5}$$

Here, Z is the z-value of a given microorganism and D_{T1} and D_{T2} are D-values of that microorganism, corresponding to the temperatures T_1 and T_2 respectively.

Table 2 presents a portion of the inactivation rate data (D-values) described by (Chmielewski et al., 2011), as well as the extrapolated data for temperatures corresponding to the NTP exhaust air and NTP reactors during plasma treatment experiments. However, it should be noted that both the microbial species and the medium supporting the microorganisms impact the inactivation rates (Swayne & Beck, 2004).

Since the present study utilized air as the supporting medium, as opposed to egg products, and utilized different strains of influenza and NDV than those used by (Chmielewski et al., 2011), the extrapolated data presented in Table 2 should be considered a rough estimate of the D-values for the microorganisms used in the present study.

If one assumes that the strains of influenza and NDV used by Chmielewski et al. (2011) are good surrogates for the strains of influenza and NDV used in the present study, and that thermal inactivation kinetics for viruses in fat free egg products and air are reasonably similar, then some important conclusions can be reached regarding the role of thermal inactivation during NTP aerosol treatment experiments. First, the D-values for all viruses exposed to temperatures of 34°C or lower appear to be sufficiently high, such that viruses were not thermally inactivated as a result of exposure to the NTP exhaust gas during sampling. Second, the D-values at 62°C vary too greatly between different strains of NDV (vNDV and INDV) to conclude whether or not rapid exposure to peak temperatures within the SDB reactor at flow rates 23 LPM and 28 LPM result in thermal inactivation of rNDV. Third, when operating the SDB reactor at a flow rate of 18LPM, the aerosol residence time in the plasma region is 1.2×10^{-2} s, and the peak temperature at this flow rate is 74°C. Comparing this residence time to the vNDV and INDV D-values at 74°C (6.74×10^{-2} and 3.18×10^{-17}) in Table 2 indicates that thermal inactivation may have played a meaningful role in airborne NDV inactivation in the SDB reactor at 18LPM. Finally, the DDB reactor experienced a greater degree of temperature fluctuation than the SDB reactor, with temperatures typically around 68°C, but occasionally, rising as high as 80°C for brief periods of time. At these temperatures, and aerosol residence times in the peak-temperature region (NTP discharge region) of the plasma reactor of 3.3×10^{-2}s, it is

quite likely that thermal inactivation played a meaningful role in airborne virus inactivation of both NDV and PR8. Therefore, based on the data presented in Table 2 it appears that thermal effects may have played a role in airborne virus inactivation, considering that air concentrations were on the order of 2-log per liter of air. Furthermore, thermal effects likely had a greater influence at lower flow rates (i.e. 18LPM and 12.5LPM).

2.4.6 Impacts of Relative Humidity on Viral Aerosol

Figures 19 and 20 show that as air flow rate increases the downstream (relative to NTP reactor) air concentration of NDV increases, despite decreasing upstream air concentrations. Furthermore, these two figures show that as air flow rate increases, the difference between upstream and downstream air concentrations at a given flow rate decreases (i.e. the upstream and downstream values converge).

The trend of decreasing upstream air concentrations with increasing flow rate is not surprising, because air flow rates were increased by increasing the rate of dry air input, while holding the rate of nebulizer air input constant. In this manner, increasing the total aerosol flow rate would lead to a dilution of the viral aerosols. However, the large discrepancy between the upstream air concentrations and the corresponding downstream air concentrations required a more in depth analysis. A brief literature review revealed that the discrepancies might be due to a very low sampling efficiency by the gelatin filters. Specifically, (Li et al, 2018) reported that gelatin membrane filters had a collection efficiency of only 1.5% when sampling aerosolized influenza virus, which is much lower than previous reports of >93% collection efficiency (Burton et al., 2006), or the virus sampling efficiencies reported by the suppliers (>99%) (Sartorius, 2019). To

determine the potential impact of a poor sampling efficiency (1.5%), the data was corrected to account for the remaining 98.5%, and plotted with upstream NDV concentrations and the measured downstream air concentrations (Figure 19 and 20). Interestingly, while the corrected data substantially closed the gap between upstream and downstream air concentrations at a given flow rate, the general trend of converging air concentrations with increasing flow rates remained. This indicated that at lower flow rates (<~25LPM), the discrepancies between upstream and downstream concentrations could not be accounted for by poor sampling efficiency.

The continued discrepancies between upstream and downstream air concentrations led to the hypothesis that the decreasing air flow rates led to increasing relative humidity (RH) levels of the aerosol, and that increasing RH levels were responsible for virus losses within the system when NTP was turned off. To explore this hypothesis, the mean NDV concentration (GFU/mL) collected at each flow rate was plotted against the corresponding mean RH value at each flow rate (Figure 21). A linear regression analysis revealed a strong ($R^2 = 0.999$) negative correlation between downstream NDV concentrations and RH. Calculated airborne NDV concentrations were also plotted against RH, in the same manner that airborne NDV concentrations were plotted against air flow rates (Figure 22). The plot shows that as RH increases, downstream air concentrations diverge from their corresponding upstream air concentrations. Therefore, it was deemed likely that virus losses within the system were the result of RH changes.

There are three possible explanations for the virus losses within the experimental system. First, a decrease in the system's RH led to increased survival rates, and perhaps improved preservation of infectivity, of aerosolized NDV reaching the gelatin filters.

Second, a decrease in RH led to a decrease in virus loss due to adhesion to the walls of the system. Third, a combination of the both effects led to the present observations.

Explanation 1: RH Impacts Virus Viability

Relative humidity (RH) is known to be an important factor governing the viability of airborne viruses, however the specific mechanism by which RH influences airborne viruses is still unclear (Yang and Marr, 2012). In general, it is believed that viruses with higher lipid content (i.e. enveloped viruses) survive better in lower humidity environments, while viruses with lower lipid content (i.e. non enveloped viruses), survive better in higher humidity environments (Sobsey & Meschke, 2003). While there are exceptions to this rule (Songer, 1967), the trend appears to be true for influenza (Lowen et al., 2007). However, previous studies investigating the effects of RH on the viability of NDV are inconclusive. For example, (Hugh-Jones et al., 1973) found that NDV survivability was greater at higher humidities (70-80%), than moderate humidities (~50%). However, (Songer, 1967) found that NDV survived best at 10% RH, but also survived better at 90% RH than 35% RH. (Boyd & Hanson, 1958) also observed similar NDV survival rates at low (0% and 9-15%) and high (100%) relative humidities for NDV stored on paper discs at a fixed temperature. However, they did not explore intermediate humidities. Therefore, although the data are not conclusive, it appears that NDV has higher survivability at extreme humidity levels (<35% or >70%), but poor survivability at intermediate RH levels (35-70%).

The observation that sampled virus concentrations increased with decreasing RH (Figure 21) is consistent with the general rule that enveloped viruses survive better in low

RH conditions (Sobsey & Meschke, 2003). However, since the present study only explored moderate RH conditions (35-70%) the findings from previous studies (Hugh-Jones et al., 1973, Songer, 1967, & Boyd & Hanson, 1958), which indicated that NDV survivability favors extreme RH conditions (i.e. <35% or >70%), were not verified. Furthermore, since virus quantification was only performed with an infectivity assay, the relationship between RH and infectivity is only speculation. If the present study had also utilized a PCR-based quantification method, which does not require virus viability, one could compare the virus concentrations measured by PCR and infectivity analysis (plaque assay) to determine a relationship between RH and preservation of virus viability. Specifically, if virus concentrations at two different RH conditions were the same by PCR analysis, but differed when measured with an infectivity assay, one might conclude that RH had an impact on virus survivability.

The specific mechanisms by which RH impacts airborne virus survivability is still uncertain, however several interesting hypothesis have been proposed. First, (Donaldson & Ferris, 1976) proposed that the rapid evaporation of water from aerosol particles, under low RH conditions, could result in viruses losing structural water molecules resulting in virus inactivation. However, one might expect that inactivation effects due to the rapid loss or aggregation of water molecules would be less drastic for enveloped viruses than non-enveloped viruses, due to the hydrophobic nature of enveloped viruses outer membrane. This hypothesis is supported by (Benbough, 1971) who found that gradual humidification, as opposed to abrupt humidification, led to increased recovery rates of non-enveloped viruses, but had little impact on enveloped viruses. (Yang & Marr, 2012) have speculated that dissolved salts in viral aerosols may play an important role in virus

inactivation during humidity fluctuations. Specifically, they report that evaporation and humidification of aerosols will either concentrate or dilute the dissolved salts in an aerosol, which leads to important changes in the salinity of the aerosol. Therefore, under conditions of very high RH (~100%), salts may be sufficiently dilute, such that virus viability is preserved or unaffected. However, under moderate RH conditions (~50%), a significant portion of the aerosol particle's water evaporates, which leads to a concentration of the dissolved salts, which may be toxic to the virus. Finally, under conditions of low RH (<50%), the dissolved salts crystallize and are no longer toxic to the virus. It should be noted that this hypothesis fits well with the observation that NDV has higher survival rates at RH extremes (<35% and >70%), and low survival rates in the moderate RH ranges (35-70%). Finally, (Yang & Marr, 2012) also hypothesized that changes in RH could lead to pH changes in the viral aerosol, which could affect virus viability. Specifically, they hypothesize that evaporation would lead to the concentration of free H^+ ions, leading to a reduction in the pH of the aerosol. This reduced pH would lead to conformational changes in viral glycoproteins, which could potentially diminish infectivity. However, more data is needed to verify this mechanism.

Explanation 2: RH Impacts Losses due to Surface Adhesion/Condensation

Humidity induced virus inactivation, while an interesting avenue of research, is not the only mechanism by which RH can affect airborne virus concentrations. Within a closed airflow system, high levels of humidity can lead to precipitation of airborne particles, such as viruses, through adhesion to the walls of the system and condensation. In this manner, a significant amount of the aerosolized viruses can be lost before reaching

the sampling site, leading to discrepancies in airborne virus concentrations throughout the length of the experimental apparatus. This phenomenon was observed in the present study, as small droplets of solution were visualized in the NTP reactor and at various points in the connective rubber tubing of the system. Of note, a sample of the condensed solution (<1mL) was taken from both the DDB and SDB reactors, following an NTP treatment experiment, and analyzed for viable viruses. No viable viruses were detected in either sample.

Due to the thin layers and widely distributed nature of the condensed aerosol, it was not feasible to collect all of the precipitated solution within the system and measure the total volume lost between the nebulizer and gelatin filters. However, using Equation 4 total volume losses were estimated, based on the assumption that condensation and adhesion losses were the only factor contributing to decreased NDV concentrations throughout the length of the system during control experiments (NTP off). The data presented in Table 1 indicates that condensation losses, not corrected for low sampling efficiencies, are almost equal to the total volume of solution nebulized in the experiments (8mL). When correcting for the possible low sampling efficiency of the gel filters, losses are still as high as 5.74mL. Physical observation of the moisture content in the system (connective tubing and SDB reactor) indicated that the estimated condensation losses were likely too large. However, it should be reiterated that it was not feasible to collect all of the condensed moisture and obtain a definitive measurement.

The condensation losses observed in the present study are consistent with other studies that utilized closed airflow systems to transport viral aerosols. For example, (Terrier et al., 2009) sampled airborne virus concentrations upstream and downstream of

a UV-based cold oxygen plasma device (COP) in a closed airflow system and found that even when the COP device was turned off, airborne concentrations of influenza decreased by 1.7-log TCID50/mL between the upstream and downstream sampling ports. (Terrier et al., 2009) attributed these losses to rapid particle aggregation and settling in the space between sampling sites. They also noted that the losses were likely explained by the high RH conditions (they did not add dry air) in their experiments. Of note, (Terrier et al., 2009) also conducted experiments with respiratory syncytial virus (RSV) and human parainfluenza virus type 3 (hPIV-3), and while hPIV-3 also exhibited substantial losses between sampling sites, RSV did not. (Xia et al., 2019) also recorded a reduction (0.35-log) in airborne virus concentrations between sampling ports located upstream and downstream of their air treatment device when the device was turned off. They attributed this loss to a filtration effect caused by a packing material in their air treatment device. However, it is interesting to note that the packing material consisted of 0.6cm diameter borosilicate beads, which despite representing a source of resistance to air flow, could hardly be believed to coalesce in a configuration capable of filtering particles as small as viruses (nanometer scale) in any manner other than direct impaction and adhesion.

It should be noted that (Terrier et al., 2009) did not dehumidify air leaving the nebulizer, while (Xia et al., 2019) did mix their aerosol with a dry air stream, and reports an RH of ~30% for 170LPM testing. It is likely that (Xia et al., 2019) measured significantly lower virus loss upstream and downstream of their reactor, when compared with (Terrier et al., 2009), because (Xia et al., 2019) utilized a lower humidity air stream. However, it is not clear if the virus losses experience by both parties was strictly due to

condensation effects, as neither group quantified the condensed moisture within their system.

Explanation 3: Combination of Viability and Adhesion Losses

The fact that condensation was visualized within the experimental system indicates that condensation losses are a significant factor contributing to discrepancies in upstream and downstream aerosol concentrations. However, even when downstream air concentrations were corrected for possible low sampling efficiencies the estimated condensation losses, necessary to completely account for NDV concentration discrepancies, appeared to be far greater than the visibly inspected moisture levels within the system. Therefore, it is possible that RH levels had an impact on virus viability, and contributed to discrepancies in air concentrations.

2.4.7 Nebulizer-Induced Virus Inactivation

The Collison 6-jet nebulizer uses a combination of shearing and impaction forces on the virus solution (MEM) to generate aerosols and separate small aerosol particles from larger aerosol particles. The fact that liquid-based viruses were continuously subjected to these forces throughout the duration of the experiment raised concerns for possible liquid-based virus inactivation within the nebulizer. Specifically, if viruses were continuously being inactivated within the nebulizer, then the viable virus concentration within the nebulizer would decrease throughout the duration of the experiment. This would lead to inconsistent aerosol NDV concentrations throughout the duration of the experiment. Therefore, samples of the nebulizer solution were taken before and after experiments (20 min duration) to see if nebulization impacted the concentration of viable

viruses. Figure 23 summarizes the data for these experiments and shows that 20minutes of continuous nebulization does not have a significant effect (99% confidence) on nebulizer virus concentration. This finding is very consistent with other studies utilizing the same nebulizer to aerosolize viruses. For instance, (Ge et al., 2014) found that 6 hours of constant nebulization at 10 psi, did not significantly decrease nebulizer virus concentrations, which included influenza. A similar finding was reported by (Appert et al., 2012), who utilized the same nebulizer solutions as (Ge et al., 2014), but with a higher applied pressure (20psi) and shorter nebulization time (15min). Finally, (Ibrahim et al., 2015) reports that after 60 min of continuous nebulization, the influenza concentration in a Collison nebulizer was unchanged. Therefore, the findings in the present study, which indicate that 20 minutes of nebulization did not cause a reduction in liquid virus concentration, are consistent with findings in the literature.

2.5 Conclusions from Laboratory Experiments

2.5.1 Airborne virus inactivation

The present study was not able to collect viable virus samples of PR8 or NDV following direct treatment of aerosols with either the SDB or DDB reactor. This data indicates that NTP is a highly effective means of inactivating poultry viruses, however the predominate inactivation mechanism remains unclear. Furthermore, this study was not able to explicitly show that viruses were inactivated while aerosolized. However, findings from other studies provide evidence that direct NTP treatment of aerosolized viruses is a dominant inactivation mechanism (Wu et al., 2015 & Xia et al., 2019).

2.5.2 Liquid-based inactivation with DDB reactor

Preliminary experiments demonstrated that indirect NTP exposure could complete inactivate (4-log reduction) aqueous NDV in ≤20 min. Liquid-based inactivation is thought to be the result of dissolved ROS and not pH change. However, the addition of sodium thiosulfate (up to 1.4M) to the collection media did not prevent virus inactivation. This is likely due to the excessively high ozone concentrations (80ppm) generated in this study.

2.5.3 Plasma Activated filter inactivation

The dissolution of gelatin membrane filters did result in a slight decrease in the pH of collection media (7.2-6.9). The pH was further decreased to 6.8 if the filters had been indirectly exposed to NTP. However, the addition of gelatin filters, NTP exposed or non-NTP exposed, did not significantly alter PR8 titers. The addition of filters did lower NDV titers, but the difference in reduction between exposed and non-exposed filters was negligible, indicating that reactive plasma species did not accumulate in the gelatin filters resulting in liquid-based virus inactivation.

2.5.4 Surface inactivation

Based on the ozone concentration (80ppm or 157.06mg/m^3) and sampling times (5min SDB and 10min DDB), ozone dosages were calculated as 785.3 min(mg/m^3) and 1570.6 min(mg/m^3) for the SDB and DDB respectively. Based on findings from other studies exploring the antiviral effects of ozone (Tseng & Li, 2008), it appears very likely that the high ozone concentrations generated during NTP treatment experiments would quickly inactivate any viable virus captured by the gelatin membrane filters. This finding

is the predominate reason that direct inactivation of aerosolized viruses cannot be confirmed.

2.5.5 Thermal inactivation Effects

D-values for the thermal inactivation of influenza and NDV at peak NTP reactor temperatures (62-80C) were calculated by extrapolating data from a previous study Chmielewski et al. (2011). If the extrapolated data are correct, even the brief exposure to peak reactor temperatures, which occurs during the aerosol's reactor and plasma discharge residence times, is sufficient to significantly reduce airborne virus concentrations. Therefore, thermal inactivation effects must be considered as a possible primary, or secondary, inactivation mechanism.

2.5.6 Impacts of relative humidity on viral aerosol

The present study observed large discrepancies in airborne virus concentrations between the nebulizer and downstream sampling port. It appears very likely that a significant portion of these discrepancies is due to an unexpectedly low sampling efficiency of the gelatin filters. However, data corrected for the low filter efficiency was not able to completely account for the low downstream NDV concentrations. Furthermore, differences between upstream and downstream NDV concentrations appeared to increase with decreasing flow rates/RH. A linear regression analysis revealed a strong negative correlation ($R^2 > 0.99$) between increasing RH and decreasing airborne NDV concentrations in the SDB system. It is currently believed that increasing RH leads to increased virus losses to condensation and adherence to the inner walls of the experimental system. However, calculated condensation losses did not appear to match visually inspected condensation losses indicating that condensation losses alone could not

completely account for the decrease in air concentrations, even when coupled with low gel filter sampling efficiency. Therefore, it is believed that increasing RH values, at least up to moderate RH values (~60%), may lead to a mild reduction in the viability of NDV aerosols .

2.5.7 Nebulizer-Induced Virus Inactivation

Twenty minutes of continuous nebulization was determined to have no significant impact on liquid NDV concentration within the Collison 6-jet nebulizer. This finding is highly consistent with other nebulization experiments reported in the literature. Therefore, it can be concluded that NDV concentrations in the nebulized aerosol do not fluctuate as a result of decreasing aqueous NDV concentrations during the nebulization process.

2.5.8 Future Research

Future studies investigating the efficacy of NTP as a microbial aerosol control technology will certainly wish to determine the minimum specific energy input required to completely inactivate aerosolized poultry viruses. This can easily be achieved by increasing the air flow rate through the system, at a fixed power input. Future studies may also wish to challenge NTP-based air treatment technologies with more hardy microorganisms, such as bacteria or fungal spores. The operating parameters required to completely inactivate hardy airborne microorganisms would almost certainly be sufficient to inactivate less hardy microorganisms, such as viruses. Therefore, a universal anti airborne pathogen technology could be developed. Finally, future studies may wish to determine the scalability of NTP systems. The present knowledge of NTP's air treatment potential is limited to laboratory scale experiments with relatively low flow

rates. The commercial realization of this technology, such as applications in an animal rearing facility, or in hospitals, will almost certainly require that the device be operated with air volumes far larger than any investigated so far.

Future studies investigating liquid-based sample collection strategies may wish to explore methods that allow for viruses to be sampled, and their viability preserved, from air streams containing high concentrations of ROS/RNS. Alternatively, studies may wish to explore methods of neutralizing ROS/RNS prior to impingement, in a manner that does not lead to significant pathogen loss as a result of inadvertent filtration by the neutralization media.

The present study found that the addition of gelatin filters to virus containing solutions led to reductions in NDV concentrations, but no reductions in PR8 concentrations, regardless of whether or not the filters were exposed to NTP. Future studies may wish to explore why the dissolution of gelatin filters reduces NDV titers. Perhaps, NDV is more sensitive to pH changes, or is more likely to aggregate to the gelatin preventing accurate plaque assays.

The ozone concentrations recorded in the present study were thought to be sufficiently high that they could lead to the inactivation of viruses accumulating on, or within, the gelatin membrane filters. Future studies may wish to run control experiments in which gelatin filters are inoculated with virus, and indirectly exposed to NTP to determine possible secondary inactivation effects. Alternatively, future studies could explore methods of neutralizing long-lived ROS/RNS prior to collection on gelatin filters, as a way of circumventing the possible issue of surface based inactivation. By eliminating

downstream inactivation effects, one could successfully demonstrate airborne inactivation.

The NTP reactor temperatures recorded in the present study were thought to be sufficiently high that even brief aerosol exposure could lead to significant thermal inactivation effects. Future studies could easily explore the contribution of thermal inactivation to the overall virus reduction by heating the reactor electrical heating tape to the normal NTP discharge temperatures, and conduct aerosol experiments in the same manner as would normally be conducted with NTP.

Relative humidity was determined to have a significant impact on virus losses throughout the length of the experimental system. While the RH effects were thought to be due to condensation losses and viability losses, the degree to which each mode contributed to the overall loss was not determined. Future studies could differentiate between the two mechanisms using two additional experiments. First, experimenters could attempt to collect all of the condensed moisture within the system and compare this with the change in viral load throughout the length of the system. Second, experimenters could include a PCR-based virus quantification procedure, in addition to a viability assay. This method would involve collecting air samples at the beginning (upstream) and end (downstream) of the experimental setup and comparing the ratio of total particles (PCR) and infectious particles (viability) assay of either end of the system. For example, if samples taken at the beginning of the experimental setup showed air concentrations of 1000 total particles (PCR) per liter of air and 10 infectious particles (viability assay) per liter of air, the upstream ratio of total to infectious particles would be 1000:10 or “100:1”. If viral losses within the system were only due to condensation effects, one would assume

that the number of particles exiting the system would be lower, but that the ratio of total particles to infectious particles would be the same (assuming that infectious particles were not more likely to condense than non-infectious particles). For example, if condensation losses were 90%, one would expect downstream concentrations of 100 total particles per liter of air and 1 infectious particle per liter of air. This would yield a ratio of 100:1 or "100", which is the same as the upstream ratio. However, if an increase in RH resulted in a loss of virus viability one would expect that increasing humidity levels would produce an increase in the ratio of total particles to infectious particles in the downstream portion of the system, because the number of infectious particles would decrease due to condensation and viability losses. For example, assuming the same upstream ratio as the previous example (1000/10 or "100") one may expect to again lose 90% of infectious particles to condensation and another 90% to viability loss. This would produce a downstream concentration of 0.1 infectious particles per liter of air. Since viability losses would not affect the total number of particles, one would expect the concentration of downstream particles to remain at 100. Therefore, the ratio of downstream particles would be 100:0.1 or 1000:1, which is greater than the upstream ratio, therefore indicating a loss of viability. Additionally, the collection efficiency of gelatin membrane filters should be further investigated.

The present study found that 20 minutes of continuous nebulization did not significantly impact the viral titer within the nebulizer. However, future studies may wish to explicitly measure changes in nebulizer output (microbes per liter) to determine the stability and consistency of nebulized aerosols.

3 Chapter 3: Pilot Scale Study

3.1 Literature Review

Chapter 2 provided conclusive evidence that NTP is an effective means of inactivating airborne viruses in a controlled laboratory setting. While this represents an important first step in developing NTP-based air treatment technology, it is not conclusive evidence that NTP is a broad solution for controlling airborne pathogen transmission. As previously discussed, airborne pathogens include a wide variety of microbial species, which exhibit varying degrees of resilience to environmental stress. Furthermore, certain environmental factors may decrease the effectiveness of different types of treatment technologies. For example, section 1.4 described how dust particles shield microbes from UV treatment, and conditions of elevated relative humidity can promote bacterial propagation on high efficiency filters. Finally, one must address the question of scalability. An effective air treatment technology must be able maintain its effectiveness when scaled to treat different volumes of air. Therefore, in order to provide conclusive evidence for the efficacy of NTP-based air treatment technology it is necessary to challenge a scalable NTP system with a variety of microorganisms under realistic environmental conditions. Animal rearing facilities, such as poultry barns, represent ideal testing conditions due to their high airborne microbe concentrations, diverse microbial profile, and challenging environmental conditions.

3.1.1 Ubiquity/diversity of airborne microorganisms in animal barns

Airborne microorganisms are ubiquitous in animal rearing facilities. In a comprehensive study of airborne pollutants in a poultry barn Hinz & Linke, (1998)

recorded airborne bacteria concentrations of $7.7x10^6$ CFU/m^3 air. Similar findings were reported for dairy production facilities (Larsson et al., 1988) and swine production facilities (Cormier et al., 1990), which showed airborne bacteria concentrations of $1.5x10^7$ CFU/m^3 and $1.5x10^5$ CFU/m^3 air respectively. In fact, airborne bacteria and fungal spores in animal (poultry) barns have been reported as high as 10^9 CFU/m^3 and $4.9x10^6$ CFU/m^3 respectively (Kasprzyk, 2008).

In addition to being highly concentrated, the airborne microbial profile in animal rearing facilities is very diverse. Dutkiewicz, (1987) and Vucemilo et al. (2005) collectively report sampling 10 different bacterial species in a farm environment including many known human pathogens such as *Staphylococcus aureus*, *Escherichia coli, and Bacillus anthracis* (Kurnatowskaka, 2002). Similarly, Lugauskas et al. (2002) report sampling over 31 species of airborne fungi in a poultry house, and voiced concern that the majority of the identified species posed a health risk to susceptible individuals. Finally, animal viruses, such as influenza and Newcastle Disease Virus, are not necessarily environmentally ubiquitous in animal rearing facilities, as viruses cannot propagate without a host organism. Therefore, if the animals within the barn are free of infection, it is likely that there will not be any detectable animal viruses. However, during periods of disease outbreaks, such as during the 2008 bird flu epidemic, airborne viruses are also present in animal rearing facilities (Jonges et al., 2015).

3.1.2 Dust, RH, and other challenging environmental factors in animal barns

In addition to containing large quantities of airborne microorganisms, the air in animal rearing facilities is also laden with non-living organic and inorganic material. In general, the airborne particulate matter in animal rearing facilities is one to two orders of

magnitude greater than other indoor environments (Zhang, 2004). Wathes (1998) reported inhalable dust concentrations up to 10.4 mg/m^3 in European poultry rearing facilities. Similarly, Ellen et al. (2000) reported inhalable dust concentrations as high as 81.33mg/m^3 in poultry houses and additional 6.5 mg/m^3 for the respirable dust fraction. These concentrations are particularly significant as the recommended threshold limit value for total dust concentration is only 2.4mg/m^3 (Donham et al., 1989).

Airborne particulate matter creates a significant challenge for any air cleaning technology designed to eliminate microbial aerosols in animal rearing facilities. However, another important environmental factor is the fluctuating humidity levels inside the barns. Most animal rearing facilities are quite large, and lack any type of humidity control system. In fact, it is quite common for barns to have open ventilation systems designed to encourage rapid air exchange with the environment. In this manner, the relative humidity inside animal rearing facilities is likely to fluctuate substantial during different seasons and even on a day-to-day basis.

3.1.3 Previous attempts at industrial cleaning devices

The highly concentrated and diverse microbial profile, heavy soil load, and fluctuating relative humidity levels, make decontaminating the air in animal rearing facilities a seemingly Herculean task. However, the ever-present economic and health threats posed by airborne pathogens have encouraged many attempts at developing air decontamination technologies for animal rearing facilities. (Lau et al., 1996) tested a fabric filter system and an electrostatic filter system in a pig barn and determined that the bacterial removal efficiencies were only 10-50% and 20-52% respectively. Interestingly, due to the intensive labor required to clean the fabric filter, the electrostatic system was

determined to be more cost effective. Another study attempted to inactivate airborne bacteria by spraying a thermo-nebulized disinfectant into the air inside a laying hen house (Adell et al., 2015). However, this strategy was deemed to be ineffective at controlling the airborne bacteria. Finally, a comprehensive study of air scrubber technology applications for controlling airborne bacteria from animal houses revealed that bio-scrubbers were unable to control airborne pathogens, and acid (peracetic) scrubbers, while effective, were too expensive to be operated continuously (Aarnink et al., 2005). Therefore, the failure of many air treatment technologies to substantially/efficiently reduce the microbial load in animal rearing facilities indicates that animal rearing facilities are a significant challenge for any air treatment system.

3.1.4 Justification of Pilot Scale Study

Chapter 2 provided conclusive evidence of NTP's effectiveness at treating viral aerosols. However, in order to provide conclusive evidence that NTP is an effective means of controlling airborne pathogens more broadly, it is necessary to demonstrate NTP's effectiveness against microorganisms other than viruses, resilience against environmental factors like dust, and scalability. Animal rearing facilities represent ideal testing facilities as they contain a variety of microorganisms, are generally dusty environments, very in size (scalability), and currently lack an effective/efficient air treatment technology. Therefore, the present study sought to determine the effectiveness of NTP as a broad air treatment technology by designing and fabricating an easily scalable pilot scale NTP system and challenging it with bacterial aerosols in a poultry barn.

3.2 Materials & Methods

3.2.1 Pilot Scale NTP System

The second set of objectives for this project involved developing a pilot scale prototype APNTP reactor, based on information gleaned from laboratory experiments, and testing it in a small, but scalable, poultry barn. The high inactivation rates and energy efficiency of the SDB reactor observed in laboratory experiments led to a pilot scale prototype that was simply a scaled-up design of the laboratory reactor. Specifically, the pilot scale plasma system consists of 25 single-cell reactors, which are identical to the SDB reactor used in laboratory experiments. The 25 reactors are operated in parallel, which allows for higher flow rates, without an increase in applied voltage. A simplified diagram of the pilot scale system is shown in Figure 27.

The pilot scale system operates by pumping air laden with infectious aerosols into the lower chamber. Continued air pressure forces the air in the lower chamber up through the plasma cells where the air is treated by NTP. The treated air (non infectious aerosol) is then expelled from the system through an outlet on the top of the device.

A photo of the pilot scale system (excluding electrical systems) is shown in Figure 28. Air is pumped through the NTP system by means of a centrifugal pump equipped with a low efficiency air filter (MERV 2), designed to remove large dust molecules that may clog the system. Although the system was designed to be operated with a 2kW pulsed AC power supply (PVM2000 Information Unlimited), technical complications forced the experiments to be conducted with a much smaller (300W) AC power supply (not pictured). Since the 300W power supply lacked sufficient power to create visible plasma discharge in the 25 cells, experiments were conducted using only 10

or 15 cells, where plasma discharge could be visualized. The remaining cells were plugged to prevent air from flowing through untreated.

3.2.2 Field-Testing Experimental Setup

The barn used in this study was a mechanically ventilated turkey barn, which contained 750 turkeys (~45lb each). Since humans and objects represent potential vectors for pathogen transmission that could threaten flock health, it was decided that project members would not enter the poultry barn. Instead, a mechanically operated barn exhaust vent was used as a source of contaminated poultry facility air. The centrifugal fan (air mover) was positioned directly under the exhaust vent, which allowed for contaminated air to be pumped through the pilot scale plasma system. A photo of the experimental setup is shown in Figure 29. Of note, while conducting field experiments, all mechanical barn exhaust vents were turned off, except for the one used for these experiments.

During field-testing, the poultry flock was recognized as being in good health, and free from viral infection. Since viruses, such as influenza, require a host to propagate they are not environmentally ubiquitous, but only exist in areas where susceptible hosts are present. This means that there were no poultry viruses during field-testing experiments. Therefore, it was decided that experiments would sample for airborne bacteria, which are environmentally ubiquitous, and also known to be potentially pathogenic. Since bacteria are much larger and hardier than viruses, it was determined that successful inactivation of airborne bacteria would be a good indicator for the NTP system's ability to inactivate viruses.

3.2.3 Experimental Procedure

Field experiment samples were taken in triplicate from either the barn exhaust vent or the plasma reactor exhaust vent using gelatin membrane filters. The sampling flow rate was 3 L/min and sampling time for each experiment was 5 minutes. After sampling, the filters were immediately dissolved in Phosphate Buffered Saline solution (PBS) and stored on ice, but not allowed to freeze, prior to sample analysis. Samples from the plasma reactor exhaust vent were taken during three different scenarios: plasma on with 10 of 25 cells in operation, plasma on with 15 of 25 cells in operation, and plasma off with 15 of 25 cells in operation.

3.2.4 Total Bacteria Count

Bacteria samples were stored on ice, without freezing, for approximately 3 hours prior to sample analysis. Liquid samples were analyzed using 4-fold serial dilution and plating on Petrifilm aerobic count plates (3M, United States). Plates were stored in an incubator at 30 C for 48 hours. Bacterial colonies were manually counted and liquid concentrations were calculated using the dilution factors as colony forming units per milliliter (CFU/mL). Air concentrations were calculated using Equation 2, with air sampling flow rate (3LPM) and sampling time (5min) and data was presented as colony forming units per liter air (CFU/L).

3.3 Results

During field-testing, the applied power to the plasma reactor was ~290W distributed over 10 or 15 cells. The flow rates were recorded for the 10 cell trial, 15 cell trial (plasma on), and 15 cell trial (plasma off) as 684LPM, 912LPM, and 988LPM

respectively, which correlated to specific energy inputs of 25.4 J/L, 19.1 J/L, and 0 J/L respectively.

Figure 30 provides a plot of the air concentrations recorded at the barn exhaust vent and the pilot scale reactor exhaust vent under different operating conditions. The barn's exhaust air had the highest bacteria concentration, with an average of approximately 3822 CFU/L of air. Air concentrations in the reactor exhaust varied based on number of plasma cells in operation and whether or not the plasma was on or off. The mean airborne bacteria concentration leaving the plasma reactor was 849 CFU/L of air when 10 cells were operated with plasma, 782 CFU/L when 15 cells were operated with plasma, and 11 CFU/L air when 15 cells were operated without plasma.

3.4 Discussion

3.4.1 Findings from the Present Study

The pilot scale NTP system used in the present study demonstrated a 99.7% reduction in airborne bacteria concentrations from the barn exhaust vent to the NTP reactor exhaust port. However, this peak reduction occurred when the NTP was not initiated and utilized 15/25 plasma cells. Interestingly, when the NTP was initiated across 15 SDB cells, the reduction level dropped to 79.5%. These findings indicate that the observed reductions in airborne bacteria across the pilot scale system were the result of filtration effects, as opposed to NTP-based inactivation. The discrepancies in air concentrations between NTP treated and untreated aerosols leaving the reactor were likely the result of the statistical inaccuracies due to the low sample size (n=3). It is likely that larger samples sizes would reveal a decrease in the difference in airborne bacteria

concentrations between NTP treated and untreated samples. However, it is clear that NTP did not have an inactivation effect on bacteria during this study.

3.4.2 Factors Contributing to the Pilot System's Low Inactivation Rates

The NTP pilot scale system's failure to inactivate bacteria with NTP during field testing was likely due to a combination of challenge microorganism, environmental factors, and low specific energy input (SEI).

The pilot scale system was based on the SDB reactor used in Chapter 2, which was originally designed to treat airborne viruses. Viruses are much smaller, and generally less hardy than bacteria. Therefore, the aerobic bacteria used as a challenge microorganism in this study represented a much more challenging pathogen, than those used in the laboratory studies.

Another important factor, which may have contributed to the low inactivation efficiencies, was the presence of particulate matter in the microbial aerosol. As previously discussed (Section 3.1) animal rearing facilities, such as poultry barns, are incredibly dusty environments. Bacteria enclosed within, or attached to, dust particles likely receive a level of protection from NTP treatment, similar to the UV shielding effect discussed in Section 1.4. The adherence to dust particles would also explain the high filtration effect between the barn exhaust and NTP exhaust ports. The MERV 2 filter used to protect the NTP system is well below the recommended filter rating to remove particulate on the size order of bacteria. However, if the bacteria were attached to dust particles, then the effective aerodynamic diameter of the infectious particle would be increased, and therefore more likely to be removed by a low efficiency filter.

The final factor that likely contributed to the poor NTP field performance was its low SEI. During laboratory testing, the SDB reactor was able to completely inactivate airborne NDV with a specific energy input of 171 J/L. In contrast, the pilot NTP system had a SEI of only 19.1 J/L, almost an order of magnitude lower than the lab scale SDB reactor, and was not able to inactivate airborne bacteria. Although this study did not perform laboratory scale testing with airborne bacteria, other studies have used bacteria as challenge microorganisms for NTP-based air treatment systems, and their findings can be used to hypothesize the minimum SEI required to inactivate airborne bacteria.

In a laboratory study, using artificially generated aerosols, Liang et al. (2012) were able to completely inactivate (~7-log reduction) *P. fluorescens* aerosols and achieved a 98.4% inactivation of *B. subtilis* aerosols after 0.12s of NTP exposure with a specific energy input of ~115.2J/L ("output" power was 24W and sampling flow rate was 12.5LPM). Liang et al. (2012) also challenged their NTP system with ambient indoor and outdoor aerosols. They found that a SEI of ~50.9 J/L was sufficient to inactivate 99% of indoor and outdoor bacteria, and fungal inactivation rates of 98% and 85% for indoor and outdoor aerosols respectively. Of note, Liang et al. (2012) did not specify whether the 24W was system power or plasma power. A similar study (Gallagher et al., 2007) used a dielectric barrier grating discharge reactor to treat aerosolized *E. coli* in a closed airflow system. This system operated with a flow rate of 25 L/s and average plasma discharge power of 330W. Therefore, their average SEI was 13.2 J/L. At this SEI, a 1.5 log reduction was observed for E. coli immediately after NTP exposure. It should be noted that Gallagher et al. (2007) did not report the total power of their NTP system, just the plasma power. Additionally, Gallagher et al. (2007) utilized a pulsed power supply with a

0.1283 duty cycle. Given that the pulse duration included almost all of the applied power, and was only 77us, the average power of the pulse duration was actually much higher (2571W) than the average discharge power. This is important because the high power inputs during the pulse duration likely produced a different NTP chemistry than if a steady 330W of AC power was applied.

The study performed by Liang et al. (2012) utilized a tubular DBD reactor and challenged it with airborne bacteria in an outdoor environment. Therefore, their data is very similar to the data generated in this study. Liang et al. (2012) demonstrated 99% inactivation of outdoor bacteria with a SEI of 50.9 J/L. Although they did not specify whether this was system power or plasma power, it still represents approximately 278% increase in applied energy compared to the system used in this study. Therefore, it is likely that if the pilot scale reactor was operated according with the same SEI used in laboratory scale testing (171 J/L), it would have been highly effective at inactivating airborne bacteria.

3.5 Conclusions From Pilot Scale Study

3.5.1 General Summary

The pilot scale NTP system was unable to inactivate airborne bacteria from a poultry barn with direct NTP treatment. This low inactivation potential was likely the result of the system being operated an order of magnitude below its specified SEI. However, findings from other studies indicate that if the pilot scale system were operated at its specified SEI; it would like have been highly effective (>99%) at inactivating airborne bacteria.

3.5.2 Future Modifications to NTP Pilot System

Future studies with the NTP pilot system will certainly wish to operate the reactor with an appropriate power supply. In this manner, it is very likely that high bacteria inactivation will be observed. Specifically, the power supply should be able to operate at 2kW, such that each of the 25 reactors can be operated at 80W, consistent with laboratory testing (Chapter 2). Additionally, future studies with this system will likely wish to add a variac voltage control unit to the centrifugal pump, to allow greater control of the flow rate through the system. Finally, samples should be taken between the MERV 2 filter and inlet of the NTP system to determine whether the high level of filtration is occurring across the filter or across the NTP reactor.

3.5.3 Future Studies

Future studies exploring NTP technology as a broad solution to airborne pathogens will certainly wish to determine the minimum SEI required to treat a variety of pathogens including viruses, bacteria, and fungal spores. In this manner, NTP systems can be calibrated operate in the most efficient manner possible. Future studies may also wish to determine how environmental factors such as dust and RH impact the inactivation efficiency of NTP reactors operating in 'real-world' settings.

4 Chapter 4: Conclusions

The present study explored the feasibility of developing NTP technology to control airborne pathogen transmission. Laboratory testing, explored in Chapter 2, revealed that NTP technology is a highly effective method of inactivating airborne viruses including NDV and influenza. Although it is unclear whether pathogens were inactivated via direct

NTP treatment, thermal effects, or long-lived species such as ozone, it is important to point out that all of these elements are intrinsic aspects of NTP. Therefore, while the specific mechanism by which NDV and influenza were inactivated remains unclear, the observed inactivation rates were the product of NTP treatment. In this manner, one can safely conclude that NTP is a highly effective method of inactivating airborne viruses.

Future laboratory scale experiments will certainly wish to explore the specific inactivation contributions of each element of NTP (i.e. short-lived species, long-lived species, thermal effects, etc.). Determination of the primary inactivation mechanism will allow future NTP systems to be optimized for maximum pathogen reduction, while minimizing the negative effects of other inactivation routes. For example, if direct NTP treatment with short-lived oxygen radicals contributed to 99% of pathogen inactivation effects, then long-lived ozone, a known pollutant could be quickly removed from the exhaust air stream without concerns that doing so would drastically reduce inactivation efficiency.

While laboratory scale experimentation is an essential tool for parsing out important NTP operating parameters, NTP's efficacy as an air treatment technology can only be determined by continued field-testing. The pilot scale study, described in Chapter 3, revealed that an NTP air treatment system could be operated continuously in a field setting, without overheating issues, electrical issues, or rapid clogging. The lack of immediate complications was itself an encouraging result from this study. Unfortunately, technical complications with a commercial high-voltage power supply prevented the pilot scale system from operating within its design parameters, which likely contributed to its poor inactivation rates. Specifically, since the pilot scale system was operated well below

its intended input power and was challenged with what were likely hardy environmental microorganisms, as opposed to sensitive laboratory generated viral aerosols, it was unable to achieve inactivation effects relative to control experiments.

Future field-experiments will certainly wish to ensure that their system is operated with an appropriate power supply. Specifically, the pilot scale reactor should be driven by a power supply that provides a specific energy input greater than or equal to the minimum specific energy input required for complete, or significant, pathogen inactivation in a laboratory setting. Additionally, future studies may wish to sample air at various points within their system to determine what aspects of the system are the greatest contributors to filtration effects. Furthermore, future studies will likely need to operate their systems continuously for time periods longer than those used in the present study (~1.5 hours) to explore the effects of prolonged operation on the systems performance.

Regardless of the scale of the NTP system (laboratory scale or pilot scale), future studies may wish to utilize a slightly different experimental process than the approach used in the present study. Specifically, in contrast with the present study, future studies should conduct preliminary experiments with bacteria, as opposed to viruses. BSL I bacteria are safe to work with and often require much shorter sample analysis times than viruses. For example, the sample analysis time for the virus samples obtained in the present study were often one week or longer. In contrast, results for aerobic bacteria samples could be obtained in 24-48 hours. The relatively rapid turn around time for bacteria samples allows researchers to obtain critical data and make necessary modifications to the NTP reactor or experimental setup at a much higher pace than when

conducting experiments with viruses. Therefore, an efficient strategy for future NTP research would be to conduct preliminary experiments with aerobic bacteria, modify the system to ensure optimal/reliable performance, and then proceed to virus testing once the system had been optimized.

Future studies should also explore NTP reactor designs that are readily adaptable to existing barn infrastructure. The multicellular pilot-scale NTP system used in the present study relied on a variety of aluminum ductwork components and connective elements to attach to the poultry barn exhaust fan during field-testing experiments. While this was an effective means testing NTP's inactivation potential, it is important that reactor designs minimize excess material and hardware in mechanical systems to minimize capital costs. As an alternative to the multicellular design, future NTP studies should consider wire-to-plate or wire-to-wire electrode configurations for their reactor designs. These simple electrode configurations can be arranged in a variety of geometries, creating a flexible design that may be readily adaptable to a variety of existing barn ventilation systems. Additionally, the wire-to-plate configuration could provide a variety of benefits to modern poultry farmers. First, the NTP discharge from this system would likely be sufficient to inactivate airborne viruses. Second, if driven by a pulsed DC power supply, the electrostatic precipitation effects of this system could also potentially remove larger microorganisms from the air stream, which may have been more resistant to direct NTP treatment (i.e. bacteria and fungal spores). In this manner, it may not be necessary to increase the NTP power to inactivate hardier microorganisms, as they are instead removed from the air stream via precipitation effects (i.e. improved energy efficiency). Third, this type of system could also potentially remove other airborne contaminates,

such as dust and therefore improve overall barn air quality. Finally, this reactor design, like others, would also be able to degrade the problematic odorous compounds (NH_3, H_2S, etc.) produced in animal rearing facilities, therefore leading to better relationships between farmers and local communities, while improving air quality, and possibly animal health.

Illustrations

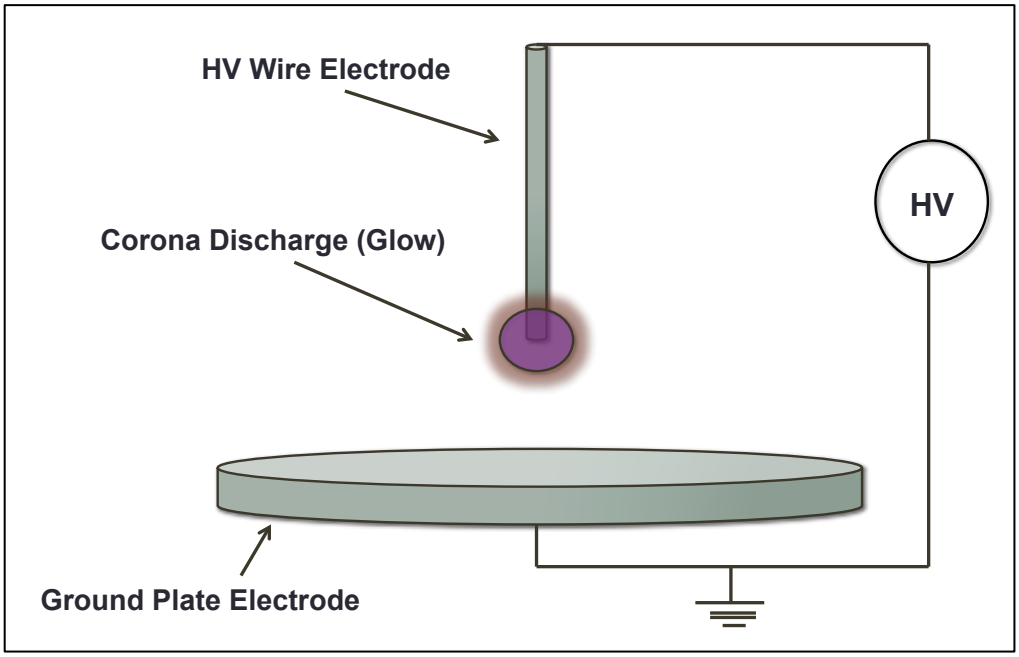

Figure 1 Simple schematic of a corona discharge reactor in wire-to-plate configuration and glow discharge regimen

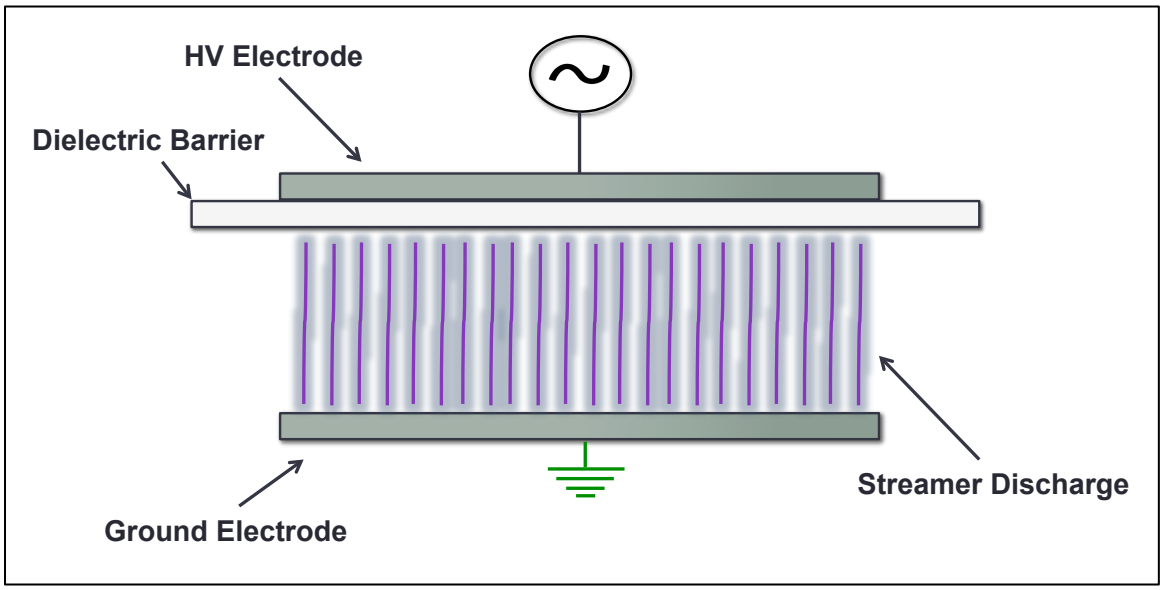

Figure 2 Simple schematic of a dielectric barrier discharge reactor with streamer discharge

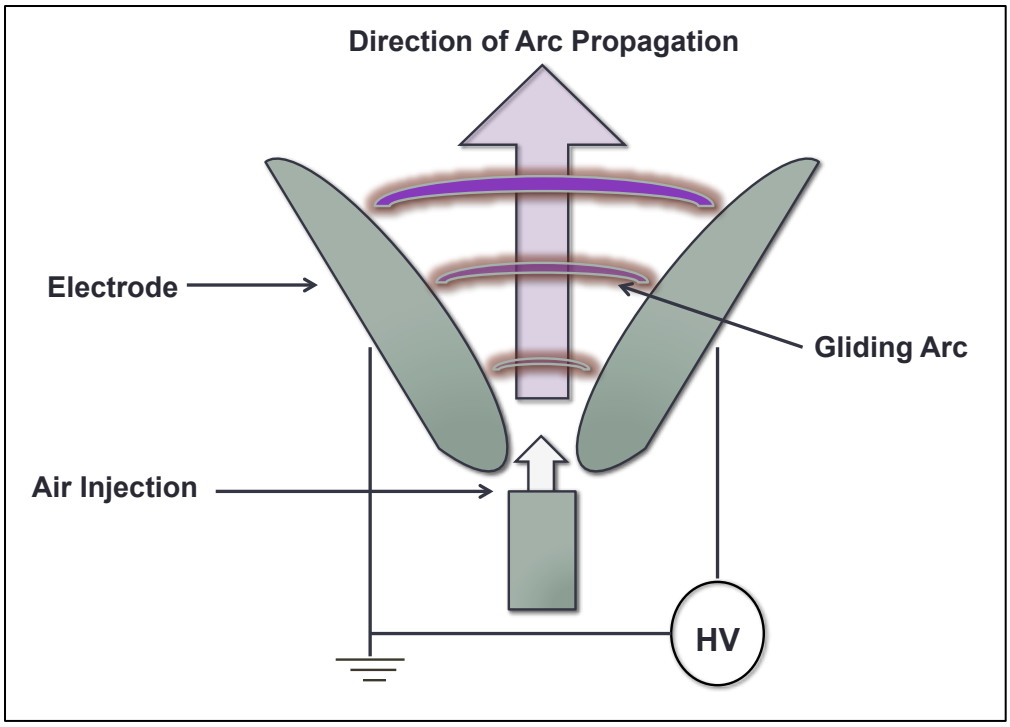

Figure 3 Schematic of a conventional gliding arc reactor

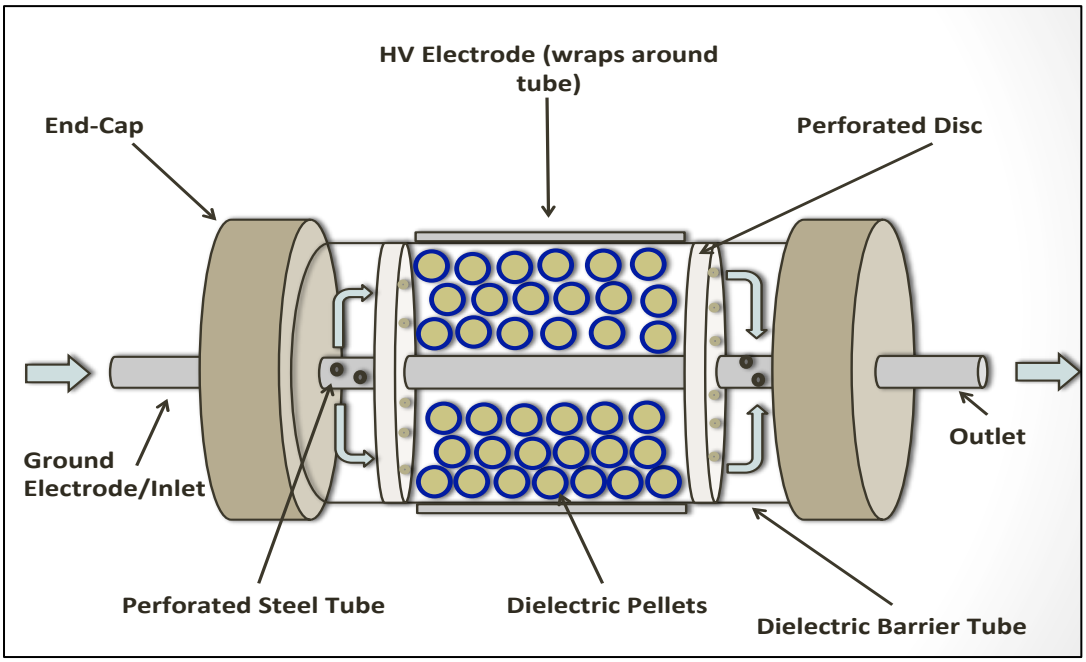

Figure 4 Schematic of a coaxial packed-bed NTP reactor

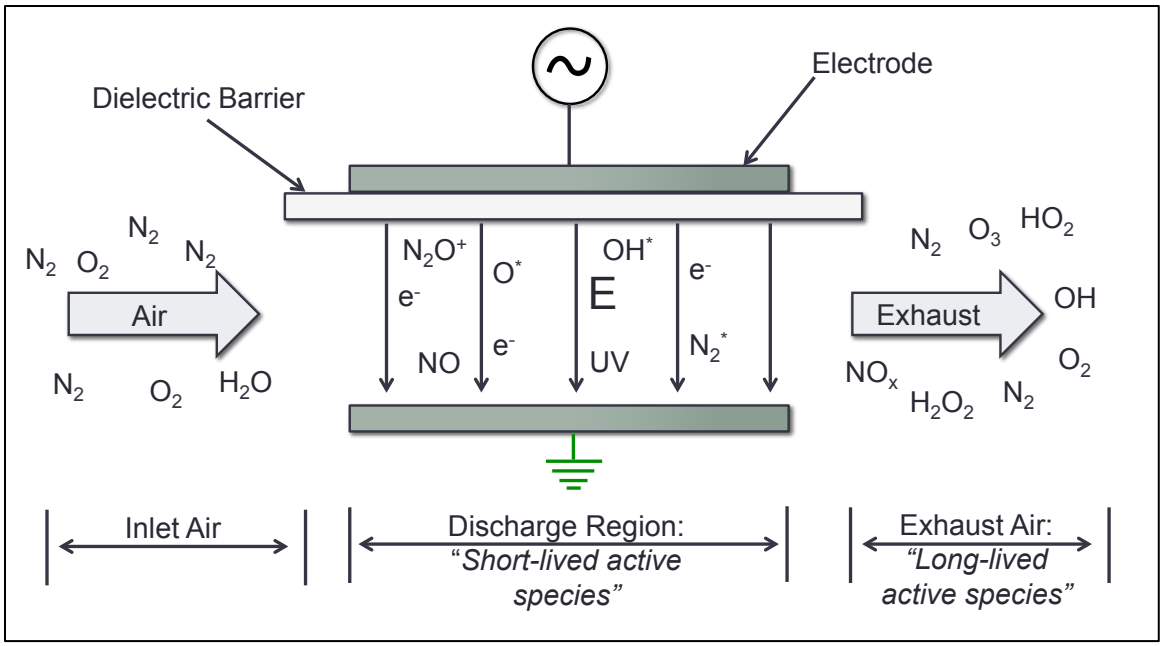

Figure 5 Diagram depicting some of the more prevalent short-lived and long-lived active species produced by a DBD reactor using air as a feed gas

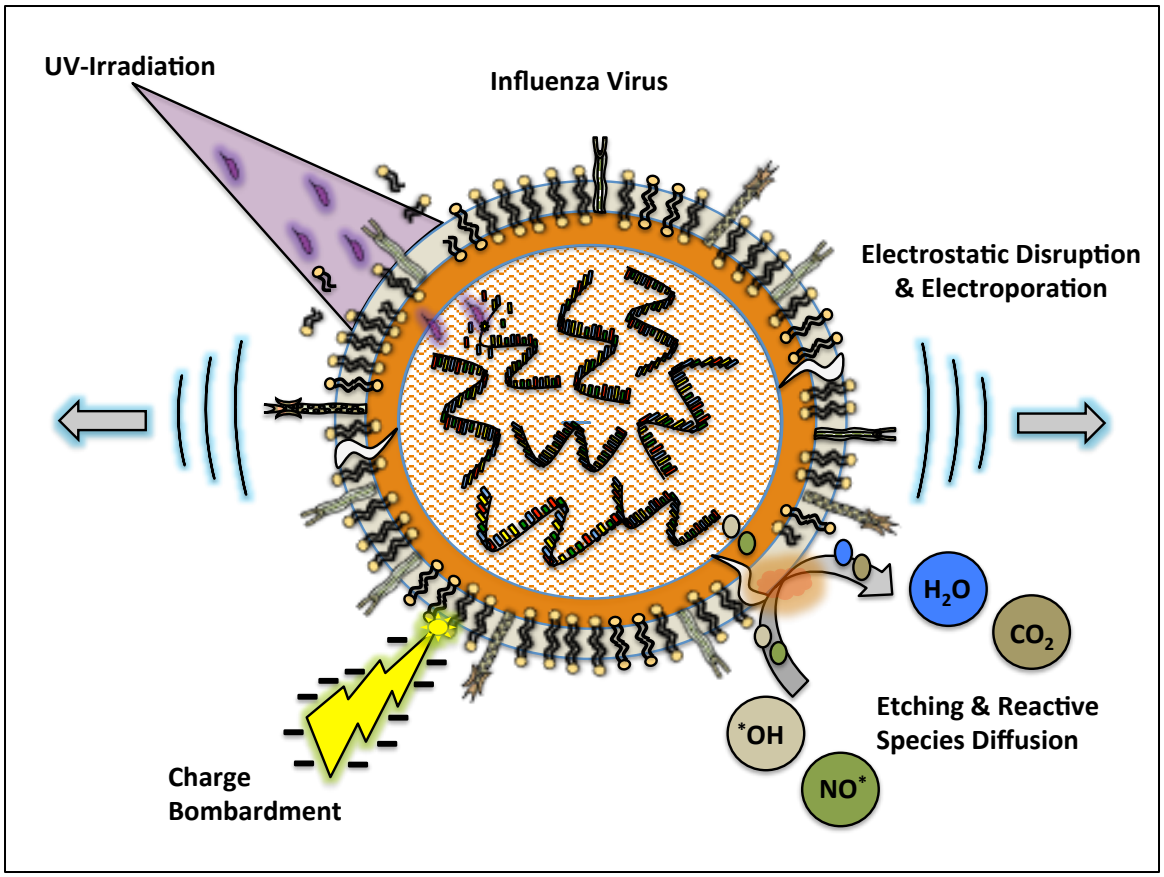

Figure 6 The many mechanisms of NTP-based pathogen inactivation

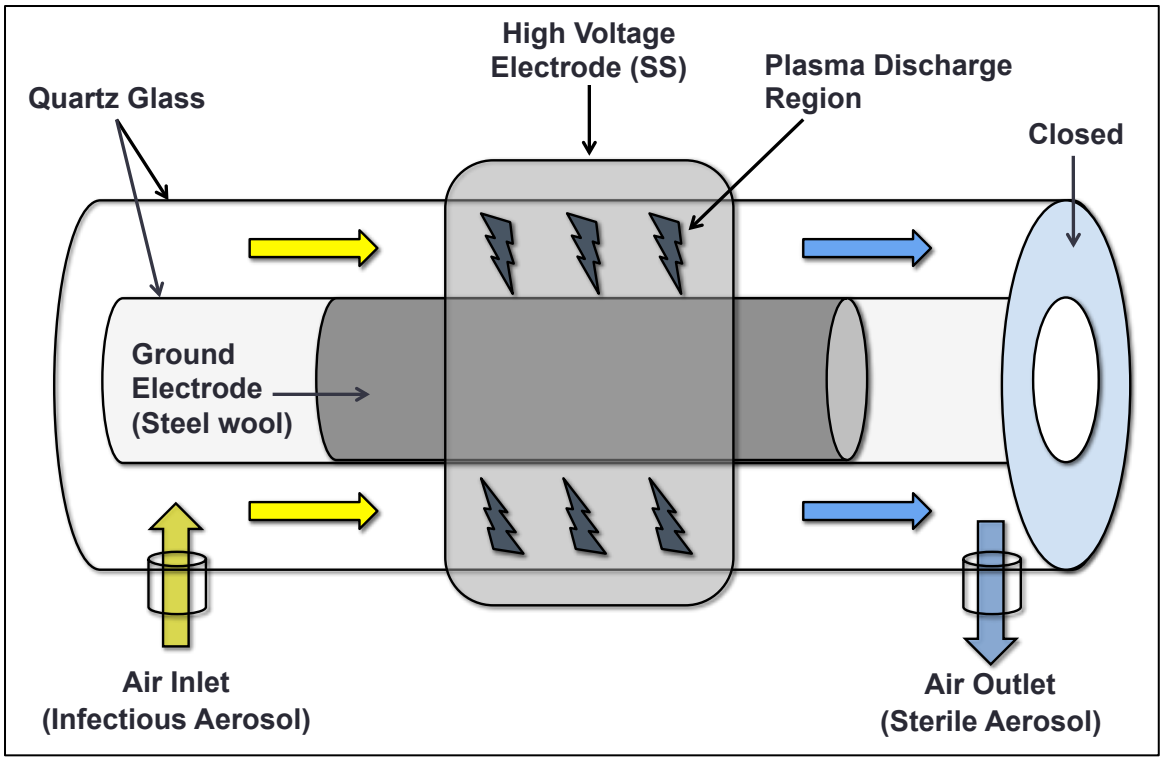

Figure 7 Flow Diagram of DDB Reactor

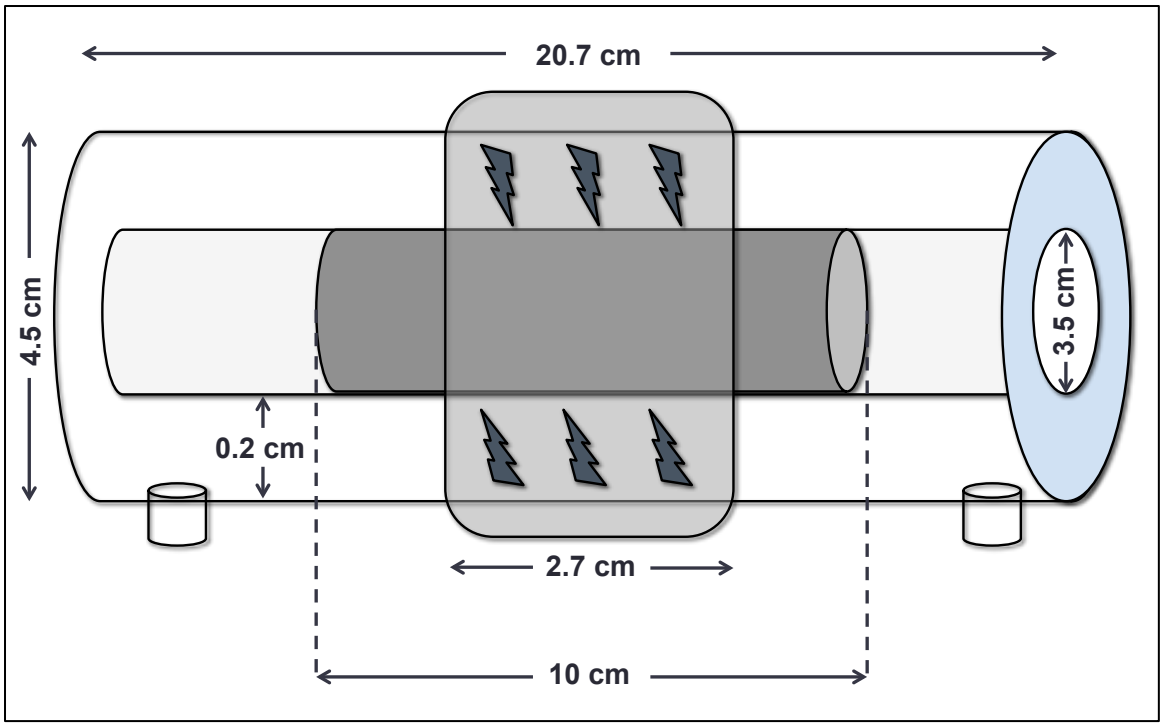

Figure 8 Dimensions of DDB Reactor

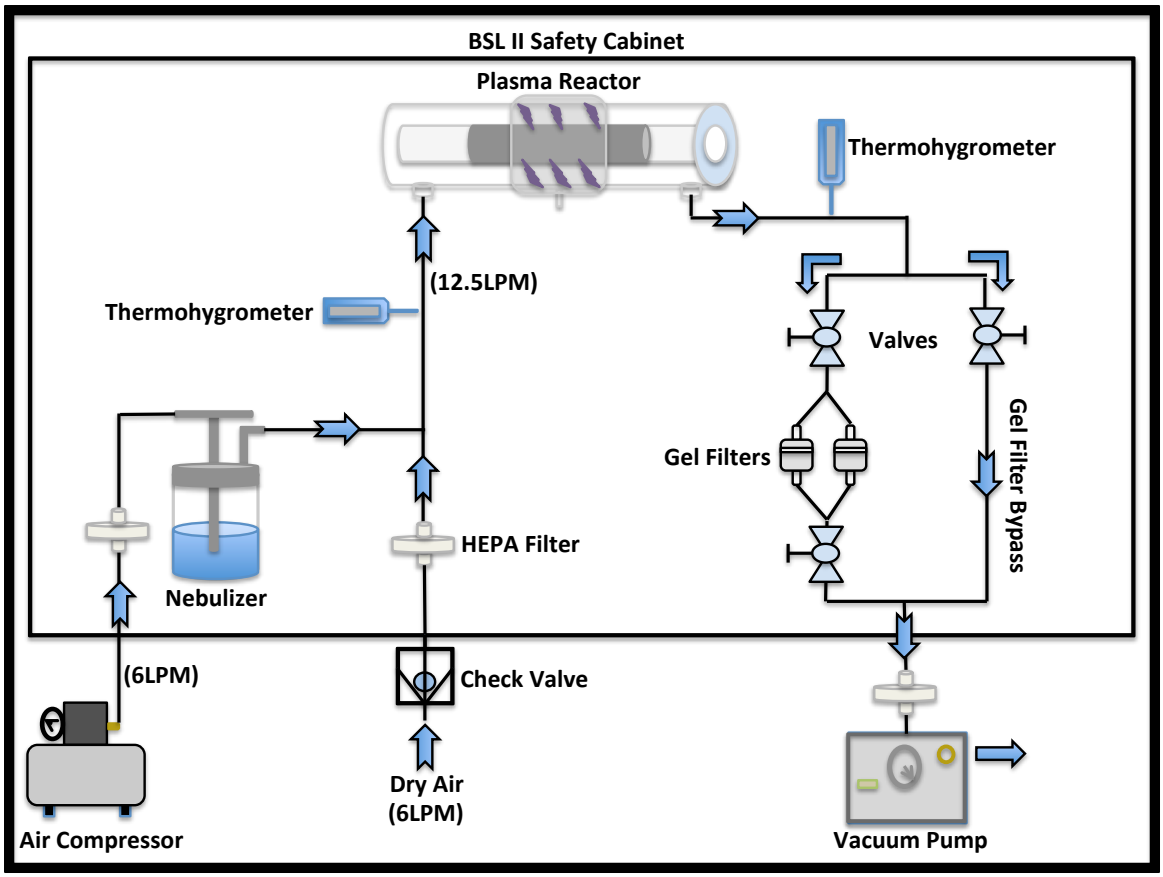

Figure 9 Experimental setup used for DDB Reactor

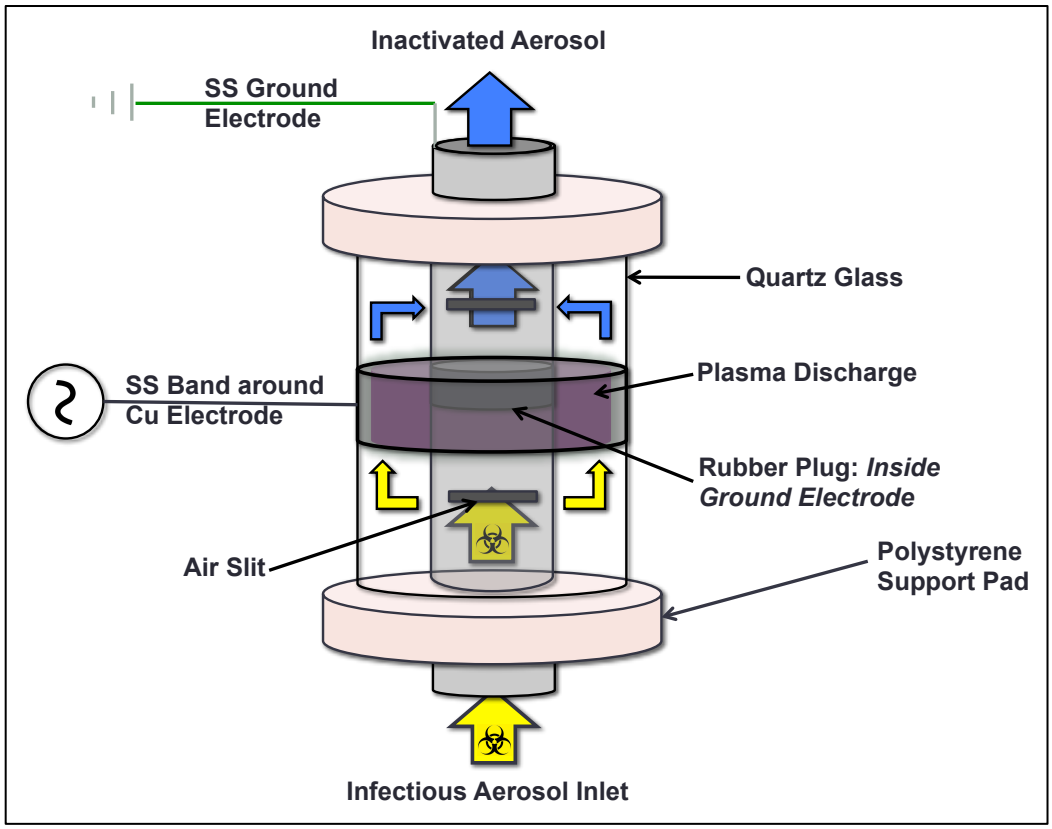

Figure 10 Component/Flow diagram of SDB reactor

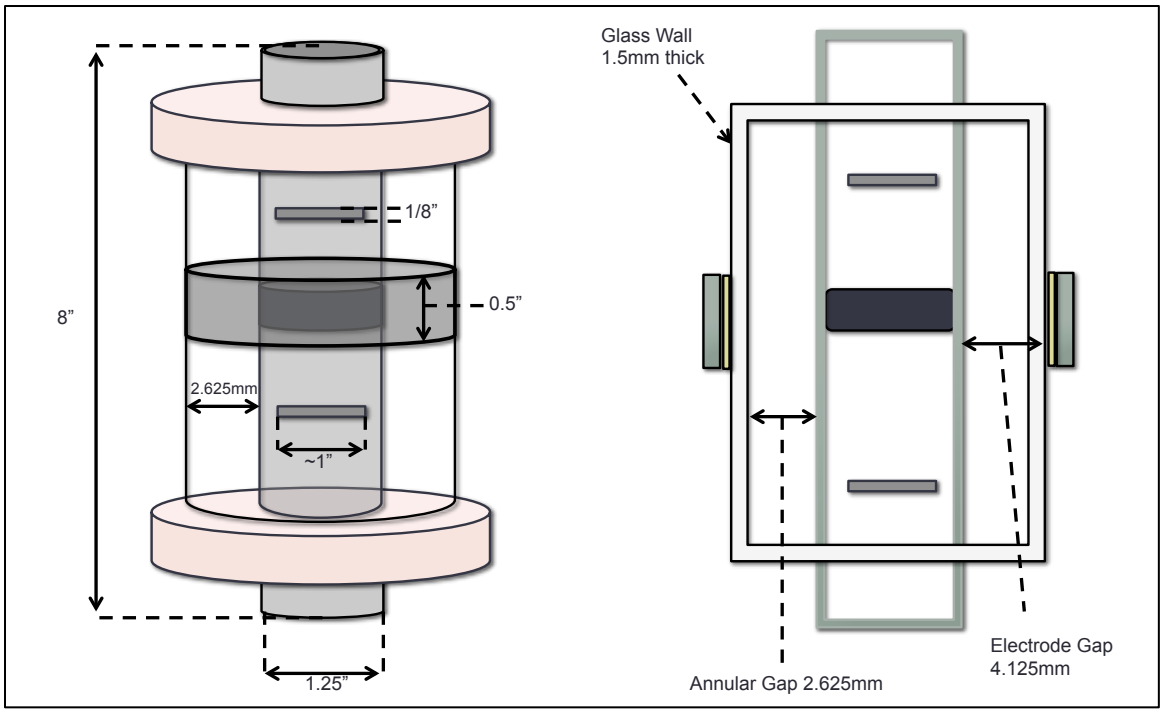

Figure 11 Dimension diagram of SDB Reactor

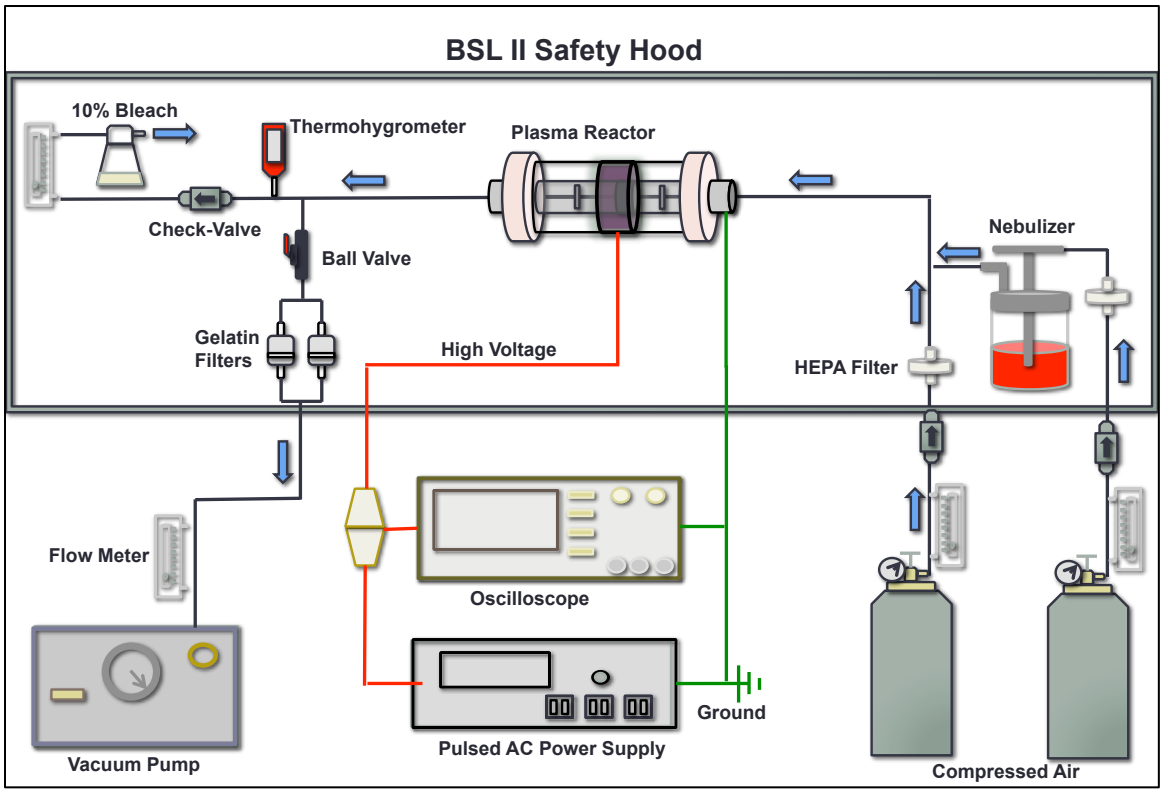

Figure 12 Experimental setup used to challenge SDB reactor

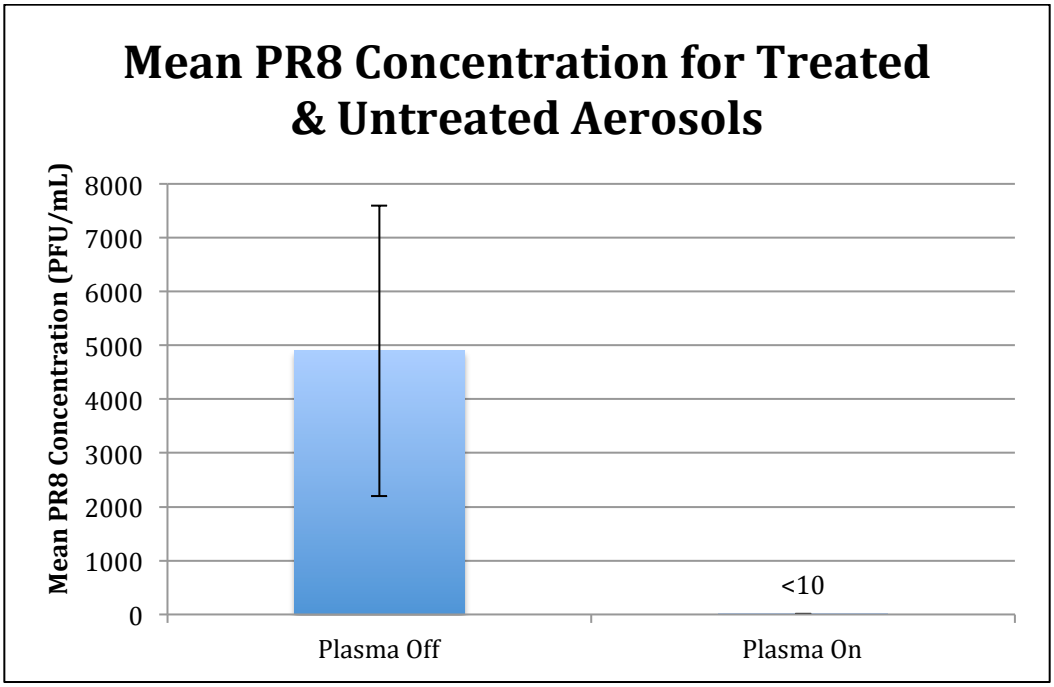

Figure 13 A plot of the mean PR8 concentrations from samples obtained from control experiments (NTP off) and treatment experiments (NTP on). The data label "<10" indicates that sample concentrations were below the limit of detection

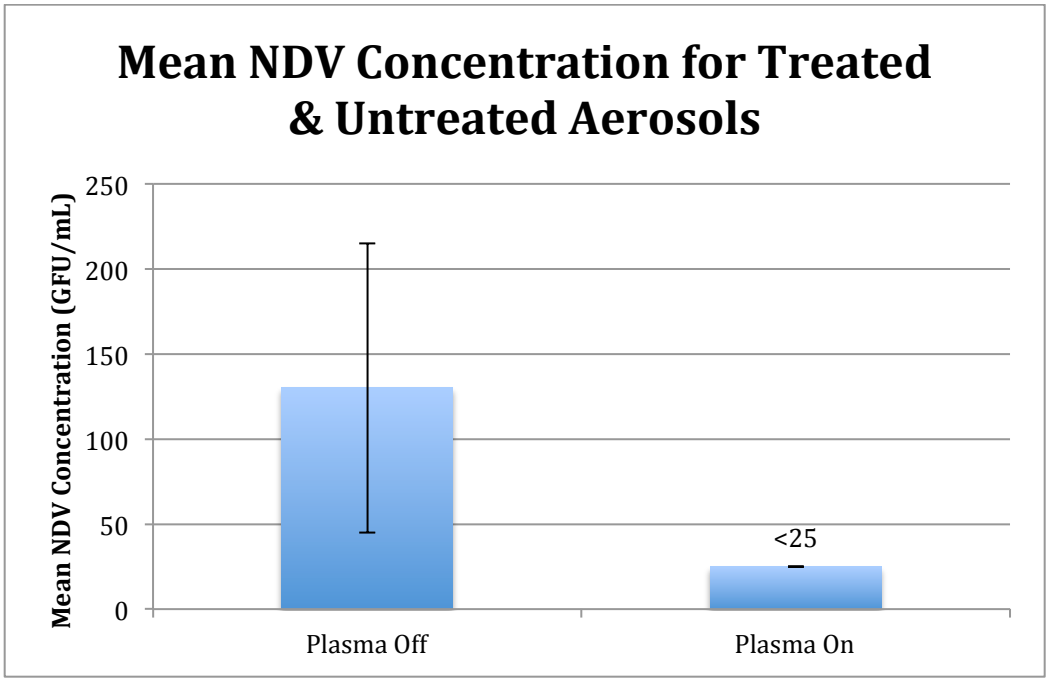

Figure 14 A plot of the mean NDV concentrations from samples obtained from control experiments (NTP off) and treatment experiments (NTP on). The data label "<25" indicates that sample concentrations were below the limit of detection

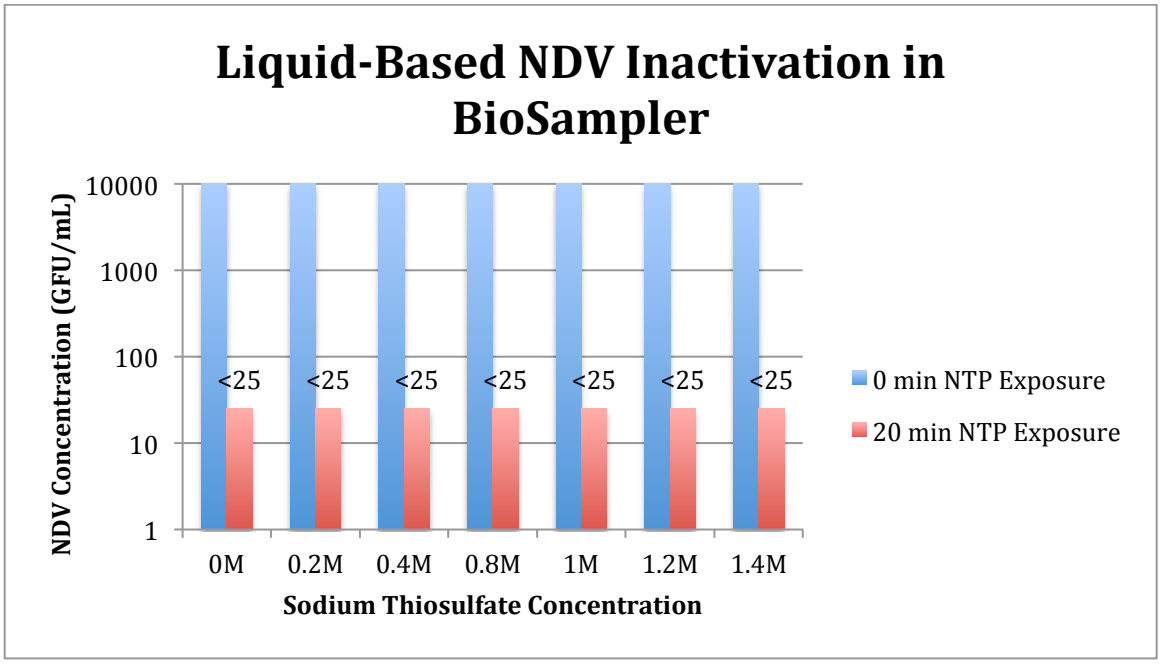

Figure 15 Plot of NDV concentrations in BioSampler with various concentrations of sodium thiosulfate added to BioSampler before and after 20 min of indirect NTP exposure

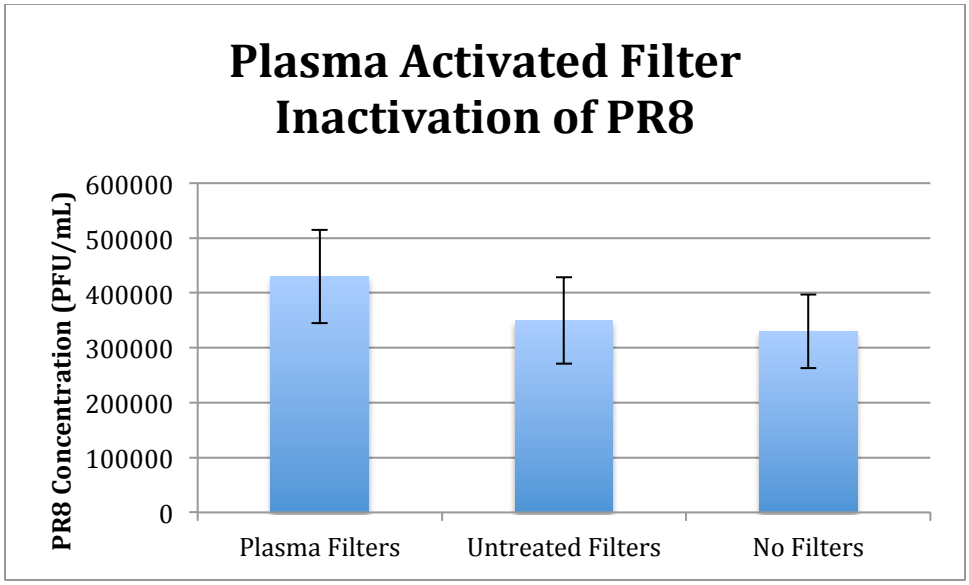

Figure 16 Plot of mean PR8 concentrations for samples mixed with NTP exposed filters, untreated filters, or no filters

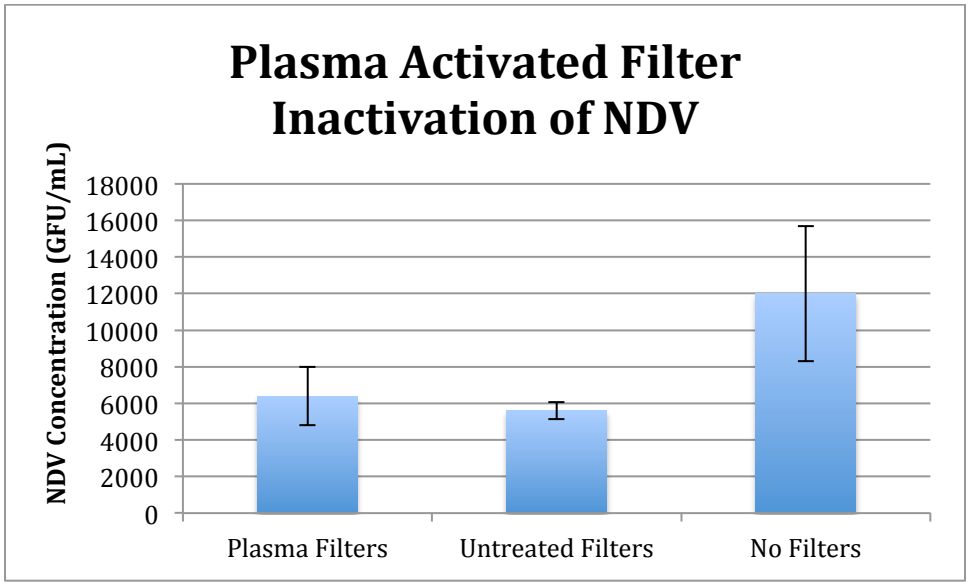

Figure 17 Plot of mean NDV concentrations for samples mixed with NTP exposed filters, untreated filters, or no filters

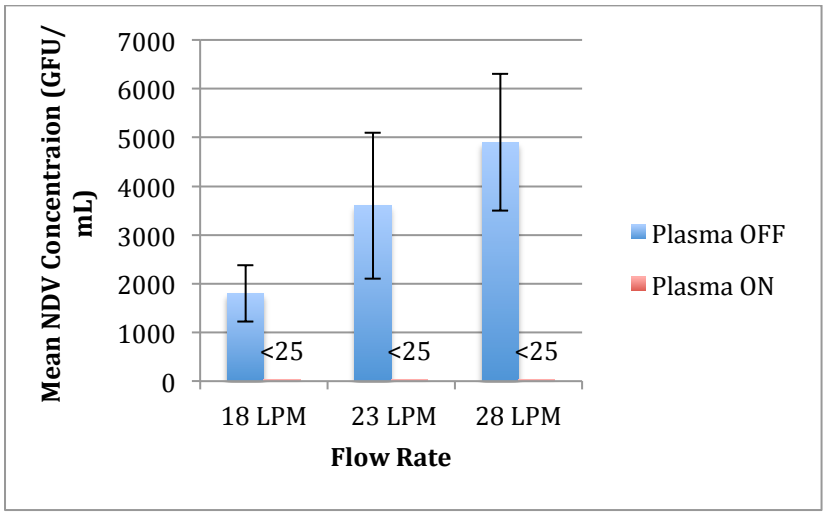

Figure 18 Plot of mean NDV concentration versus flow rate for treated and untreated samples. Treated samples (NTP on) were below limit of detection (<25 GFU/mL)

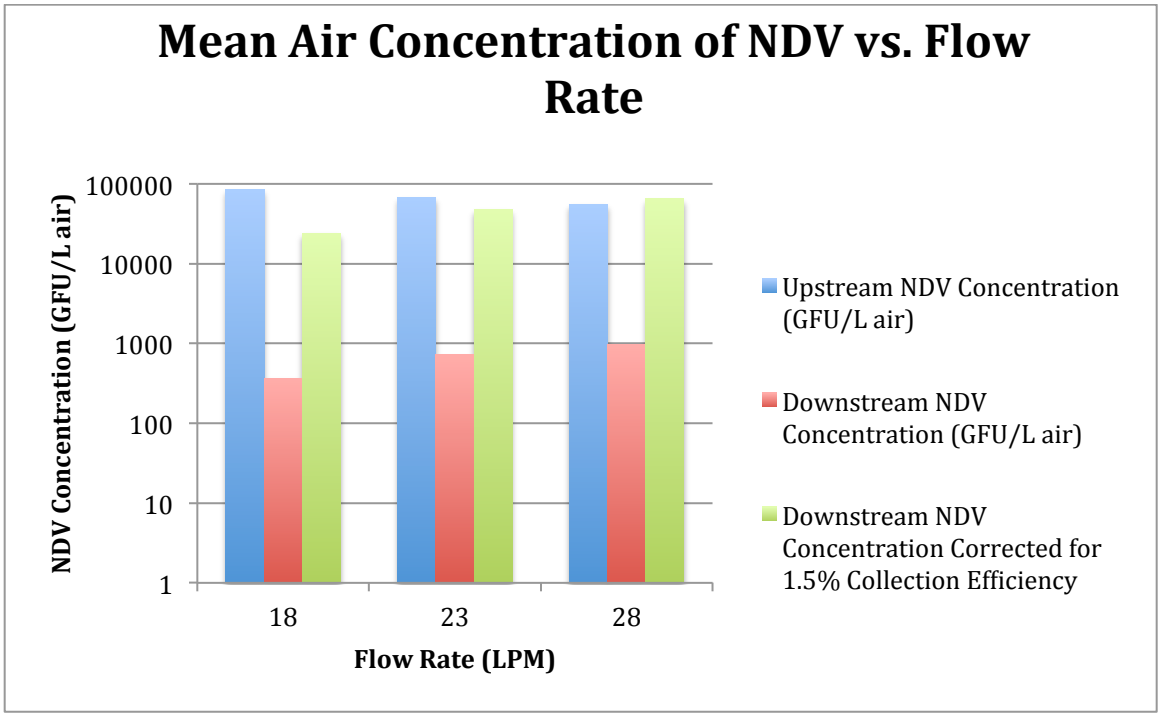

Figure 19 Calculated mean air concentrations of NDV upstream and downstream of SDB reactor at different air flow rates without NTP treatment

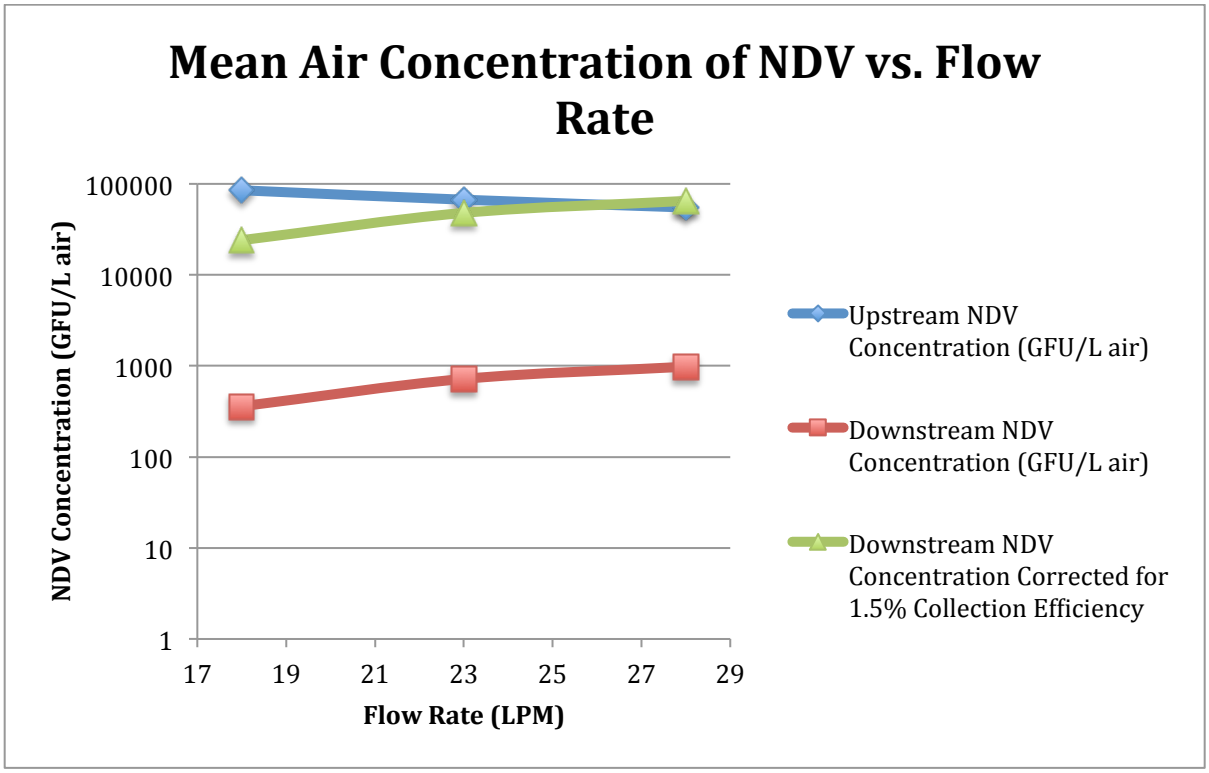

Figure 20 Scatter plot of airborne NDV concentration vs. flow rate

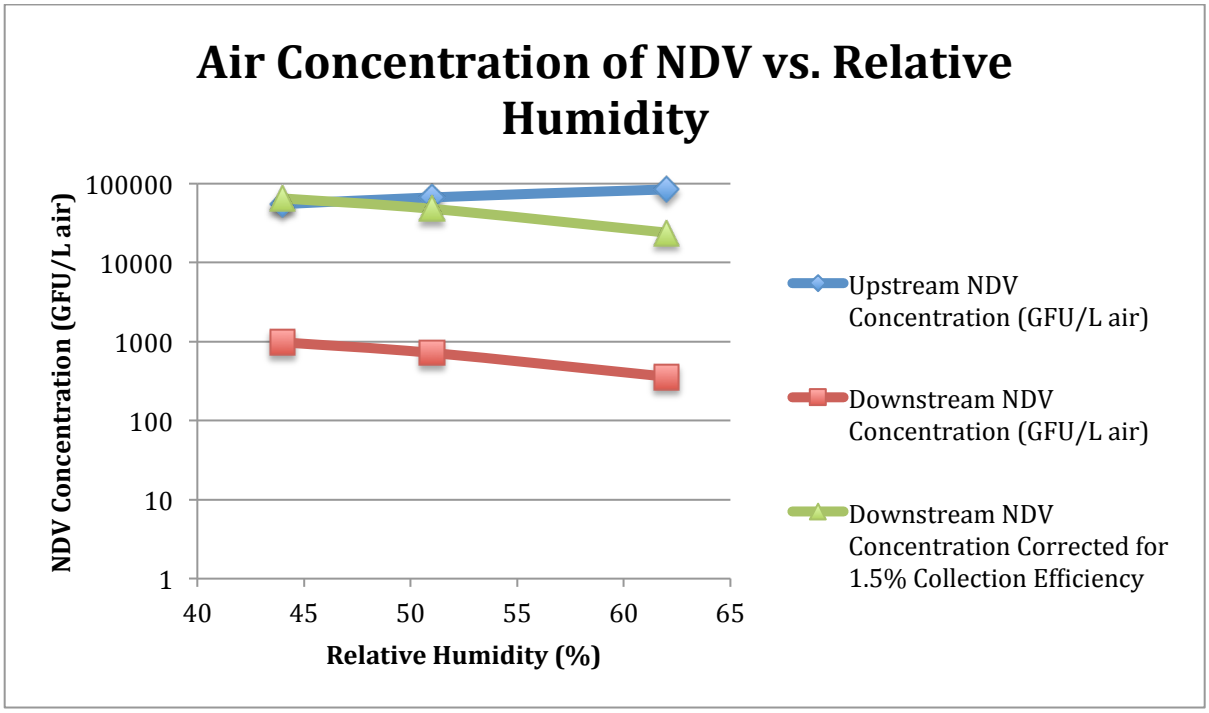

Figure 21 Scatter plot of airborne NDV concentration vs. relative humidity

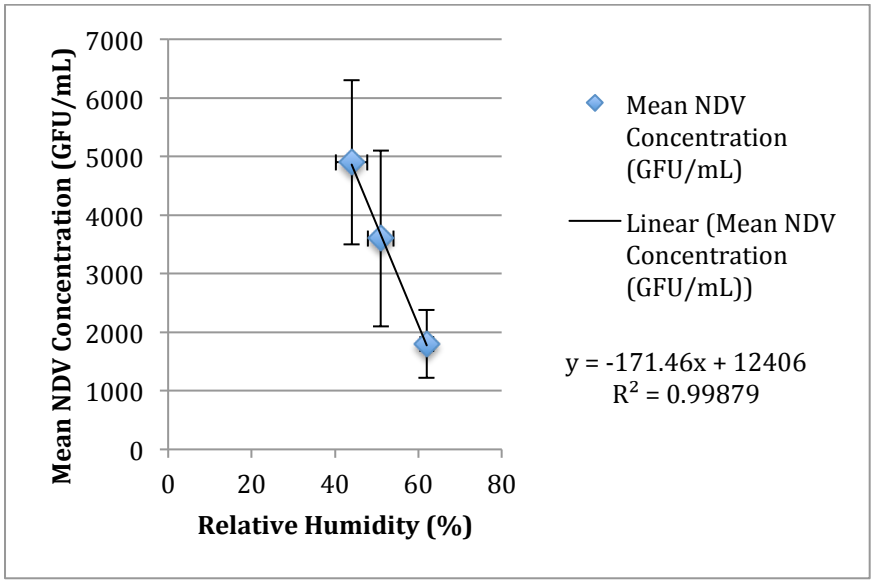

Figure 22 Plot of mean NDV concentration vs. mean relative humidity

Table 1 Estimated condensation losses of nebulized solution at each flow rate and corresponding relative humidity value. Includes losses corrected for error introduced by possible low sampling efficiency of gelatin filters

Flow Rate (LPM)	Relative Humidity (%)	Condensation Losses (mL)- *Uncorrected*	Condensation Losses (mL)- *Corrected for 1.5% Sampling Efficiency*
18	62	7.97	5.74
23	51	7.91	2.27
28	44	7.86	-1.49

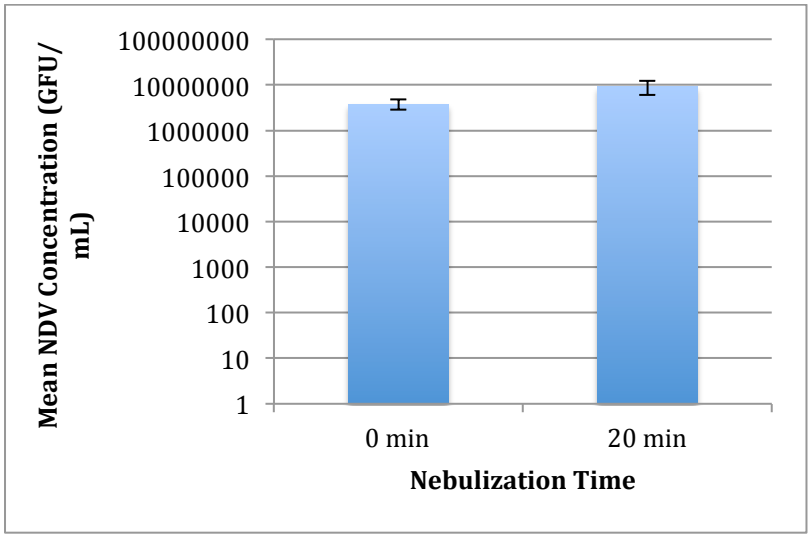

Figure 23 Plot of nebulizer virus concentrations before and after nebulization

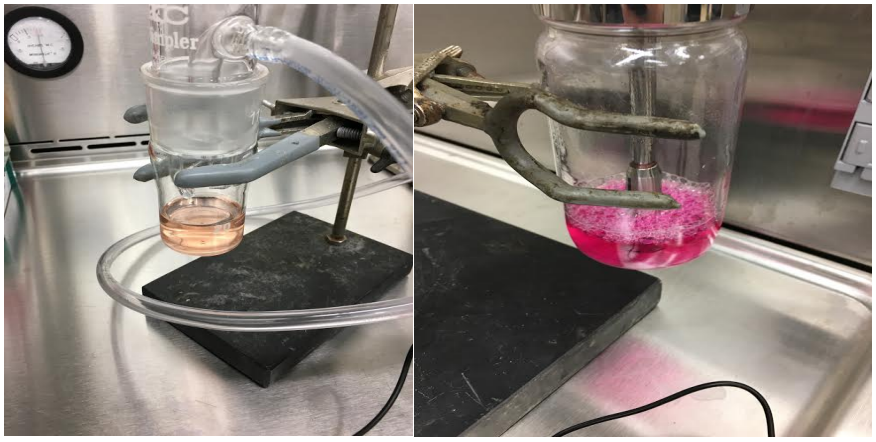

Figure 24 (Left) collection media after 20 min of indirect NTP exposure. (Right) original color of collection media (shown in nebulizer)

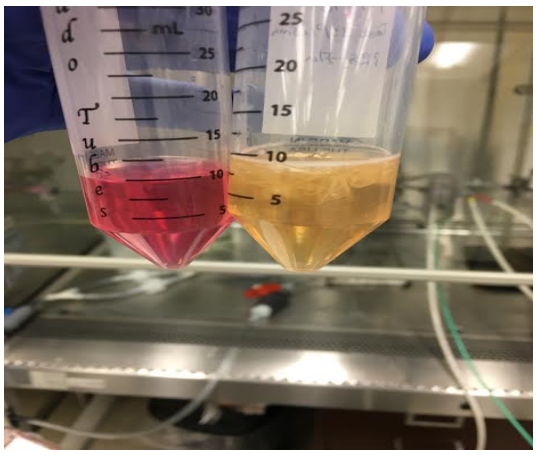

Figure 25 Comparison of MEM solution without the addition of NTP exposed gelatin filters (left) and after the addition of NTP exposed gelatin filters

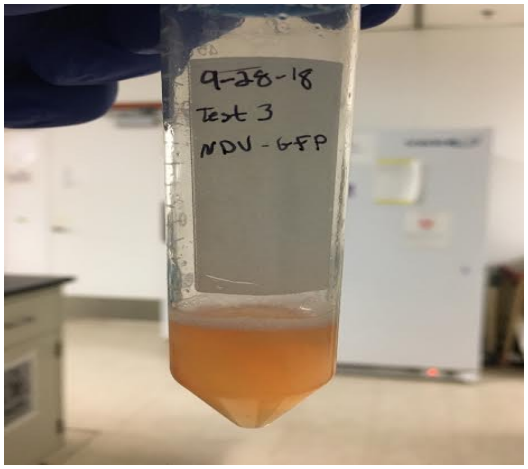

Figure 26 MEM solution after the addition of two non-NTP exposed gelatin filters

Table 2 Data obtained from Chmielewski et al. (2011) for influenza and NDV D-values for thermal inactivation in fat free egg products and extrapolated data for virus inactivation at temperatures corresponding to NTP exhaust air and NTP reactor temperatures

	NTP Exhaust Air Temperatures (°C)			Fat Free Egg Product Temperatures (°C)		NTP Reactor Temperatures (°C)			
	27	29	34	55	59	62	68	74	80
	D-Value (s)								
H5N2	2.59E+09	9.05E+08	6.61E+07	1.116E+03	2.4E+1	2.86E+1	1.24	5.37E-	2.32E-

								02	03
H7N2	1.74E+72	1.74E+67	5.50E+54	1.74E+2	4.2E+1	5.50E-16	5.50E-31	5.50E-46	5.50E-61
vNDV	6.75E+08	2.53E+08	2.19E+07	7.44E+2	1.02E+3	2.41E+1	1.28	6.74E-02	3.57E-03
INDV	3.18E+30	3.18E+28	3.18E+23	3.18E+2	3.3E+1	3.18E-5	3.18E-11	3.18E-17	3.18E-23

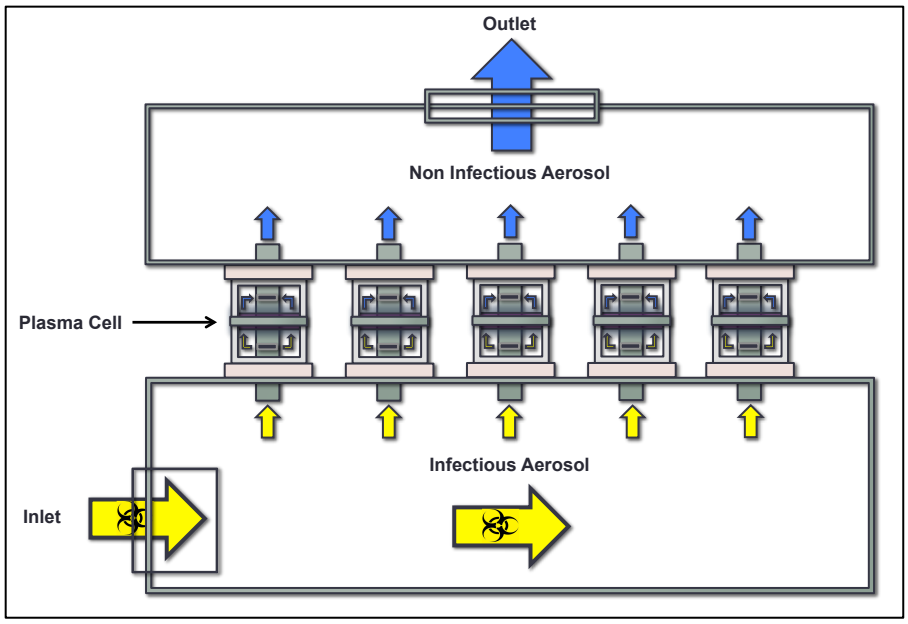

Figure 27 Simplified (cross sectional) diagram of pilot scale system. Only 5 of 25 single cell reactors shown

Figure 28 Pilot scale NTP system (excludes electrical equipment)

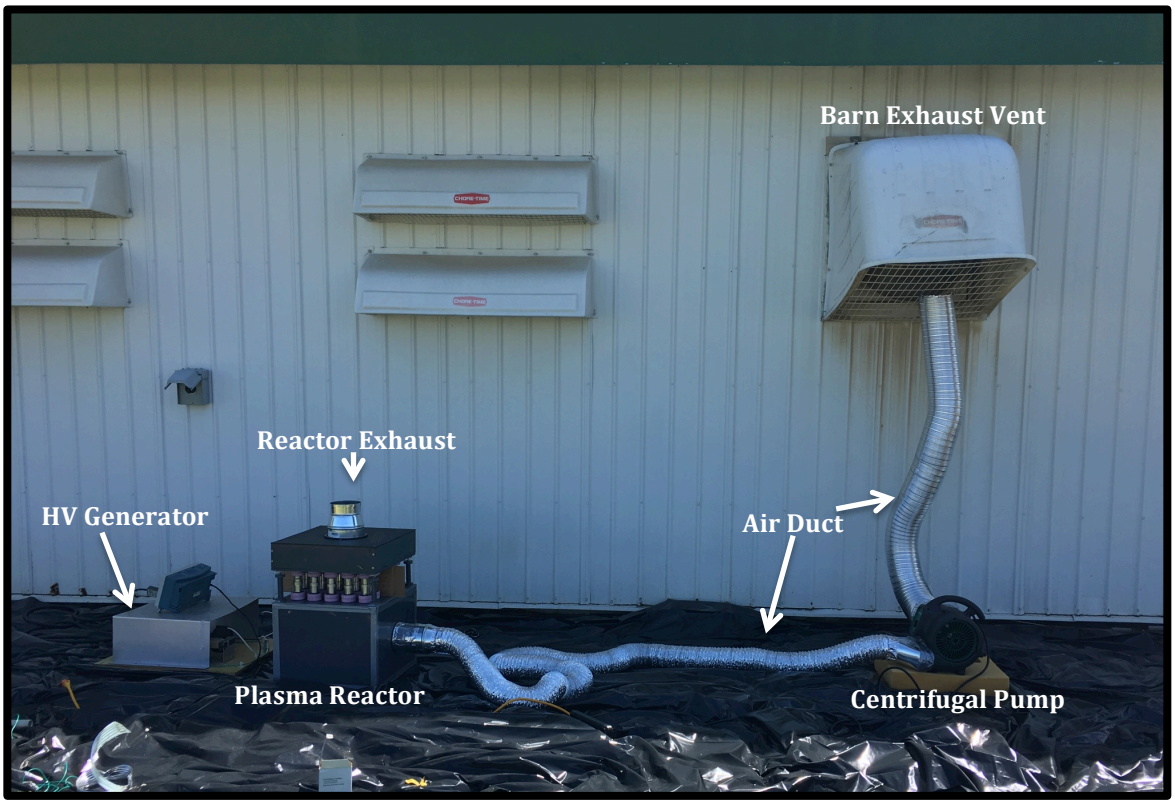

Figure 29 Photo of experimental setup for pilot scale testing experiments

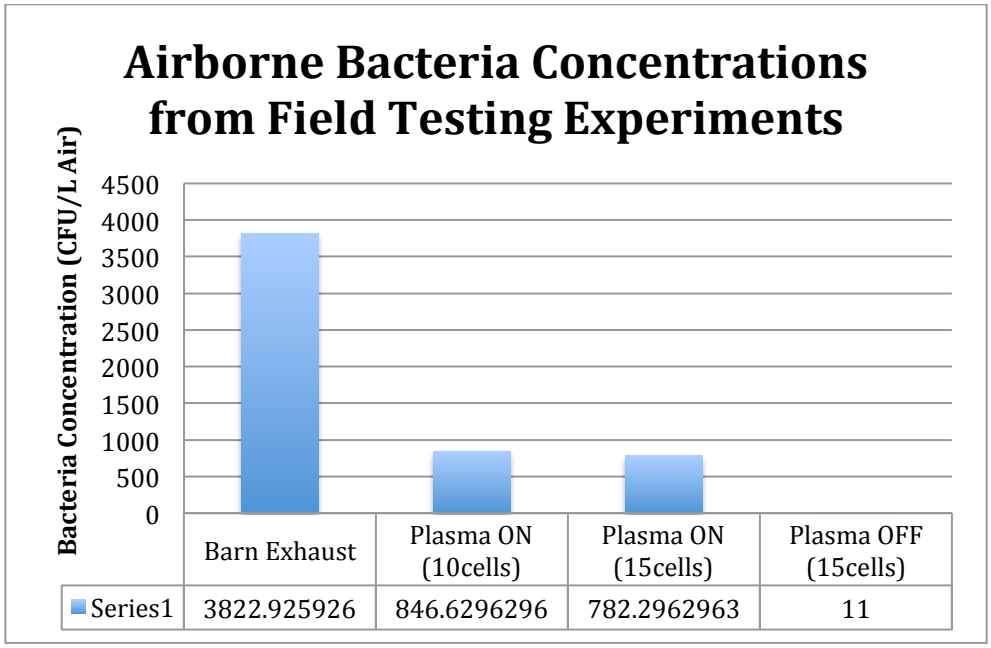

Figure 30 Plot of airborne bacteria concentrations from pilot scale experiments

Bibliography

1.] Centers for Disease Control and Prevention. (2012). *Principles of Epidemiology in Public Health Practice, Third Edition, An Introduction to Applied Epidemiology and Biostatistics.* Retrieved from: https://www.cdc.gov/csels/dsepd/ss1978/lesson1/section10.html (June 7, 2019)

2.] Terrier O., Essere B., Yver M., Barthélémy M., Bouscambert-Duchamp M., Kurtz P., VanMechelen D., Morfin F., Billaud G., Ferraris O., Lina B., Rosa-Calatrava M., Moules V. (2009). Cold oxygen plasma technology efficiency against different airborne respiratory viruses. *Journal of Clinical Virology, 45*(2), 119-124.

3.] Lonc, E., & Plewa, K. (2009). Microbiological Air Contamination in Poultry Houses. *Polish Journal Of Environmental Studies, 19*(1), 15-19.

4.] L. Morawska, "Droplet fate in indoor environments, or can we prevent the spread of infection?" *Indoor Air*, vol. 16, no. 5, pp. 335–347, 2006.

5.] Tellier, R. (2006). Review of aerosol transmission of influenza A virus. *Emerging Infectious Diseases,12*(11), 1657-62.

6.] Colbeck, I., & Lazaridis, M. (2014). *Aerosol science : Technology and applications*. Chichester, West Sussex, U.K.: John Wiley and Sons Limited.

7.] Alonso, C., Raynor, P., Goyal, S., Olson, B., Alba, A., Davies, P., & Torremorell, M. (2017). Assessment of air sampling methods and size distribution of virus-laden aerosols in outbreaks in swine and poultry farms. *Journal of Veterinary Diagnostic Investigation,29*(3), 298-304.

8.] Knight, V. (1980). VIRUSES AS AGENTS OF AIRBORNE CONTAGION. *Annals of the New York Academy of Sciences, 353*(1), 147-156.

9.] Centers for Disease Control and Prevention. (2016). *How Infections Spread*. Retrieved from https://www.cdc.gov/infectioncontrol/spread/index.html on (June 11, 2019).

10.] Bourouiba, L., Dehandschoewercker, E., & Bush, J. (2014). Violent expiratory events: On coughing and sneezing. *745*, 537-563.

11.] Jonges M, van Leuken J, Wouters I, Koch G, Meijer A, Koopmans M (2015) Wind-Mediated Spread of Low-Pathogenic Avian Influenza Virus into the Environment during Outbreaks at Commercial Poultry Farms. PLoS ONE 10(5): e0125401. doi:10.1371/journal.pone.0125401

12.] Torremorell, M., Alonso, C., Davies, P. R., Raynor, P. C., Patnayak, D., Torchetti, M., & McCluskey, B. (2016). Investigation into the airborne dissemination of H5N2 highly pathogenic avian influenza virus during the 2015 spring outbreaks in the Midwestern United States. *Avian diseases*,*60*(3), 637-643.

12.] Zuo, Z., Kuehn, T., Verma, H., Kumar, S., Goyal, S., Appert, J., Raynor P., Ge S., Pui, D. (2013). Association of Airborne Virus Infectivity and Survivability with its Carrier Particle Size. *Aerosol Science and Technology, 47*(4), 373-382.

13.] Woo, M. H., Grippin, A., Anwar, D., Smith, T., Wu, C. Y., and Wander, J. D. (2012). Effects of Relative Humidity and Spraying Medium on UV Decontamination of Filters Loaded with Viral Aerosols. Appl. Environ Microbial., 78:5781–5787.

14.] Scott, G. H., and Sydiskis, R. J. (1976). Responses of Mice Immunized with Influenza Virus by Aerosol and Parenteral Routes. Infect. Immunity, 13:696–703.

15.] Druett, H., Henderson, D., Packman, L., & Peacock, S. (1953). Studies on respiratory infection: I. The influence of particle size on respiratory infection with anthrax spores. *Journal of Hygiene, 51*(3), 359-371.

16.] Ching P, Harriman K, Li Y, et al. Infection prevention and control of epidemic- and pandemic-prone acute respiratory diseases in health care: WHO interim guidelines. Document WHO/CDS/EPR/2007.6, Geneva, Switzerland, World Health Organization, pp. 90, 2007.

17.] Weber TP, Stilianakis NI. Inactivation of influenza A viruses in the environment and modes of transmission: a critical review. Journal of Infection 2008;57:361e73.

18.] Hinds, W. C. (1999). *Aerosol technology: properties, behavior, and measurement of airborne particles*. John Wiley & Sons.

19.] Sze To, G. N., & Chao, C. Y. H. (2010). Review and comparison between the Wells–Riley and dose-response approaches to risk assessment of infectious respiratory diseases. *Indoor Air*, *20*(1), 2-16.

20.] Alford, R.H., Kasel, J.A., Gerone, P.J. and Knight, V. (1966) Human influenza resulting from aerosol inhalation, Proc. Soc. Exp. Biol. Med., 122, 800–804.

21.] Hatch, T. F. (1961). Distribution and deposition of inhaled particles in respiratory tract. *Bacteriological reviews*, *25*(3), 237.

22.] Centers for Disease Control and Prevention (2019). *1918 Pandemic (H1N1 virus)*. Retrieved from https://www.cdc.gov/flu/pandemic-resources/1918-pandemic-h1n1.html on (June 17, 2019)

23.] Herfst S., Böhringer, M., Karo, B., Lawrence, P., Lewis N., Mina M., Russell C., Steel J., Swart R., Menge C. Department of Virology. (2017). Drivers of airborne human-to-human pathogen transmission. *Current Opinion in Virology, 22*, 22-29.

24.] Centers for Disease Control and Prevention. (2015, August 4). *H5 Viruses in the United States*. Retrieved from: https://www.cdc.gov/flu/avianflu/h5/index.htm

25.] Center for Animal Health and Food Safety, UMN, *Epidemiologic Study of Highly Pathogenic Avian Influenza H5N2 among Turkey Farms*, 2015, University of Minnesota.

26.] Gatherer, D. (2009). The 2009 H1N1 influenza outbreak in its historical context. *Journal of Clinical Virology, 45*(3), 174-178.

27.] Alexandratos, N., & Bruinsma, J. (2012). *World agriculture towards 2030/2050: the 2012 revision* (Vol. 12, No. 3). FAO, Rome: ESA Working paper.

28.] Silbergeld, E. K., Graham, J., & Price, L. B. (2008). Industrial food animal production, antimicrobial resistance, and human health. *Annu. Rev. Public Health*, *29*, 151-169.

29.] Chen P-S, Lin CK, Tsai FT, Yang C-Y, Lee C-H, Liao Y-S, et al. Quantification of Airborne Influenza and Avian Influenza Virus in a Wet Poultry Market using a Filter/Real-time qPCR Method. Aerosol Sci- ence and Technology. 2009; 43(4):290-7.

30.] Seedorf, J., Hartung, J., Schroder, M., Linkert, K.H., Phillips, V.R., Holden, M.R., Sneath, R.W., Short, J.L., White, R.P., Pedersen, S., Takai, H., Johnsen, J.O., Metz,

J.H.M., Groot Koerkamp, P.W.G., Uenk, G.H., Wathes, C.M., 1998. Concentrations and emissions of airborne endotoxins and microorganisms in livestock buildings in Northern Europe. J. Agric. Eng. Res. 70, 97–109.

31.] Köllner, B., Heller, D., 2006. Ambient air concentrations of bioaerosols in the vicinity of a pigpen – results of the project ‘‘health-related effects of bioaerosols emitted by livestock husbandries” | [Bioaerosolimmissionen im umfeld eines schweinemastbetriebes – Ergebnisse aus dem projekt ‘‘gesundheitliche wirkungen von stall-luft-komponenten aus tierhaltungsbetrieben”]. Gefahrst. Reinhalt. Luft 66, 349–354.

32.] Millner, P. D. (2009). Bioaerosols associated with animal production operations. *Bioresource technology*, *100*(22), 5379-5385.

33.] Centers for Disease Control and Prevention, National Center for Emerging and Zoonotic Infectious Diseases (2017). *Zoonotic Diseases*. Retrieved from https://www.cdc.gov/onehealth/basics/zoonotic-diseases.html on (June 18, 2019).

34.] World Health Organization (2018, November 18). *Influenza (Avian and Other Zoonotic).* Retrieved from https://www.who.int/en/news-room/fact-sheets/detail/influenza-(avian-and-other-zoonotic) on (June 18, 2019).

34.] World Health Organization. (2019 A, February 12). *Cumulative Number of Confirmed Human Cases of Avian Influenza A(H5N1) Reported to WHO*. Retrieved from:

https://www.who.int/influenza/human

animal_interface/H5N1_cumulative_table_archives/en/

35.] World Health Organization. (2019 B). *Zoonoses: Diseases.* Retrieved from https://www.who.int/zoonoses/diseases/en/ on (June 18, 2019).

36.] Lonc, E., & Plewa, K. (2010). Microbiological Air Contamination in Poultry Houses. *Polish Journal Of Environmental Studies, 19*(1), 15-19.

37.] Gurzadyan, G. G., Nikogosyan, D. N., Kryukov, P. G., Letokhov, V. S., Balmukhanov, T. S., Belogurov, A. A., & Zavilgelskij, G. B. (1981). Mechanism of high power picosecond laser UV inactivation of viruses and bacterial plasmids. *Photochemistry and photobiology*, *33*(6), 835-838.

37.] Wells, W. F., and G. M. Fair. 1935. Viability of E. coli exposed to ultra-violet radiation in air. Science 82:280-281.

38.] Wells, W. F., and H. W. Brown. 1936. Recovery of influenza virus suspended in air and its destruction by ultraviolet radiation. Am. J. Hyg. 24:407-413.

39.] Tseng, C. C., & Li, C. S. (2005). Inactivation of virus-containing aerosols by ultraviolet germicidal irradiation. *Aerosol Science and Technology*, *39*(12), 1136-1142.

40.] McDevitt, J. J., Rudnick, S. N., & Radonovich, L. J. (2012). Aerosol susceptibility of influenza virus to UV-C light. *Appl. Environ. Microbiol.*, *78*(6), 1666-1669.

41.] Griffin, D.W., Kellogg, C.A., Garrison, V.H., Lisle, J.T., Borden, T.C., Shinn, E.A., 2003. Atmospheric microbiology in the northern Caribbean during African dust events. Aerobiologia 19, 143e157

42.] Martin Jr, S. B., Dunn, C., Freihaut, J. D., Bahnfleth, W. P., Lau, J., & Nedeljkovic-Davidovic, A. (2008). Ultraviolet germicidal irradiation: current best practices. *Ashrae Journal*,*50*(8), 28.

43.] Aarnink, A. J. A., Mosquera, J., Winkel, A., Cambra-Lopez, M., Van Harn, J., de Buisonje, F. E., & Ogink, N. W. M. (2009). Options for dust reduction from poultry houses. In *Agricultural Technologies In a Changing Climate: The 2009 CIGR International Symposium of the Australian Society for Engineering in Agriculture* (p. 47). Engineers Australia.

44.] Pyankov, O., Usachev, E., Pyankova, O., & Agranovski, I. (2012). Inactivation of Airborne Influenza Virus by Tea Tree and Eucalyptus Oils. *Aerosol Science and Technology, 46*(12), 1295-1302.

45.] Kettleson, E. M., Ramaswami, B., Hogan Jr, C. J., Lee, M. H., Statyukha, G. A., Biswas, P., & Angenent, L. T. (2009). Airborne virus capture and inactivation by an electrostatic particle collector. *Environmental science & technology*, *43*(15), 5940-5946.

46.] Kettleson, E. M., Schriewer, J. M., Buller, R. M. L., & Biswas, P. (2013). Soft-X-ray-enhanced electrostatic precipitation for protection against inhalable allergens, ultrafine particles, and microbial infections. *Appl. Environ. Microbiol.*, *79*(4), 1333-1341.

47.] Mainelis, G., Górny, R. L., Reponen, T., Trunov, M., Grinshpun, S. A., Baron, P., ... & Willeke, K. (2002). Effect of electrical charges and fields on injury and viability of airborne bacteria. *Biotechnology and bioengineering*, *79*(2), 229-241.

48.] Manuzon, R., Zhao, L., & Gecik, C. (2014). An Optimized Electrostatic Precipitator for Air Cleaning of Particulate Emissions from Poultry Facilities. *ASHRAE Transactions*,*120*(1).

49.] Sleytr,U. B. (1978). Regular Arrays of Macromolecules on Bacterial Cell Walls: Structure, Chemistry, Assembly, and Function, Int. Rev. Cytol. 53:1.

50.] Eliasson, B., & Kogelschatz, U. (1991). Nonequilibrium volume plasma chemical processing. *IEEE transactions on plasma science*, *19*(6), 1063-1077.

51.] Kim, H. H. (2004). Nonthermal plasma processing for air-pollution control: a historical review, current issues, and future prospects. *Plasma Processes and Polymers*, *1*(2), 91-110.

52.] Conrads, H., & Schmidt, M. (2000). Plasma generation and plasma sources. *Plasma Sources Science and Technology*,*9*(4), 441.

53.] Chang, J. S., Lawless, P. A., & Yamamoto, T. (1991). Corona discharge processes. *IEEE Transactions on plasma science*,*19*(6), 1152-1166.

54.] Kogelschatz, U. (2003). Dielectric-barrier discharges: their history, discharge physics, and industrial applications. *Plasma chemistry and plasma processing*, *23*(1), 1-46.

55.] Moreau, M., Orange, N., & Feuilloley, M. G. J. (2008). Non-thermal plasma technologies: new tools for bio-decontamination. *Biotechnology advances*, *26*(6), 610-617.

56.] Chen, H. L., Lee, H. M., Chen, S. H., & Chang, M. B. (2008). Review of packed-bed plasma reactor for ozone generation and air pollution control. *Industrial & Engineering Chemistry Research*, *47*(7), 2122-2130.

57.] Chang, J. S.; Kostov, K. G.; Urashima, K.; Yamamoto, T.; Okayasu, Y.; Kato, T.;

Iwaizumi, T.; Yoshimura, K. Removal of NF3 from Semiconductor-process Flue Gases by Tandem Packed-bed Plasma and Adsorbent Hybrid Systems. IEEE Trans. Ind. Appl. 2000, 36, 1251.

58.] Al-Abduly, A., & Christensen, P. (2015). An in situ and downstream study of non-thermal plasma chemistry in an air fed dielectric barrier discharge (DBD). *Plasma Sources Science and Technology*, *24*(6), 065006.

59.] Sasaki, S., Kanzaki, M., & Kaneko, T. (2016). Calcium influx through TRP channels induced by short-lived reactive species in plasma-irradiated solution. *Scientific reports*, *6*, 25728.

60.] Li, R., Liu, Y., Cheng, W., Zhang, W., Xue, G., & Ognier, S. (2016). Study on remediation of phenanthrene contaminated soil by pulsed dielectric barrier discharge plasma: the role of active species. *Chemical Engineering Journal*, *296*, 132-140.

61.] Thomas, R. S. (1964). Ultrastructural localization of mineral matter in bacterial spores by microincineration. *The Journal of cell biology*, *23*(1), 113-133.

62.] Farr, S. B., & Kogoma, T. O. K. I. O. (1991). Oxidative stress responses in Escherichia coli and Salmonella typhimurium.*Microbiology and Molecular Biology Reviews*, *55*(4), 561-585.

63.] Cabiscol Català, E., Tamarit Sumalla, J., & Ros Salvador, J. (2000). Oxidative stress in bacteria and protein damage by reactive oxygen species. *International Microbiology, 2000, vol. 3, núm. 1, p. 3-8*.

64.] Gaunt, L. F., Beggs, C. B., & Georghiou, G. E. (2006). Bactericidal action of the reactive species produced by gas-discharge nonthermal plasma at atmospheric pressure: a review. *IEEE Transactions on Plasma Science*, *34*(4), 1257-1269.

65.] Gallagher, M. J., Vaze, N., Gangoli, S., Vasilets, V. N., Gutsol, A. F., Milovanova, T. N., S. Anandan, D. Murasko, & Fridman, A. A. (2007). Rapid inactivation of airborne bacteria using atmospheric pressure dielectric barrier grating discharge. *IEEE Transactions on Plasma Science*, *35*(5), 1501-1510.

66.] Moisan, M., Barbeau, J., Moreau, S., Pelletier, J., Tabrizian, M., & Yahia, L. H. (2001). Low-temperature sterilization using gas plasmas: a review of the experiments and an analysis of the inactivation mechanisms. *International journal of Pharmaceutics*, *226*(1-2), 1-21.

67.] Lerouge, S., Wertheimer, M. R., & L'H, Y. (2001). Plasma sterilization: a review of parameters, mechanisms, and limitations. *Plasmas and Polymers*, *6*(3), 175-188.

68.] Moreau, M., Orange, N., & Feuilloley, M. G. J. (2008). Non-thermal plasma technologies: new tools for bio-decontamination. *Biotechnology advances*, *26*(6), 610-617.

69.] Ohshima, T., Sato, M., & Saito, M. (1995). Selective release of intracellular protein using pulsed electric field. *Journal of Electrostatics*, *35*(1), 103-112.

70.] Mitchell, B. W., & King, D. J. (1994). Effect of negative air ionization on airborne transmission of Newcastle disease virus. *Avian diseases*, 725-732.

71.] Nishikawa, K., & Nojima, H. (2003). Airborne virus inactivation technology using cluster ions generated by discharge plasma. *Sharp Tech J*, *86*, 10-15.

72.] Hagbom, M., Nordgren, J., Nybom, R., Hedlund, K. O., Wigzell, H., & Svensson, L. (2015). Ionizing air affects influenza virus infectivity and prevents airborne-transmission.*Scientific reports*, *5*, 11431.

73.] Wu, Y., Liang, Y., Wei, K., Li, W., Yao, M., Zhang, J., & Grinshpun, S. A. (2015). MS2 virus inactivation by atmospheric-pressure cold plasma using different gas carriers and power levels. *Appl. Environ. Microbiol.*, *81*(3), 996-1002.

74.] Xia, T., Kleinheksel, A., Lee, E. M., Qiao, Z., Wigginton, K. R., & Clack, H. L. (2019). Inactivation of airborne viruses using a packed bed non-thermal plasma reactor. *Journal of Physics D: Applied Physics*, *52*(25), 255201.

75.] Bergeron, V., Chalfine, A., Misset, B., Moules, V., Laudinet, N., Carlet, J., & Lina, B. (2011). Supplemental treatment of air in airborne infection isolation rooms using high-throughput in-room air decontamination units. *American journal of infection control*, *39*(4), 314-320.

76.] Sakudo, A., Shimizu, N., Imanishi, Y., & Ikuta, K. (2013). N2 gas plasma inactivates influenza virus by inducing changes in viral surface morphology, protein, and genomic RNA: *BioMed research international*, *2013*.

78.] Sheffield, P. E., Knowlton, K., Carr, J. L., & Kinney, P. L. (2011). Modeling of regional climate change effects on ground-level ozone and childhood asthma. American journal of preventive medicine, 41(3), 251-257.

79.] Goudarzi, G., Geravandi, S., Foruozandeh, H., Babaei, A. A., Alavi, N., Niri, M. V., ... & Mohammadi, M. J. (2015). Cardiovascular and respiratory mortality attributed to ground-level ozone in Ahvaz, Iran. Environmental monitoring and assessment, 187(8), 487.

80.] Wang, G., Zhu, R., Yang, L., Wang, K., Zhang, Q., Su, X., ... & Fang, J. (2016). Non-thermal plasma for inactivated-vaccine preparation. Vaccine, 34(8), 1126-1132.

81.] Aboubakr, H. A., Williams, P., Gangal, U., Youssef, M. M., El-Sohaimy, S. A., Bruggeman, P. J., & Goyal, S. M. (2015). Virucidal effect of cold atmospheric gaseous plasma on feline calicivirus, a surrogate for human norovirus. Appl. Environ. Microbiol., 81(11), 3612-3622.

82.] Zimmermann, J. L., Dumler, K., Shimizu, T., Morfill, G. E., Wolf, A., Boxhammer, V., ... & Anton, M. (2011). Effects of cold atmospheric plasmas on adenoviruses in solution. Journal of Physics D: Applied Physics, 44(50), 505201.

83.] Shahid, M. A., Abubakar, M., Hameed, S., & Hassan, S. (2009). Avian influenza virus (H 5 N 1); effects of physico-chemical factors on its survival. Virology Journal, 6(1), 38.

84.] Uhm, H. S., Lee, K. H., & Seong, B. L. (2009). Inactivation of H 1 N 1 viruses exposed to acidic ozone water. Applied Physics Letters, 95(17), 173704.

85.] Hogan Jr, C. J., Kettleson, E. M., Lee, M. H., Ramaswami, B., Angenent, L. T., & Biswas, P. (2005). Sampling methodologies and dosage assessment techniques for submicrometre and ultrafine virus aerosol particles. Journal of Applied Microbiology, 99(6), 1422-1434.

86.] Jaschhof, H. (1992). Sampling Virus Aerosols Using the Gelatin Membrane Filter. Bio Tech, 6.

87.] Lazarova, V., Janex, M. L., Fiksdal, L., Oberg, C., Barcina, I., & Pommepuy, M. (1998). Advanced wastewater disinfection technologies: short and long term efficiency. Water Science and Technology, 38(12), 109-117.

88.] Shin, G.A., & Sobsey, M.D. (2003). Reduction of norwalk virus, poliovirus 1, and bacteriophage ms2 by ozone disinfection of water. Applied and Environmental Microbiology, 69, 3975-3978

89.] Tseng, C., & Li, C. (2008). Inactivation of surface viruses by gaseous ozone. Journal of environmental health, 70(10), 56-63.

90.] Thomas, C., King, D. J., & Swayne, D. E. (2008). Thermal inactivation of avian influenza and Newcastle disease viruses in chicken meat. Journal of food protection, 71(6), 1214-1222.

91.] Swayne, D. E., & Beck, J. R. (2004). Heat inactivation of avian influenza and Newcastle disease viruses in egg products. Avian Pathology, 33(5), 512-518.

92.] Chmielewski, R. A., Beck, J. R., & Swayne, D. E. (2011). Thermal inactivation of avian influenza virus and Newcastle disease virus in a fat-free egg product. Journal of food protection, 74(7), 1161-1168.

93.] Li, J., Leavey, A., Wang, Y., O'Neil, C., Wallace, M. A., Burnham, C. A. D., ... & Biswas, P. (2018). Comparing the performance of 3 bioaerosol samplers for influenza virus. Journal of Aerosol Science, 115, 133-145.

94.] Burton, N. C., Grinshpun, S. A., & Reponen, T. (2006). Physical collection efficiency of filter materials for bacteria and viruses. The Annals of occupational hygiene, 51(2), 143-151.

95.] Sartorius (2019). *Disposable Gelatin Membrane Filters*. Retrieved from https://www.sartorius.com/shop/ww/en/usd/applications-laboratory-microbiological-quality-control-pharmaceutical-quality-control-air-monitoring-equipment/disposable-gelatine-membrane-filters%2c-diameter-80mm%2c-1-fold%2c-pack-size-10/p/17528--80----ACD

96.] Yang, W., & Marr, L. C. (2012). Mechanisms by which ambient humidity may affect viruses in aerosols. Appl. Environ. Microbiol., 78(19), 6781-6788.

97.] Sobsey MD, Meschke JS. 2003. Virus survival in the environment with special attention to survival in sewage droplets and other environmental

media of fecal or respiratory origin. WHO, Geneva, Switzerland. https://www.researchgate.net/publication/228551421_Virus_Survival_in_the_Environment_with_Special_Attention_to_Survival_in_Sewage_Droplets_and_Other_Environmental_Media_of_Fecal_or_Respiratory_Origin

98.] Songer, J. R. (1967). Influence of relative humidity on the survival of some airborne viruses. Appl. Environ. Microbiol., 15(1), 35-42.

99.] Lowen, A. C., Mubareka, S., Steel, J., & Palese, P. (2007). Influenza virus transmission is dependent on relative humidity and temperature. *PLoS pathogens*, *3*(10), e151.

100.] Boyd, R., & Hanson, R. (1958). Survival of Newcastle Disease Virus in Nature. Avian Diseases, 2(1), 82-93.

101.] Hugh-Jones, M., Allan, W. H., Dark, F. A., & Harper, G. J. (1973). The evidence for the airborne spread of Newcastle disease. Epidemiology & Infection, 71(2), 325-339.

102.] Donaldson AI, Ferris NP. (1976). The survival of some air-borne animal viruses in relation to relative humidity. Vet. Microbiol. 1:413– 420.

103.] Benbough JE. 1971. Some factors affecting the survival of airborne viruses. J. Gen. Virol. 10:209 –220.

104.] Ge, S., Kuehn, T. H., Abin, M., Verma, H., Bekele, A., Mor, S. K., ... & Zuo, Z. (2014). Airborne virus survivability during long-term sampling using a non-viable Andersen cascade impactor in an environmental chamber. Aerosol Science and Technology, 48(12), 1360-1368.

105.] Appert, J., Raynor, P. C., Abin, M., Chander, Y., Guarino, H., Goyal, S. M., et al. (2012). Influence of Suspending Liquid, Impactor Type, and Substrate on Size-Selective Sampling of MS2 and Adenovirus Aerosols. Aerosol Sci. Technol., 46:249–257.

106.] Ibrahim, E., Harnish, D., Kinney, K., Heimbuch, B., & Wander, J. (2015). An experimental investigation of the performance of a Collison nebulizer generating H1N1 influenza aerosols. Biotechnology & Biotechnological Equipment, 29(6), 1142-1148.

107.] Hinz, T., & Linke, S. (1998). A comprehensive experimental study of aerial pollutants in and emissions from livestock buildings. Part 2: Results. Journal of Agricultural Engineering Research, 70(1), 119-129.

108.] Larsson, K., Malmberg, P., Eklund, L., Belin, L., & Blaschke, E. (1988). Exposure to microorganisms, airway inflammatory changes and immune reactions in asymptomatic dairy farmers. International Archives of Allergy and Immunology, 87(2), 127-133.

109.] Cormier, Y., Tremblay, G. U. Y., Meriaux, A., Brochu, G., & Lavoie, J. (1990). Airborne microbial contents in two types of swine confinement buildings in Quebec. American Industrial Hygiene Association Journal, 51(6), 304-309.

110.] Kasprzyk, I. (2008). Aeromycology–main research fields of interest during the last 25 years. Ann Agric Environ Med, 15(1), 1-7.

111.] Dutkiewicz, J. (1987). Bacteria in farming environment. European journal of respiratory diseases. Supplement, 154, 71.

112.] Vucemilo, M., Vinkovic, B., Tofant, A., Simpraga, B., Pavicic, Ž., & Matkovic, K. (2005, September). Microbiological air contamination in intensive poultry breeding. In Proceedings of the XIIth Congress on Animal Hygiene.

113.] Kurnatowskaka A. Reservoirs of biological pathogenic agents in aerosphere, hydrosphere and lithosphere. In: KURNATOWSKA A. (Ed.). Ecology. Its connections with different scientific disciplines. Wyd. Naukowe PWN. 2002 [In Polish].

114.] Lugauskas, A., Krikstaponis, A., & Sveistyte, L. (2004). Airborne fungi in industrial environments--potential agents of respiratory diseases. Annals of agricultural and environmental medicine: AAEM, 11(1), 19-25.

115.] Zhang, Y. (2004). Indoor air quality engineering. CRC press.

116.] Wathes, C. M. (1998). Aerial emissions from poultry production. World's poultry science journal, 54(3), 241-251.

117.] H. H. Ellen, R. W. Bottcher, E. Von Wachenfelt, & H. Takai. (2000). Dust Levels and Control Methods in Poultry Houses. Journal of Agricultural Safety and Health, 6(4), 275-282.

118.] Donham, K., Haglind, P., Peterson, Y., Rylander, R., & Belin, L. (1989). Environmental and health studies of farm workers in Swedish swine confinement buildings. Occupational and Environmental Medicine, 46(1), 31-37.

119.] Lau, A. K., Vizcarra, A. T., Lo, K. V., & Luymes, J. (1996). Recirculation of filtered air in pig barns. Canadian Agricultural Engineering, 38, 297-304.

120.] Adell, E., Calvet, S., Pérez-Bonilla, A., Jiménez-Belenguer, A., García, J., Herrera, J., & Cambra-López, M. (2015). Air disinfection in laying hen houses: Effect on airborne microorganisms with focus on Mycoplasma gallisepticum. Biosystems Engineering, 129, 315-323.

121.] Aarnink, A. J. A., Landman, W. J. M., Melse, R. W., & Huynh, T. T. T. (2005). Systems for eliminating pathogens from exhaust air of animal houses. In Livestock

Environment VII, 18-20 May 2005, Beijing, China (p. 239). American Society of Agricultural and Biological Engineers.